OPTIMAL PLANNING AND DESIGN OF HYBRID RENEWABLE ENERGY SYSTEM FOR RURAL HEALTHCARE FACILITIES

OLATOMIWA LANRE JOSEPH

FACULTY OF ENGINEERING
UNIVERSITY OF MALAYA
KUALA LUMPUR

2016

OPTIMAL PLANNING AND DESIGN OF HYBRID RENEWABLE ENERGY SYSTEM FOR RURAL HEALTHCARE FACILITIES

OLATOMIWA LANRE JOSEPH

THESIS SUBMITTED IN FULFILMENT OF THE REQUIREMENTS FOR THE DEGREE OF DOCTOR OF PHILOSOPHY

FACULTY OF ENGINEERING
UNIVERSITY OF MALAYA
KUALA LUMPUR

2016

UNIVERSITY OF MALAYA

ORIGINAL LITERARY WORK DECLARATION

Name of Candidate: **Olatomiwa Lanre Joseph**

Matric No: **KHA120160**

Name of Degree: **Doctor of Philosophy (PhD)**

Title of Project Paper/Research Report/Dissertation/Thesis ("this Work"):

Optimal Planning and Design of Hybrid Renewable Energy System for Rural Healthcare Facilities

Field of Study: **Renewable Energy**

I do solemnly and sincerely declare that:

(1) I am the sole author/writer of this Work;
(2) This Work is original;
(3) Any use of any work in which copyright exists was done by way of fair dealing and for permitted purposes and any excerpt or extract from, or reference to or reproduction of any copyright work has been disclosed expressly and sufficiently and the title of the Work and its authorship have been acknowledged in this Work;
(4) I do not have any actual knowledge nor do I ought reasonably to know that the making of this work constitutes an infringement of any copyright work;
(5) I hereby assign all and every rights in the copyright to this Work to the University of Malaya ("UM"), who henceforth shall be owner of the copyright in this Work and that any reproduction or use in any form or by any means whatsoever is prohibited without the written consent of UM having been first had and obtained;
(6) I am fully aware that if in the course of making this Work I have infringed any copyright whether intentionally or otherwise, I may be subject to legal action or any other action as may be determined by UM.

Candidate's Signature Date:

Subscribed and solemnly declared before,

Witness's Signature Date:

Name:

Designation:

ABSTRACT

This thesis focused on the feasibility of off-grid hybrid renewable energy in delivering basic healthcare services in rural areas without electricity access. Renewable energy resource (RES) such as solar and wind energy is considered abundant in many rural places, it is also environmental friendly, hence suitable for providing electricity in rural healthcare facilities where there is no electricity access. These energy resources have received greater attention in recent years due to their cost effectiveness in operation. Optimum planning and design of hybrid renewable power system based on location selection, component types, system configuration as well as sizing to meet the load requirements of rural healthcare facility has been considered in this study. In this case, long-term meteorological data from six selected locations across the six climatic zones of Nigeria (Sokoto, Maiduguri, Jos, Iseyin, Enugu and Port-Harcourt) were first examined to determine the feasibility of utilizing the energy resources (solar and wind) to power a typical rural healthcare facilities at respective remote locations. Followed by development of prediction algorithm for solar radiation using soft-computing methodologies. Then, utilization of cost-effective optimization algorithm for optimal sizing of the energy resources and other system components with accurate mathematical models for energy management of the entire hybrid system. The final aim is the minimization the proposed hybrid system total annual cost during the project lifetime while considering the reliability of power supply to the rural clinics and pollutant emission reduction. To this aim, cost function of PV, wind, diesel generator and battery were derived by considering the rural clinics load demand, sites meteorological (solar radiation, wind speed, temperature) data and diesel price.

Findings from the study showed that Sokoto and Jos exist in the high wind potential regions, while the remaining sites are only suitable for small wind applications. Values obtained for global, beam and diffuse radiation as well as clearness index, show that all

the sites enjoy considerable solar energy potential suitable for varying degree of solar energy applications. The feasibility simulation carried out with Hybrid Optimization Model for Electric Renewable (HOMER) software indicates that hybrid system is the best option for all the sites considered in this study. The PV/wind/diesel/battery hybrid system configuration is considered optimum for RHC applications at Iseyin, Sokoto, Maiduguri, Jos and Enugu, while hybrid systems involving PV/diesel/battery is considered ideal for RHC at remote location in Port-Harcourt, due to the quality of renewable energy potential. Hence, it was concluded that, the abundance of wind and solar resources in the country create an ideal environment for inclusion of renewable energy systems, such as PV and wind in the design and implementation of standalone power supply systems to improve rural health delivery. The reliability of hybrid systems is found to be enhanced when solar, wind and diesel generator are used together; the size of battery storage is also reduced because there is less dependence on one method of energy production.

ABSTRAK

Tesis ini memberi tumpuan kepada kemungkinan luar grid tenaga boleh diperbaharui hibrid dalam menyampaikan penjagaan kesihatan asas perkhidmatan di kawasan luar bandar yang tidak mempunyai akses elektrik. sumber tenaga yang boleh diperbaharui (RES) seperti solar dan angina tenaga dianggap banyak di banyak tempat luar bandar, ia juga mesra alam sekitar, oleh itu sesuai untuk membekalkan tenaga elektrik dalam kemudahan penjagaan kesihatan luar bandar di mana tidak ada akses elektrik. Sumber-sumber tenaga telah menerima perhatian yang lebih besar dalam tahun-tahun kebelakangan ini kerana kos mereka keberkesanan dalam operasi. perancangan dan reka bentuk sistem kuasa boleh diperbaharui hibrid Optimum berdasarkan pemilihan lokasi, jenis komponen, konfigurasi sistem serta saiz untuk memenuhi keperluan beban kemudahan penjagaan kesihatan luar bandar telah dipertimbangkan dalam kajian ini. Data meteorologi jangka panjang di enam lokasi terpilih di seluruh enam kawasan geo-politik Nigeria (Sokoto, Maiduguri, Jos, Iseyin, Enugu dan Port-Harcourt) adalah pertama dipetimbangkan untuk menentukan kemungkinan menggunakan sumber tenaga (sumber angin dan solar) dalam menjanakan kuasa kepada pusat kesihatan luar bandar (RHC) di lokasi masing-masing jauh. Ini diikuti dengan pembangunan algoritma ramalan untuk radiasi solar dengan kaedah mesra pengkomputeran, oleh itu, pembangunan dengan kos yang efektif, pengoptimuman algoritma untuk saiz optimum sumber-sumber tenaga dan komponen sistem lain yang menggunakan kaedah mesra pengkomputeran. Di ikuti dengan pembangunan model matematik yang tepat untuk pengurusan keseluruhan tenaga sistem hibrid.

Hasil dari kajian setakat ini, menunjukkan bahawa Sokoto dan Jos wujud di kawasan-kawasan yang berpotensi angin kuat, manakala kawasan lain hanya sesuai untuk aplikasi angin kecil. Nilai yang diperolehi untuk global, pemancaran dan radiasi resapan serta indeks kejelasan, menunjukkan bahawa semua laman web yang memiliki potensi tenaga

solar yang besar sesuai untuk pelbagai tahap aplikasi tenaga solar. Simulasi pra-kemungkinan dijalankan menggunakan perisian tenaga boleh dipebaharui iaitu (HOMER) menunjukkan bahawa sistem hibrid adalah pilihan yang terbaik untuk semua laman web yang dipertimbangkan dalam kajian ini. Konfigurasi PV /angin / diesel / sistem bateri hibrid angin dianggap optimum untuk aplikasi RHC di Sokoto, Maiduguri, Jos dan Enugu, manakala sistem hibrid yang melibatkan PV / diesel / bateri dianggap sesuai untuk RHC di lokasi yang jauh dalam Iseyin dan Port-Harcourt, kerana kualiti potensi tenaga boleh diperbaharui. Oleh itu, kesimpulan menunjukkan bahawa, banyak angin dan sumber solar di negara ini mewujudkan persekitaran yang sesuai untuk kemasukan sistem tenaga boleh diperbaharui, seperti PV dan angin dalam reka bentuk dan pelaksanaan sistem bekalan kuasa yang tunggal untuk menambah baik penyampaian tenaga ke pusat kesihatan luar bandar. Kebolehpercayaan sistem hibrid dapat dipertingkatkan apabila penjanaan tenaga daripada solar, angin dan diesel digunakan bersama; saiz bateri yang digunakan juga dapat dikurangkan kerana tidak kurang bergantung kepada satu kaedah pengeluaran kuasa sahaja.

ACKNOWLEDGEMENTS

Foremost, I appreciate God Almighty, for His faithfulness, grace, love, mercy, strength and inspiration throughout the course of this work. My profound appreciation goes to Prof. Dr. Saad Mekhilef for his interest, contributions and encouragement towards the successful completion of this research. The bright spark unit of University Malaya, for the SBSUM scholarship award under the Federal University of Technology Minna and University of Malaya Memorandum of Understanding (MOU). My Parent (Deacon and Mrs. E.B Olatomiwa), for their immeasurable sacrifices towards my attainment in life. My lovely wife (Funmilayo Olatomiwa) and children (Olamiposi, Olafimihan and Oluwakoyinsolami), for their love, encouragements and understanding throughout the course of this work. My siblings (Olaniyi, Oluwakemi, Kolawole, Ayoola, Olayinka and Olabisi) for their continual prayers and encouragements. Finally, to everyone too numerous to mention that have contributed in one way or the other to the successful completion of this programme.

TABLE OF CONTENTS

LIST OF FIGURES

LIST OF TABLES

LIST OF SYMBOLS AND ABBREVIATIONS

ANFIS	:	adaptive neuro fuzzy inference system
ANN	:	artificial neural network
GP	:	genetic programming
RET	:	renewable energy technologies
RES	:	renewable energy sources
HRES	:	hybrid renewable energy system
RHC	:	rural health clinic
SEG	:	solar energy gain
NIMET	:	Nigerian metrological agency
RMSE	:	root-mean square error
MAPE	:	mean absolute percentage error
COE	:	cost of energy
LCOE		levelized cost of energy
CRF		capital recovery factor
SS	:	south-south
SW	:	south-west
SE	:	south-east
NE	:	north-east
NW	:	north-west
NC	:	north-central
R^2	:	coefficient of determination
r	:	correlation coefficient
$\bar{H}$	:	monthly mean global solar radiation
$\bar{H}_0$	:	monthly mean extraterrestrial radiation

$\bar{H}_b$	:	monthly mean beam radiation
$\bar{H}_d$	:	monthly mean global solar radiation on tilted surface
$\bar{H}_T$	:	monthly mean global solar radiation on tilted surface
$\overline{K_t}$	:	monthly mean clearness index
$\bar{T}_{max}$	:	monthly mean maximum temperature (^{o}C)
$\bar{T}_{min}$	:	monthly mean minimum temperature (^{o}C)
$\bar{n}$	:	monthly mean sunshine duration (hr)
$f(v)$	:	Weibull probability density
k	:	Weibull shape parameter
c	:	Weibull scale parameter (m/s)
$\Gamma(x)$	:	gamma function
ρ	:	air density (kg/m3)
α	:	surface roughness coefficient
β_{opt}	:	optimum angle of inclination (degree)

LIST OF APPENDICES

CHAPTER 1: INTRODUCTION

1.1 Background

Reliable electricity access is a pre-requisite for improving humans live in rural areas, enhancing healthcare delivery, education as well as other developmental growths within the local communities. At present, 17 percent of world population do not have access to electricity, out of which an estimated 85 percent of this population lives in rural settlement of Sub-Saharan Africa, South Asia and others countries, with Sub-Saharan Africa occupying the largest share (IRENA, 2012). The majority of these people have limited possibility to access electricity. According to the projection of International Energy Agency (IEA), the population without electricity will not decrease due to incessant population growth (IEA, 2008). The growing population, with the associated increase in socio-economic activities, makes continuous energy supply imperative, in order to meet the teeming energy demand.

It has also been reported that, close to 1.3 billion worldwide are provided with healthcare facilities without electricity access (Practical Action, 2013). This deficiency implies that medical equipment such as; ultrasound, autoclave, centrifuge and medical x-ray cannot be used in such places. Surgery is occasionally conducted with light from windows or kerosene lamps. The report also indicated that, many women die on a daily basis during pregnancy and childbirth in rural places due to poor medical care, and that provision of minimum lighting and minor surgical equipment would reduce this high maternal mortality rate by 70% if provided. Modern advances in the distribution of vaccines and other cold-chain dependent drugs have presented demands for electricity in health centers where there is no or limited access to reliable power supply as presented in Figure 1.1.

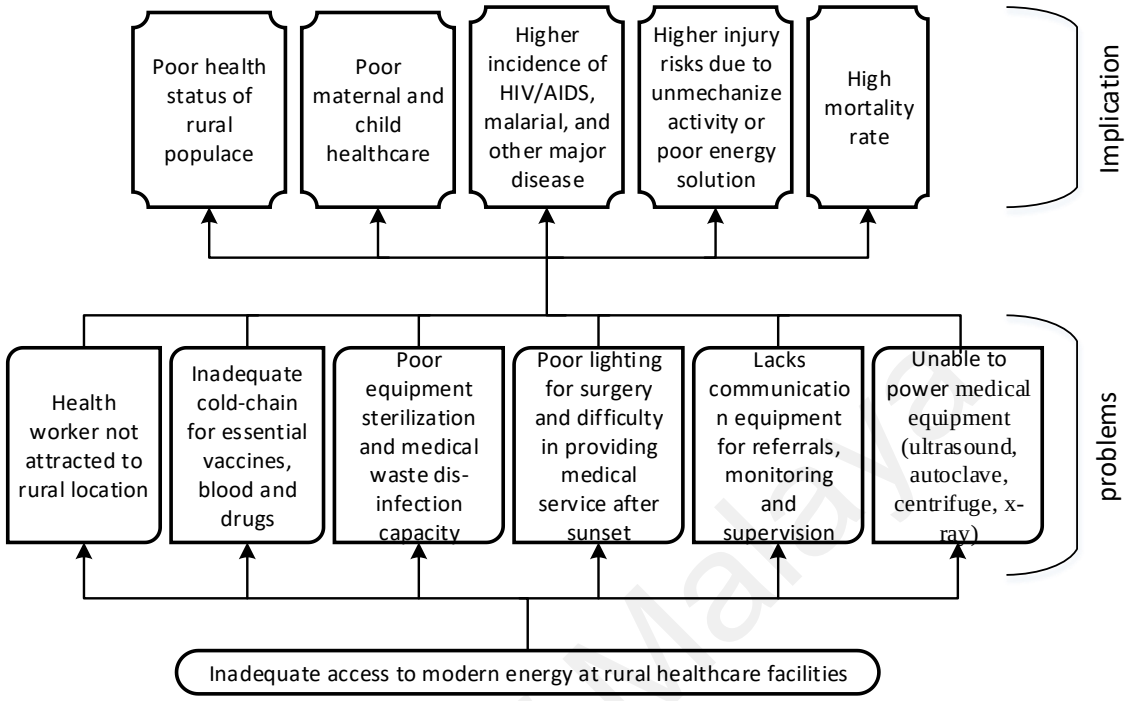

Figure 1.1: Impact of energy access on rural healthcare services

In a recent World Health Organization (WHO) survey for 11 countries in Sub-Saharan Africa, Nigeria inclusive, covering about 4,000 clinics and hospitals (Adair-Rohani et al., 2013). It was observed that, one-quarter health facilities in the considered countries have no access to electricity supply, and about three-quarter with unreliable power supply. Even in facilities linked to the national grid, insufficient generation as characterized by erratic power supply, has often been the case. Diesel generators have traditionally been used to power these off-grid clinics, and in supplementing unreliable grid supply in grid-connected facilities, with attendant huge price of diesel fuel, unreliable delivery and high CO_2 pollutant emission contributing to air pollution exposures and climate change. Operators of rural health facilities in Nigeria and developing nations in general, are challenged with many problems, which have hindered effective delivery of the healthcare to the rural populace. For example, unreliable power supply has rendered cold-chain activities inoperable, while a healthcare facility without means of illumination usually keeps the patients arriving late in the night for medical attention to wait until the following

morning before medical attention can be rendered. This has often led to many problems, including obstetric complications, which is one of the root causes of the high maternal mortality rates in the rural area. Lack of antenatal care, absences of skilled birth attendants and limited availability of emergency obstetrics procedures due to lack of electricity are reasons behind this situation. Therefore, electricity should be a priority for effective public health delivery.

1.2 Problem statements

Since the beginning of the democratic dispensation in Nigeria (1999), a number of reforms have been established to open up power sector to privatization in the country, thus improving energy supplies to the infrastructure to cope with the ever-increasing population growth. These reforms include the National Energy Policy (NEP), the Electric Power Sector Reform Act (EPSR), and the establishment of the Nigerian Electricity Regulatory Commission (NERC) and the Rural Electrification Agency (REA). Consequently, involvement of the government in the regulation of energy production and distribution was withdrawn and the undertakings of all stakeholders and issuing of operational licenses to several parties in the power sector were well managed (O. S. Ohunakin, Ojolo, & Ajayi, 2011). These reforms led into the development of various independent power projects (IPPs), to complement the existing power infrastructure across the nation (Vincent-Akpu, 2012). Nevertheless, even with these reforms, the provision of electricity to the rural communities has not improved due to non-access to the grid, coupled with grid unreliability; other constraints include inaccessible terrain, communities' hostilities, and the high cost of grid extension to the communities (A. S. Sambo, 2009). Since about 70% of the rural areas are still without any form of electricity (NBS, 2013), it is thus obvious that rural communities are not likely to benefit from power reforms. Extension of the national grid to most rural areas via thick jungles and difficult

terrain is challenging and inefficient due to the concomitant high cost and loss of transmission from the grid to the load center (Sen & Bhattacharyya, 2014). Power generation in rural villages through the use of diesel generators may seem to be a reliable option if there is proper operation and regular maintenance. However, the noise and environmental pollution resulting from the emission of CO_2 and other harmful gasses, and their negative effects on the health of patients and health personnel in the rural clinics, pose a serious drawback. Furthermore, the unstable diesel prices and the additional cost of transportation to such locations make this alternative a difficult one to maintain.

Given the fact that improvement of rural accessibility to electricity via connection the national grid seems impracticable at the moment, the establishment of a system that is autonomous and off-grid in such locations becomes imperative. A solution based on renewable energy (RE) technologies, would be a viable option due to the vast deposits of the resources, coupled with the associated environmental friendliness. Moreover, such rural locations have lower electricity demand. These alternative technologies for electricity production have received immense attention recently, due to their cost effectiveness in operation as well as sustainability (Akikur, Saidur, Ping, & Ullah, 2013; Dihrab & Sopian, 2010; Hiendro, Kurnianto, Rajagukguk, & Simanjuntak, 2013). In the case of rural health facilities, a solar/wind/diesel generator hybrid system can be deployed to cater for the need of the un-electrified rural health center. It will enable power supply to certain medical equipment, critical lighting, and mobile communication devices in an off-grid area for timely delivery and critical medical care for the rural dwellers. Hence, the role of off-grid renewable energy in delivering basic healthcare services to rural areas that are without grid extension or stable power supply, cannot be over emphasized.

Various renewable sources are available for electric power generation, these include; solar, biomass, wind, fuel cells, geothermal and small hydro. Over the years, several

research have been conducted in different parts of the world to assess the potentials of these resources for various applications, and the results have shown their significant contributions to global climate protection efforts through the reduction of greenhouse gas emission while meeting rapid energy growth demand (Azoumah, Yamegueu, Ginies, Coulibaly, & Girard, 2011). Similarly, in Nigeria, several researchers have evaluated the prospects of some renewable energy sources as means of power generation, however, no particular considerations were given for rural healthcare application, and in most cases, the studies were based mainly on single source renewable energy systems (Nnaji, Uzoma, & Chukwu, 2010; O. S. Ohunakin, Adaramola, Oyewola, & Fagbenle, 2014). Even in many of these studies where renewable energy are assessed, one of the greatest challenges is inadequate meteorological data, such as solar irradiance, this is because of unavailability of these resources data in several government-operated meteorological stations in Nigeria. The few meteorological stations that have records are not up-to-date, and this is likely because of improper calibration of the measuring equipment.

In technical terms, a system that wholly depends on single source renewable energy alone is not considered reliable. This is especially true for remote areas with isolated loads. This is because the availability of the RE sources may not be guaranteed at all times, due to the varying nature of the resources' outputs. Hence, the need for hybrid power systems that combined conventional and renewable energy sources.

A renewable hybrid system has been described as a cluster of distinct renewable energy sources which operate independently and with coordination (C. Wang, 2006). Hybrid energy system that combines two or more energy sources when properly operated, will overcome the inherent limitations of each source when considered separately (Bajpai & Dash, 2012). Proper selection of renewable power sources will substantially lower the use of fossil diesel and also increase the sustainability of power supply. Furthermore,

conventional power sources will complement the renewable sources during varying weather conditions, which will definitely improve the consistency of the electric power system. In literature, various hybrid renewable energy system configurations utilized in providing power to different applications in various region of the world have proofed to be cost-effective and environmental friendly. Among which includes; PV/battery(Mulder et al., 2013), wind/battery (W. Wang, Mao, Lu, & Wang, 2013), wind/PV/battery (Nandi & Ghosh, 2010a), wind/diesel/battery (Xu Liu, Islam, Chowdhury, & Koval, 2008), PV/diesel/battery (Shaahid & El-Amin, 2009), PV/FC/electrolyzer/battery (Elbaset, 2011), PV/FC/electrolyzer/Super-capacitor (Payman, Pierfederici, & Meibody-Tabar, 2009) etc.

Among the different configurations, a hybrid system such as solar PV, wind, battery and diesel generator, combining conventional and renewable energy sources, can be considered a good option for isolated loads; such as rural healthcare applications. Such a hybrid power scheme comprises of wind and solar PV as major sources of energy, with diesel generator backup source, and battery bank for storage. The system is expected to among other benefits, meet the load demands, reduce energy costs, ensure maximal utilization of renewable sources, optimize the operation of battery bank, ensure efficient operation of the diesel generator and reduce environment pollution emissions.

1.3 Motivation

Since optimal planning and design of the hybrid renewable energy system are essential measures for efficiency and for the economic utilization of energy resources in any application, guaranteeing low life-cycle cost with full usage of all the constituent energy resources in the hybrid system, and enabling system operation in optimum conditions with respect to investment and power system reliability requirements. Therefore, the main motivation for this research is to study and analyze the hybrid renewable energy system

based on solar and wind as the RE source and conventional diesel generator as a backup source with a battery energy storage devices as shown Figure 1.2 for providing electricity to selected off-grid rural healthcare facilities in Nigeria. The main questions therefore, include;

- Will soft-computing methodologies be suitable for estimating solar radiation, for energy resource analysis in locations where there is limited meteorological data?
- Can wind/solar-based RE resources be a viable option to a conventional diesel generator in providing reliable power to the considered rural healthcare facilities?
- Which system configuration offers the most technically-feasible and cost-effective option to meet the electricity demand of the considered rural health facilities?
- What is the economic and environmental benefit of the proposed configurations?

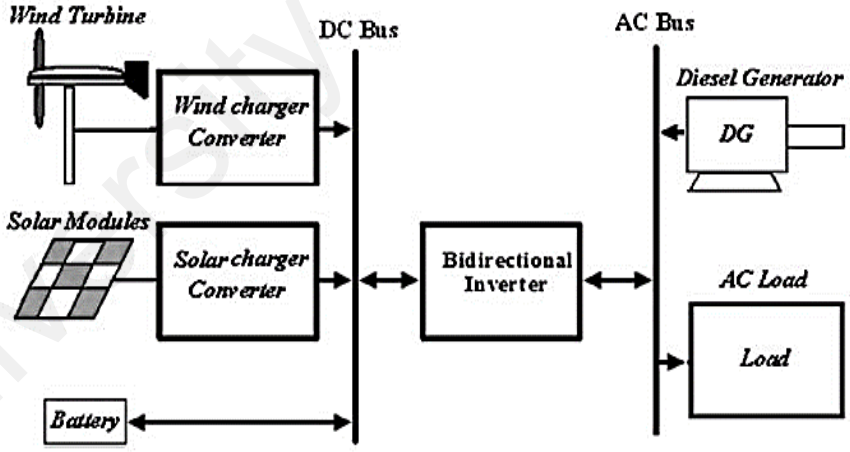

Figure 1. 2: Proposed hybrid energy model

Foremost in this study is the analysis of long-term meteorological data of six selected locations across the six different climatic zones in Nigeria and techno-economic feasibility of utilizing hybrid renewable power systems to meet the load demand of a typical rural healthcare facility at such locations, with the lowest cost of energy. Since the capital cost of the hybrid systems is usually influenced by technical factors such as

efficiency, technology, reliability, and site conditions, the influence of each of these factors needed to be considered for the performance study of the system. The major factors, that determined the electricity cost is accurate sizing mechanism of the system components. Inaccurate sizing of hybrid system components may make the system more costly or unreliable. Therefore, optimal sizing of different components of the hybrid system will proffer a cost-effective and reliable benefit system.

In this regard, accurate modeling and optimal sizing of the various components, constituting the hybrid power scheme is vital for this study. To design an optimal power solution, load analysis and location data assessment is required. A control strategy/energy management will be designd to operate in different modes. At normal mode, the RE sources (PV and wind) have priority to supply the load and the excess energy deployed to charge the batteries, while the remaining excess energy can be used by dump loads, such as; water heating, water pumping, etc. In the case of inadequate energy from either the RE sources or the battery bank to power the load, a conventional diesel generator will be operated automatically to power the load and charge the batteries.

1.4 Research objectives

The broad aim of this thesis is optimal planning and design of hybrid renewable energy interventions that will enable quality healthcare delivery to rural areas of Nigeria. While the specific objectives are as follows:

1. To statically access the potential of wind and solar energy resources in six selected locations, representing different climatic zones of Nigeria.
2. To develop an algorithm for solar radiation prediction with soft computing techniques.

3. To perform techno-economic feasibility of introducing wind and solar energy resources in providing electricity access to off-grid rural healthcare facilities in Nigeria.
4. To employ a cost-effective optimization model (HOMER) for optimal sizing of the hybrid power scheme that meets the energy demand of the selected rural health clinic at optimum energy dispatch.

1.5 Thesis outline

The remaining parts of the thesis are organized as follows: in Chapter 2, the energy status in Nigeria with the potential of renewable energy in meeting the energy demand of the country was discussed. Review of solar energy conversion system, including previous approaches to solar radiation prediction as well as PV array performance prediction. The chapter also includes a review of wind energy conversion system with various wind turbine performance and behaviour prediction models. A review of optimum sizing methodologies in the hybrid system for purpose of efficient and economic utilization of renewable energy resources was conducted. Chapter 3 presents the methodology employed in caring out the study objectives. In this chapter, the approaches to renewable energy resource data collection were described, followed by the methodology for solar radiation prediction, then approach to assessment of renewable energy resources in the selected sites. Mathematical modeling of the hybrid system components is also included within this chapter, followed by the adopted approach to optimal sizing of the proposed hybrid renewable energy system. In Chapter 4, the results and discussion of each aspect of the methodology are presented. This includes validation of optimal sizing of the proposed hybrid renewable energy system configuration based on different scenarios at the selected sites. Finally, the conclusion based upon the finding from this study, recommendations and suggestion for future study is presented in chapter 5.

CHAPTER 2: LITERATURE REVIEW

2.1 Introduction

In this chapter, energy status in Nigeria with the potentiality of renewable energy in meeting the energy demand of the country were brief discussed, followed by review of solar and wind energy conversion system, including; previous approaches to the solar radiation prediction, PV array performance prediction, wind turbine performance and behaviour prediction models. The chapter also contains a review of the hybrid renewable energy system with different configurations and system topologies. Finally, it discussed various approaches to optimum sizing of hybrid system components for efficient and economic utilization of renewable energy resources.

2.2 Energy status in Nigeria

Generally, the economic development of any country depends upon its energy supply (Ikeme & Ebohon, 2005). Nigeria is divided into six climatic zones with a total land area of 923.769 sq. km (NBS, 2013). The rural population in Nigeria constitute 50.4% with merely 36% of this population having access to electricity, while the areas with electricity access hardly have up to 4 hours of uninterrupted power supply in a day (UN, 2014; WorldBank, 2013). The conventional electricity production in Nigeria is currently distributed from seven power stations and several independent power projects across the nation. Therefore, the present generation capacity of the nation is 3.9GW with per-capita capacity of 28.6W (Worldbank, 2015). This amount is obviously insufficient for the domestic consumption of the entire nation. For the country to achieve its energy requirement, it will need per-capita capacity of 1000W or a power production capacity of 140GW contrary to the present capacity. Therefore, the accessibility to electricity in the Nigeria ranges between ~27% and ~60% of the capacity installed, whereas, the transmission and distribution deficit is up to the tune of ~28% of the generated power (ECN, 2013). According to International Fund for Agricultural Development (IFAD,

2012), about 80% of Nigeria rural communities' lives below the poverty line. The rural regions are generally difficult to access because of bad road networks, despite the on-going power sector reforms and privatization of the electricity firms. Due to logistic and economic reasons, rural areas far away from the grid and having a low potential for power procurement cannot attract private power investors. However, energy supply is essential for the basic amenities and economic development. A rural location without electricity supply frequently lacks indispensable amenities such as communication, school, portable water supply and healthcare. The Human Development Index (HDI) of electrified communities is higher compared with non-electrified communities (Chaurey & Kandpal, 2010). Several small and medium-sized enterprises (SME) owners in the rural community are not financially buoyant to acquire or fuel power generator. Furthermore, the condition became worse due to fuel subsidy removal by the Federal Government of Nigeria in 2012. Consequently, several businesses in rural areas suffer stagnation and some close down due to frustration. In most cases, these have resulted in massive rural-urban migration, while the vibrant youths that are supposed to boost the HDI of the community migrate into the cities leaving the old and feeble behind. Furthermore, lack of stable power supply has resulted into the social backwardness of the rural communities and their economic potentials unexploited.

For Nigeria to achieve her energy requirements there is an urgent need to consider alternative power sources, especially for the rural communities. However, RE alternative cannot sufficiently end the power shortage in Nigeria. RE technology is said to have a significant amount of untapped potential, which could help the country to meet her increasing energy need. If the RE is synergistically harnessed, erratic power supply will be a history with less deteriorating environmental impact. Therefore, adopting the use of distributed generation approaches will definitely solve the electricity supply problem.

2.3 Renewable energy resources assessment

RE resources, provide excellent and consistent electricity for various uses in the different rural area around the world (Dihrab & Sopian, 2010; Hiendro et al., 2013). Among the several RE sources, wind and solar are very abundant and accessible regardless of the location. Hence, they are commonly explored. A comprehensive study of available long-term solar radiation data and wind regime in a specific location is therefore, vital for design and prediction of energy output of their respective energy conversion devices; the in-depth knowledge will help in determining their suitability for any specific applications.

Over the years, research has been conducted in different part around the world to assess the potentials of these RE resources for various applications. In Iran, the potentials of solar radiations in different parts of the country were assessed, and the results obtained showed greater potential for energy application in the central and southern part of the country (Besarati, Padilla, Goswami, & Stefanakos, 2013). In Borj-Cedrin, gulf of Tunis Tunisia, an assessment of global solar radiation on an hourly, daily, monthly and seasonal basis was conducted to determine its suitability for power application, and performance of the developed experimental model was validated with the actual measured data, and results showed good agreement (El Ouderni, Maatallah, El Alimi, & Nassrallah, 2013). In a related study at a certain location in Saudi Arabia, examination of optimal tilt angle for solar collector orientation for energy production enhancement was performed. The results from the study showed a gain of 8% at a tilt of solar collector in a particular angle on a monthly basis as compared to yearly tilt (Benghanem, 2011).

Studies on wind speed assessment from various locations around the world have also shown encouragements for power applications. In Malaysia, (Islam, Saidur, & Rahim, 2011), assessed wind energy characteristics and potentials for power generation at two

locations with wind data measured at 10m hub height. Maximum monthly wind speeds of 4.8 and 4.3 m/s, and power density of 67.4 and 50.8 W/m^2 were observed at Kudat and Labuan respectively. Furthermore, in a related study (Mohammadi & Mostafaeipour, 2013), an assessment of the possibility of wind energy for power application at a particular location in Kurdistan provinces on hourly, daily, monthly, seasonal and annual basis was conducted using Weibull distribution function. Outcome of the study showed the site to be marginally suitable for wind power application.

In Nigeria, several investigations had been conducted on solar and wind energy assessment for power generation, but with no particular considerations for rural healthcare application. In (O. S. Ohunakin et al., 2014), solar applications and developments in Nigeria were comprehensively discussed; various irradiation levels as distributed within the six climatic region across the country were categorized into zones. Furthermore, since there are limited meteorological sites in the country, several empirical models were developed for some locations around the country, to predict global and diffuse radiation data, needed for diverse solar applications (Adaramola, 2012; Ajayi, Ohijeagbon, Nwadialo, & Olasope, 2014; Okundamiya & Nzeako, 2011). In wind availability assessment, Nigeria has a poor/moderate wind regime with wind speeds that range from 2.12 to 4.13 m/s in the south, excluding the coastal regions; while in the northern region, the wind speeds is considered reasonable, this is within the range 4.0 to 8.60 m/s (Adaramola, Oyewola, Ohunakin, & Akinnawonu, 2014; O. S. Ohunakin, 2011b).

2.4 Renewable energy potential and applications in Nigeria

Energy is an important factor to economic advancement of any nation. It also plays a vital role towards economic partnership with international communities. Energy is expected to contribute more to the economic development if the RE potentials are

properly harnessed especially in the rural area where electric energy distribution from National grid looks like a mirage. Nigeria has a vast deposit of RE resources, these include; hydropower, wind, solar, biomass, etc. (O. S. Ohunakin, 2010). All these are available with promising potentials at different sites within the country. Unfortunately, this availability is not reflected on their contribution to the energy balance. One of the Nigeria government's interests is investing in these RE resources to enhance the reliability of power supply and mitigate the environmental effect caused by excessive dependence on fossil fuel for power generation (ECN, 2006). This will indeed lead to a more independent power system for all and sundry. To achieve this purpose, small and large-scale renewable energy systems have been implemented in some locations in Nigeria. Despite financial and technical issues, the availability of natural resources and the required technology encourage the implementation of such projects.

2.4.1 Solar Energy

Nigeria possesses great solar radiation potentials with high duration of sunshine throughout the year. Solar radiation levels as distributed within the six climatic region in the country were categorized into zones (O. S. Ohunakin et al., 2014). Zone I comprised the entire states in the North-Eastern part of the country. This zone has high solar radiation incident on the horizontal surface and it has great potential for large-scale solar power, mostly in the semi-arid region. In Zone II, which is made up of the North-West and North-Central parts of the country, there is viable solar radiation, which is suitable for most solar projects. Zone III, which comprises of all locations in the southern part of the country, including the coastal region exhibits low potential of annual global solar radiation, and is only appropriate for stand-alone PV systems. Nevertheless, certain states/locations in the South-Western and South-Eastern regions are viable for decentralized energy projects Figure 2.1 shows the solar radiation map of Nigeria (O. S. Ohunakin et al., 2014).

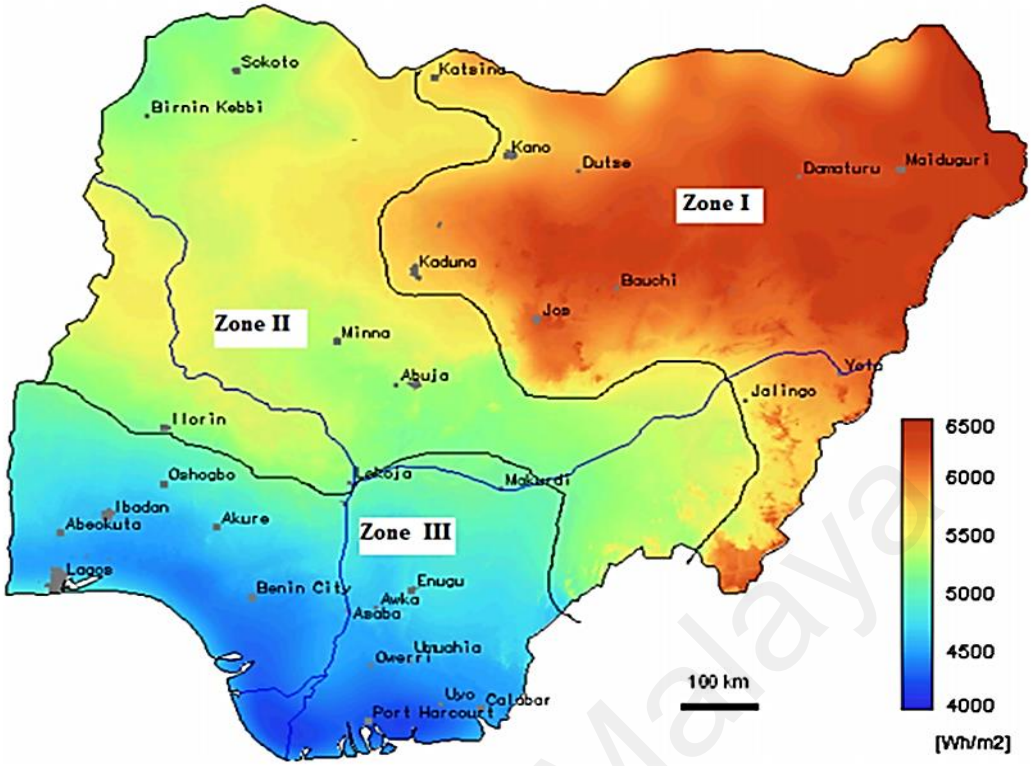

Figure 2. 1: Solar radiation map of Nigeria

Mean monthly solar radiation with clearness index of a particular location in Nigeria (Lat.13.130, Long. 4.330) is shown in Figure 2.2. The annual average radiation for this location stands at 5.92 kWh/m^2/day. The good values for these averages are obtainable if the PV panel is inclined to optimum tilt angle. The value is reasonably high and promising to utilize solar energy for PV and solar water heating applications.

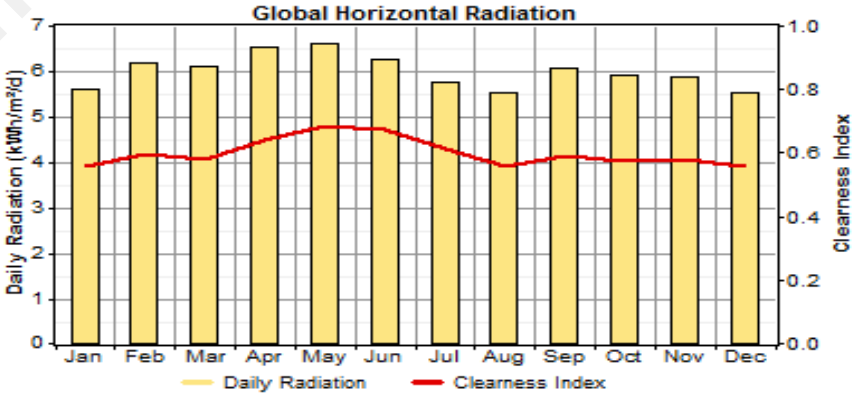

Figure 2. 2: Monthly average daily solar radiation of a particular place in Nigeria

The Energy Commission of Nigeria (ECN) have implemented and supervised different small standalone PV projects, while others have been implemented under state governments (O. S. Ohunakin et al., 2014). These projects are intended for remote rural communities to provide electricity and for an agricultural purpose, in other to boost the social-economic development of such places. Many challenges facing this implementation include; high financing and technological requirements, non-availability of highly qualified personnel for design and installations, availability of space and infrastructure for storage system. These challenges have limited the wide spread of the technology. Although obtaining a loan for small-scale standalone PV project is usually easier due to government interventions. The success of these pilot projects expected to make way for more investment in the larger-scale projects. The implementation of these projects has proven to be feasible and the possibility of it sustainability is high despite the above-mentioned challenges. In fact, the implementation requires different steps; it begins from the study of the community's needs, obtaining the technical information i.e; data, preparing design and obtaining the necessary fund for implementation. This will be followed by equipment installation and finally sharing the relevant information with the local community to enable them operates and maintains the system.

2.4.2 Wind Energy

The wind energy technology has enjoyed rapid attention recently. Different pre-technical and economic assessment needed to be conducted before a decision pertaining to its implementation can be made (Dalton, Lockington, & Baldock, 2009; Giannoulis & Haralambopoulos, 2011). This also entails a thorough investigation of the wind potential at the specific site. This will involve several years of wind speed and direction measurements to guarantee a more reliable assessment. Furthermore, the distribution of wind speed, energy available in wind and the appropriate type of wind turbine will need to be studied using the measured meteorological data.

Presently, the contribution of wind energy in the national energy consumption is low because there is lack of marketable wind turbine connected to the national grid. However, quite a few numbers of stand-alone wind power stations were previously installed. This cuts across five (5) northern states around the country primarily to power water pumps. One of which is a 5 kW wind energy conversion system for electrification of Sayyan Gidan Gada village in Sokoto State (Uzoma et al., 2011). Over the years, only limited researches have been conducted on assessments of wind velocity characteristics and accompanying wind energy potentials in different part of the country. Nonetheless, encouraging efforts in designing a suitable wind-powered generator are being made at the Sokoto Energy Research Centre (SERC) as well as the Abubakar Tafawa Balewa University, Bauchi.

Another alternative and feasible application of small wind turbine in Nigeria is for water pumping purposes, especially in a rural area for irrigation farming. Over the years, diesel generators have traditionally been used for such purposes (ECN, 1997). These remote sites served by this technology are far from existing grid and considering grid extension installation to these locations is too expensive. The use of wind turbine to replace diesel generators is more beneficiary in terms of lowering operating cost of the system and non-pollutant emission into the environment as often associated with diesel power generator. Another drawback of such traditional technology is bad roads condition in these locations, which have alarming influence on the total cost of transporting the diesel fuel. Figure 2.3 represent the wind map of Nigeria at 10m height (A. S. Sambo, 2009).

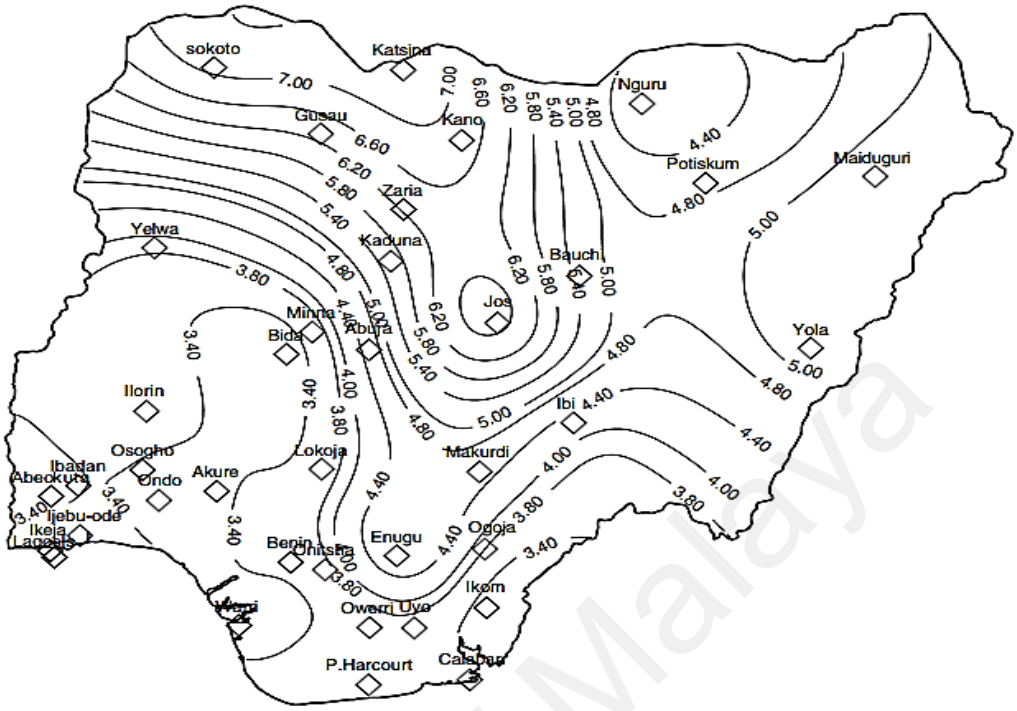

Figure 2. 3 Wind speed map of Nigeria at 10m height

2.5 Solar Energy Conversion System

Solar energy conversion system (SECS) utilized solar irradiance incident on the earth's surfaces to generate electricity. Most of the energy resources on the earth are produced directly or indirectly by the solar energy except the like of geothermal energy. The two major approach for electricity generation through sunlight, are; solar photovoltaic (PV) and solar thermal systems as shown in Figure 2.4.

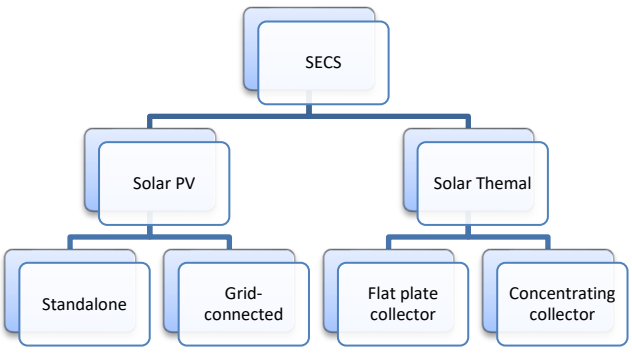

Figure 2. 4: Classification of SECS

Besides the wind energy, solar energy through PV is another fast emerging RE technology. Although the total size of the globally solar power generation capacity is lower than the wind energy generation, nevertheless, it has seen increasing growth rate over the last decade (Hossain & Ali, 2016; Ibrahim, Othman, Ruslan, Mat, & Sopian, 2011). This technology has attracted enormous attention worldwide, because of its sustainability, abundant deposit and environmental friendliness, thereby making its wide applications leading to the abatement of prevalent global warming (Akikur et al., 2013).

The photovoltaic effect is a process by which solar energy is directly converted to electrical energy. The behavior of a solar panel or PV panel is comparable with the classical p-n junction diode. A typical PV cell can be likened to a diode at night, when illuminated. The photons energy is attracted to the semiconductor material, leading towards the formation of electron-hole pairs. The electric field produced by the p-n junction separates the photon-created electron-hole pairs. The electrons are transferred to the n-region (N-type material), and the holes are drawn to the p-region (P-type material). The n-region electrons flow via the external circuit to deliver the electricity to the load (Luque & Hegedus, 2011) . The PV cell is the basic component within a PV energy system. In a typical PV cell, less than 2W at about 0.5 V DC is produced. Therefore, it is essential to connect PV cells in series-parallel arrangements to generate the required voltage and power. Figure 2.5 illustrates single PV cells arranged to make a module, and modules connected together to produce an array. A module may generate power from a few watts to hundreds of watts, while available power of an array may range between hundreds of watts to megawatts.

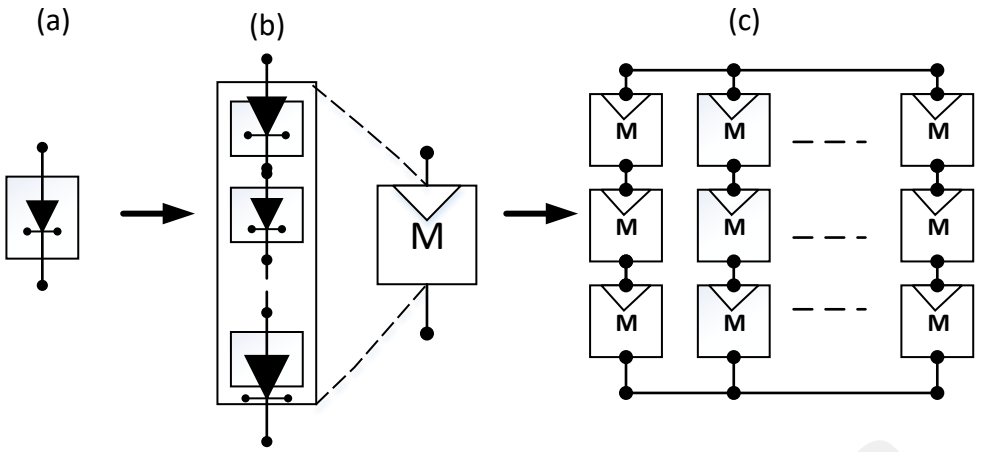

Figure 2. 5 PV System (a) cell (b) module (c) array

2.5.1 Approaches to solar radiation prediction

Long-term knowledge of accessible solar radiation data in a specific location is vital for the design and prediction of energy output of solar conversion systems. Such data are usually obtained from remote measurements at certain locations using solar radiation measuring instruments. However, owing to the high cost of calibration and maintenance of the instruments, available solar radiation data at many meteorological stations around the world are limited (Hunt, Kuchar, & Swanton, 1998). The challenges associated with the measurement of global solar radiation have led into the development of several models and algorithms for its estimation using a number of available measured meteorological variables. These include sunshine hours, maximum, minimum and average air temperature, relative humidity and cloud factor. In several government-operated meteorological stations in Nigeria, records of solar radiation data are not available. The few meteorological stations that have records are not up-to-date, and this is likely as a result of improper calibration of the measuring equipment.

Over the years, several methods for estimation of solar radiation on horizontal surfaces have been developed; these include; empirical models (Besharat, Dehghan, & Faghih, 2013), satellite-derived models(Pinker, Frouin, & Li, 1995) and stochastic algorithm

models (Hansen, 1999). Empirical models have been widely employed in the correlation of global solar radiation with various routinely-measured meteorological and geographical parameters. Such parameters include sunshine duration, pressure, cloudiness index, humidity maximum and minimum temperatures. Records from literature have shown that sunshine duration and minimum and maximum temperature relations have been recognized as the best correlations for solar radiation prediction (Besharat et al., 2013). However, in a situations where sunshine duration data were not readily available, commonly measured maximum and minimum temperature alone had also produced good results (Xiaoying Liu et al., 2009). While the application of satellite-based methods appears promising for the estimation of solar radiation over large regions, the high cost and insufficient historical data are considerable drawbacks since such methods are somewhat new. The methodology as demonstrated low performance in the long-term forecasting of solar radiation data. More so, they are also not entirely applicable in the case of having missing data on the dataset. Nevertheless, the application of artificial intelligence techniques is one way to overcome these challenges.

Artificial and computational intelligence techniques have been widely deployed in the estimation of solar radiation around the world. In Oman, (Al-Alawi & Al-Hinai, 1998) predicted solar radiation at certain location without measured data. Monthly mean daily values of temperature, pressure, relative humidity, sunshine duration hours and wind speed were used as inputs for an artificial neural network (ANN) method to predict global solar radiation. Comparison of the results obtained with an empirical model revealed that and the ANN-based model was highly accurate. In Algeria, (Mellit, Benghanem, & Kalogirou, 2006) predict daily solar radiation for sizing photovoltaic (PV) application using a combination of neural and wavelet networks . The wavelets served as activation functions. The results showed the more satisfactory performance of the proposed approach compared to other neural network models. In China, an ANN model was

developed to estimate monthly mean daily solar radiation for eight cities across the country in (Jiang, 2009). Comparing the obtained results with results from conventional empirical models and using statistical analysis, it was obvious that the results showed good correlation between ANN model-estimated values and the actual data, with higher accuracy than other empirical models.

Behrang *et al* developed a model based on particle swarm optimization (PSO) technique to estimate monthly mean daily global solar radiation on a horizontal surface for 17 cities in Iran. (Behrang, Assareh, Noghrehabadi, & Ghanbarzadeh, 2011). The results showed the superior performance of the PSO-based models compared with traditional empirical models. Mohandes employed a PSO algorithm to train an ANN in order to model the monthly mean daily global solar radiation values in Saudi Arabia (Mohandes, 2012). Different parameters such as the number of months, sunshine duration, and location latitude, longitude and altitude were considered as inputs. The developed hybrid model displayed better performance compared to the backpropagation trained neural network (BP-NN). Benghanem et al, developed six ANN-based models to estimate horizontal global solar radiation in Al-Madinah, Saudi Arabia (Benghanem, Mellit, & Alamri, 2009). They utilized different combinations of input parameters consisting of sunshine hours, ambient temperature, relative humidity and days of the year. According to the results, the model with higher accuracy is dependent upon sunshine duration and air temperature. Ramedani et al. employed support vector regression (SVR) to develop a model for predicting global solar radiation in Tehran, Iran (Ramedani, Omid, Keyhani, Shamshirband, & Khoshnevisan, 2014b). In the study, two SVR models were proposed: radial basis function (SVR-rbf) and polynomial function (SVR-poly). The results indicated that the SVR-rbf model is superior to the polynomial function model (SVR-poly). Table 2.1 presents the summary of the reviewed solar radiation prediction model.

Table 2. 1 Summary of the reviewed solar radiation prediction models

Model	Input Parameters	Country	Reference	Remarks
Emperical	Sunshine hours, temperature, relative humidity, mean sea level and vapour pressure	Bahrain	(Abdalla, 1994)	Measured based on regression constants
Emperical	Global solar radiation and sunshine	Turkey	(Bakirci, 2009)	Measured based on regression constants
Emperical	Sunshine hours, Solar radiation, cloudiness	Nigeria	(Yohanna, Itodo, & Umogbai, 2011)	Developed based on Angstrom–Page equation
Stochastic algorithm	Global solar radiation extraterrestrial solar irradiance	USA	(Hansen, 1999)	Based on Gaussian, linear transformation and analytical approximation of empirical distributions
ANN	Temperature, relative humidity, pressure, wind speed and sunshine duration hours	Oman	(Al-Alawi & Al-Hinai, 1998)	Based on Artificial neural network
ANN	Average air temperatures, extraterrestrial solar radiation, sunshine duration precipitation and number of day	Iran	(Ramedani, Omid, & Keyhani, 2013)	Five different input combinations based on ANN
BNN	Average air temperature, sunshine duration, relative humidity, and extraterrestrial solar radiation	Saudi Arabia	(Yacef, Benghanem, & Mellit, 2012)	Prediction based on Bayesian neural network (BNN)
PSO	Extraterrestrial solar radiation and sunshine duration	Iran	(Behrang et al., 2011)	Five new sunshine duration models developed with particle swarm optimization (PSO)
PSO-ANN	Latitude, longitude, altitude, month of the year and sunshine duration	Saudi Arabia	(Mohandes, 2012)	Hybrid approach using PSO to train ANN
SVR	Maximum and minimum temperature, extraterrestrial radiation sunshine duration, number of days,clear-sky and solar radiation	Iran	(Ramedani, Omid, Keyhani, Shamshirband, & Khoshnevisan, 2014a)	Four distinctive models based on artificial intelligence to predict global solar radiation

The review highlights the competency of soft computing methodologies in accurate estimation of solar radiation, based on available meteorological data. The basic paradigm behind soft computing methodologies is the collection of input/output data pairs in order for the proposed network to learn from these data. In this study, soft-computing methodology called; adaptive neuro-fuzzy inference system (ANFIS), that merges the learning power of ANNs with the knowledge representation of fuzzy logic has been proposed to predict solar radiation in the selected sites, and the results will be compared with empirical model.

2.5.2 PV array performance predictions models

Since the performance of PV array is dependent upon the availability of solar radiation at a specific site as well as the PV module temperature, therefore, adequate knowledge of PV array performance under various operating conditions is necessary for precise selection and accurate prediction of energy performance of a solar energy conversion system. PV modeling is a mathematical representation of the PV output current-voltage (I-V), and power-voltage (P-V) relations. General equivalent circuit of single-diode PV model representing PV operation is shown in Figure 2.6. A comprehensive model is a two-diode model that utilized two diodes.

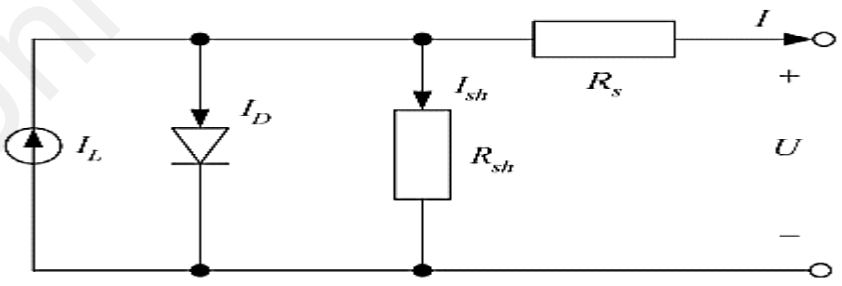

Figure 2. 6: Single-diode PV equivalent circuit

Many researchers have employed single-diode model to simulate PV module operation in the past (Chouder, Silvestre, Sadaoui, & Rahmani, 2012; Sera, Teodorescu, & Rodriguez, 2007). The authors in these studies depended on the manufacturer's data to

determine the value of the series and shunt resistances. Moreover, the ideality factor, saturation current and photon current are required for this evaluation according to the relation employed. Since, many PV manufacturers do not provide values for these parameters; therefore, assumptions for each of these parameters or iterative method are usually made. Ishaque *et al* employed a two-diode to model a PV cell (Ishaque, Salam, & Taheri, 2011). Two-diode PV model has more parameters than the ideal single-diode model; however, some assumptions are needed to simplify the computations. An Iterative method was used to determine the model parameters of the PV modules in this study. Although, the influence of temperature and solar irradiance were considered for different values for these parameters, it is however discovered that global optimization fitting any irradiance/temperature of these parameters were not computed.

A PV model for the primary purpose of maximum power point identification was developed in (El Shahat, 2010). In this work, the author assumed value for the ideality factor, and employed manufacturer's data sheet curve to calculate the series resistance, while genetic algorithm (GA) was employed to fix the maximum power point. A methodology for identification of parameter of solar PV cell with single-diode model is presented in (Zagrouba, Sellami, Bouaïcha, & Ksouri, 2010). In this study, the model validation was conducted with the results obtained by Pasan cell software; however, the software does not provide value for all PV parameters. As earlier stated, the temperature and solar radiation variation influence solar PV cell parameters, but in this study, this effect was not considered.

Based on the foregoing, ideality factor of a PV cell is seen as one of major parameters that require further analysis for PV performance evaluation. A more precise value in this parameter can be obtained by curve fitting or by trial and error according to (El Shahat, 2010). This approach seems inappropriate for its estimation in some instances because

the value may fit only selected I-V curve at specific temperature and solar radiation, but not all temperature and radiation levels. In this thesis, the ideality factor and other parameter will be estimated with simple iterative code developed using MATLAB. Furthermore, different points on I-V curve at various solar radiation and temperatures levels will be used for the computation, and this will not only be limited to the maximum power point at STC rather at various solar radiation or temperature level. The result from the simulation will be compared with real data from manufacturer's datasheet for validation purposes.

2.6 Wind Energy Conversion System

The principle of electricity generation from the wind is through conversion of kinetic energy of the wind into electrical energy. The wind turbine transforms the wind's kinetic energy in a rotor consisting of two or more blades mechanically coupled to an electric generator. The amount of energy received is enhanced by mounting the turbine on a tall tower. The power production capacity can be enhanced by installing more wind turbines at the site to make a wind farm (Burton, Jenkins, Sharpe, & Bossanyi, 2011). Two major wind turbine configurations are available in the market; the horizontal axis and vertical axis configuration. Most modern turbines employed horizontal axis configuration due to its many advantages over the other as summarized in Table 2.2 (Caló & Pongrácz, 2011; C. Wang & Nehrir, 2008).

Table 2. 2: Difference between horizontal and vertical axis wind turbine

Type	**Performance metrics**				
	Yield	**Strength**	**Violent wind resistance**	**Installation on frame**	**Installation area**
Horizontal axis	high	high	good	no	open
Vertical axis	low	low	moderate	yes	semi

Figure 2.7 shows the basic power stages within wind energy conversion system while Figure 2.8, depict a typical wind energy conversion system (Dadhania, Venkatesh, Nassif, & Sood, 2013).

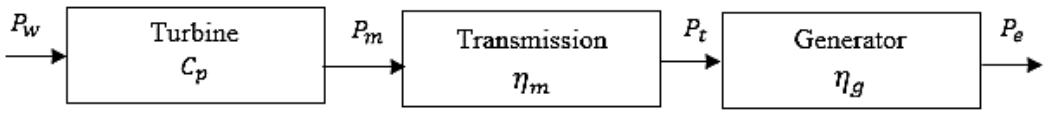

Figure 2. 7: Basic power stages of wind energy conversion system

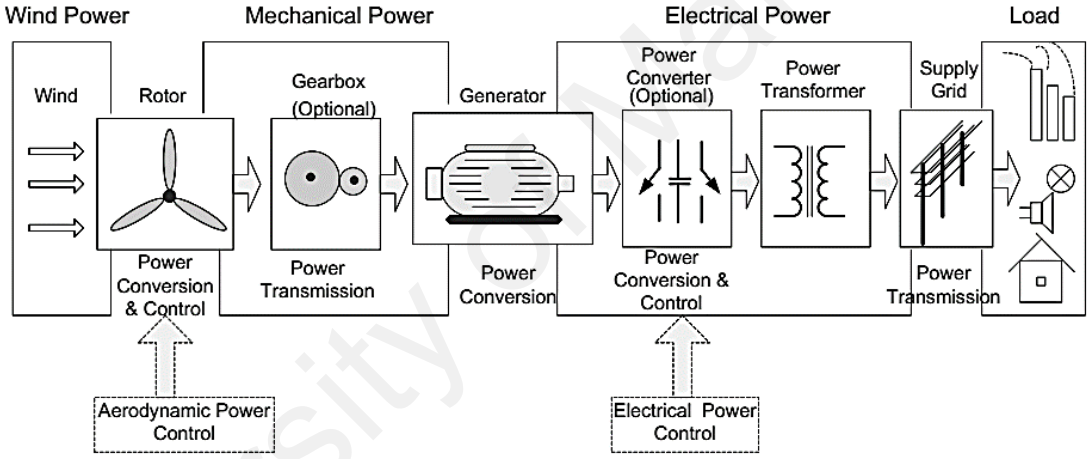

Figure 2. 8: Basic power stages of wind energy conversion system

The principal components of a modern wind turbine include; yaw, mast, nacelle, rotor, gearbox and generator. Wind turbine captures the wind energy potential with the help two or more blades attached to the rotor. The gearbox converts the rotational speeds of the wind turbine into high rotational speeds on the generator side. The electric generator, generate power when the shaft is propelled by the wind turbine and maintained constant output according to specifications by engaging an appropriate control and supervisory algorithms (C. Wang, 2006).

Instantaneous power in the wind is the product of wind velocity v (m/s) and cross-sectional area A (m^2), perpendicular to the wind stream having air density ρ as expressed as;

$$P_w = \frac{1}{2}\rho A v^3 \tag{2.1}$$

The wind power is converted into mechanical power P_m by the wind turbine as;

$$P_m = C_p P_w \tag{2.2}$$

where $C_p$is the power coefficient of the turbine rotor blade. The mechanical power is transmitted through the gear system to the electrical generator and the output is given by;

$$P_e = C_p \eta_m \eta_g P_w \tag{2.3}$$

where η_m and η_g are wind turbine and generator efficiency respectively.

Induction machines are usually used for wind power generation due to their ruggedness and cost effectiveness (Naikodi, 2011). Induction type generators are often seen in grid-connected application owing to their excitation requirement, and are only applicable in stand-alone applications given that sufficient reactive excitation is available for self-excitation (C. Wang & Nehrir, 2008). Induction generators can handle a slight increment speed from the rated value due to saturation, and the rate of increase in generated voltage is not linear with speed. Wind turbine can further be classified into; fixed-speed (FSWT) and variable-speed wind turbine (VSWT) each with different features (Burton et al., 2011). In order to make optimal use of the available wind energy, variable wind turbine is considered the best, and this can be achieved using doubly-fed induction generator (DFIG) or permanent magnet synchronous generator (PMSG).

Furthermore, wind turbine can also be grouped according to sizes and applications. For example; the European Wind Energy Association (EWEA, 2011) grouped wind turbines into several classifications as shown in Table 2.3

Table 2. 3: Wind turbine classification according to sizes

Type	**Rating**	**Features**	**Application**
Micro	Less than 3kW	Direct drive PMSG	Battery charging, farms, rural load
Small	3 to 30kW	Low maintenance and high reliability PMSG	Small home, remote area, residential area
Medium	30 to 200kW	PSMG or Wound rotor , Direct drive, variable speed	Village power, hybrid system, distributed power
Large	More than 200kW	PSMG or Wound rotor , Direct drive, variable speed	Off shore wind farm

2.6.1 Wind turbine performance prediction models

The application of wind energy conversion system (WECS) has gained popularity over the years due to the economic viability of wind energy technology, which justifies their utilization in standalone and grid-connected application (C. Wang, 2006). A thorough understanding of expected energy output of wind turbine is a prerequisite for effective design and implementation of wind power projects. Since various available wind turbines have different power output curve, different models have been developed to describe their performance. Proper choice among these models is therefore, important in wind turbine power simulation.

As wind speed in a location varies continuously with change in weather conditions, the energy available in the wind also changes. Hence, the need for dynamic modeling of all systems involved, for proper understanding of the entire system. Designing an optimum system requires an accurate modeling; however, a critical and a prerequisite step for optimization is the knowledge of all the factors that affects the performance of the

system before modeling. Three main factors affecting the wind turbine's performance are; the power curve of a selected wind turbine, the site wind speed distribution and the height of the hub. Each of these factors is briefly discussed in the following paragraphs;

1) *Power curve of wind turbine:* power output of any wind turbine at a specific wind speed can be estimated from the power curve of the respective wind turbine obtained from the manufacturer datasheet. Figure 2.9 represent a typical power curve of a wind turbine.

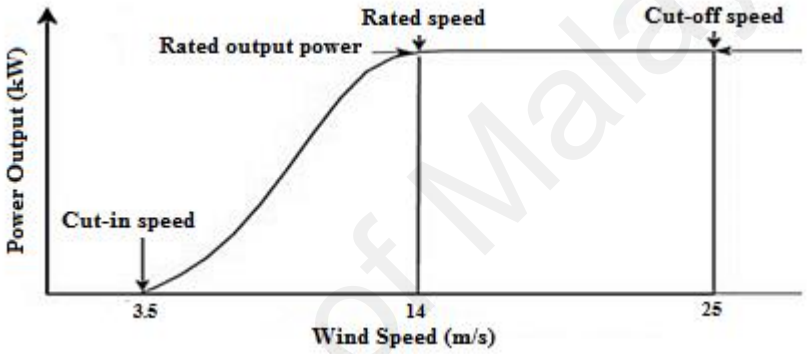

Figure 2. 9: Typical power curve of a wind turbine

2) *Wind speed distribution in the selected site:* The wind turbine electrical power output is proportional to cube of the wind speed as given in Equation (2.1); therefore, effective study of wind speed distribution at a specific site is required in determining the energy yield of the wind turbine (Thapar, Agnihotri, & Sethi, 2011). In most applications, Weibull probability distribution function has been widely used for wind speed distribution assessments, since the approach provides a suitable match with experimental data when compared to other statistical models. Weibull probability density function (PDF) is given as (Gökçek, Bayülken, & Bekdemir, 2007);

$$f(v,k,c) = \frac{k}{c}\left(\frac{v}{c}\right)^{k-1} exp\left[-\left(\frac{v}{c}\right)^{k}\right] \quad (2.4)$$

while the corresponding cumulative probability function (CPF) is expressed as (O. S. Ohunakin, 2011a);

$$F(v,k,c) = 1 - exp\left[-\left(\frac{v}{c}\right)^{k}\right] \quad (2.5)$$

where v is the wind speed, while c and k are scale and shape parameters respectively and $v \geq 0, k > 1, c > 0$. These parameters can be computed by employing different approaches including; the graphical method (Rinne, 2010), standard deviation method, maximum likelihood method (El Alimi, Maatallah, Dahmouni, & Nasrallah, 2012), power density method (Akdağ & Dinler, 2009), etc.

3) *Hub Height*: Several complex relationships have been used to study the influence on the hub height on the wind speed variation, but many of these are sophisticated for general engineering studies. However, many researchers have proposed simplified expressions, which may give satisfactory results, even though not theoretically precise. One of the most simple and common expressions is the power law and expressed as (Burton et al., 2011);

$$\frac{v}{v_0} = \left(\frac{h}{h_0}\right)^{\alpha} \quad (2.6)$$

where v is the wind velocity at required hub height 'h', v_0 is the wind velocity at reference height h_0' and α is site surface roughness coefficient with value ranges from 0.14 for flat surfaces and more than 0.25 for heavily forested landscape. From the above, it is clear that the wind turbine output energy depends on the location height of the wind turbine. To calculate the wind turbine performance using this formula, the measured wind speed at the height of the anemometer must

be converted to desired height of the turbine (Thapar et al., 2011). All these factors must be accurately computed for the modeling of the wind turbines.

Over the years, various models have been proposed by different authors to predict the wind turbines' performance. Generally, these models are classified under two categories; models based on fundamental equations of power available in the wind and those based on the concept of a power curve of wind turbine. Modeling of wind turbine, based on fundamental equations of available power in the wind are not considered accurate, and do not represent the behaviour of wind turbines accurately, due to its dependence on various parameters, including; wind velocity, wind turbine, rotational speed, mechanical transmission efficiency and turbine blade parameters. However, the concept of a power curve is often preferred in wind turbine's performance modeling, because it directly gives the generated power, independent of other wind turbine parameters. The electrical output power from a wind turbine is directly provided by the power curve at a given wind turbine speed. In this model, a power curve of the wind turbine is presumed to match its typical curve as shown in Figure 2.9.

A set of characteristic equations can be developed to predict the wind turbine power output for the wind speed ranges. The power generated from a wind turbine is assumed to be linearly increase with an increase in wind speed from cut-in to rated speed, then remain constant at the rated until cut-off speed. Models based on the concept of the presumed power curve employed in literature are categorized into (a) linear power curve and (b) cubic law.

2.6.1.1 Model based on linear power curve

The following equations characterized model based on linear power curve of the wind turbine (Thapar et al., 2011);

$$p_e = \begin{cases} 0 & (for\ v < v_c\ ) \\ P_{er}.\left(\dfrac{v - v_c}{v_r - v_c}\right) & (for\ v_c \leq\ v \leq v_r) \\ P_{er} & \left(for\ v_r \leq\ v \leq v_f\right) \\ 0 & \left(for\ \ v > v_f\right) \end{cases} \quad (2.7)$$

where p_e is the electrical power available from the wind turbine, P_{er} is the rated power of the turbine, while v_c , v_r and v_f are the cut-in speed, rated speed and cut off speed of the wind turbine respectively.

In some case studies (Borowy & Salameh, 1996; Chedid & Rahman, 1997) a similar model employing Weibull shape parameter *k* have been applied to predict wind turbine output performance as:

$$P_e = \begin{cases} 0 & (for\ v \leq v_c\ and\ v \leq v_f) \\ P_{er}.\dfrac{(v^k - v_c^k)}{(v_r^k - v_c^k)} & (for\ v_c \leq\ v \leq v_r) \\ P_{er} & \left(for\ v_r \leq\ v \leq v_f\right) \\ 0 & \left(for\ \ v > v_f\right) \end{cases} \quad (2.8)$$

2.6.1.2 Model based on cubic law

This model is mathematically represented as (Khatod, Pant, & Sharma, 2010);

$$P_e = \begin{cases} 0 & (for\ v \leq v_c\ and\ v \leq v_f) \\ av^3 - bP_{er} & (for\ v_c \leq\ v \leq v_r) \\ P_{er} & \left(for\ v_r \leq\ v \leq v_f\right) \\ 0 & \left(for\ \ v > v_f\right) \end{cases} \quad (2.9)$$

where the constants *a* and *b* are function of rated speed and cut-in speed of the wind turbine mathematically represented as:

$$a = {p_{er}}/{(v_r^3 - v_c^3)} \quad \text{and} \quad b = {v_c^3}/{(v_r^3 - v_c^3)}$$

The above models are more simplified when wind speed is higher than the rated speed of wind turbine. They have popularly been utilized in evaluation and predictions of wind energy generation for different applications (Adaramola, Paul, & Oyewola, 2014; Akdağ & Dinler, 2009; Celik, 2003).

2.7 Hybrid renewable energy system

Over the years, immense efforts have been channeled into the development of renewable energy technologies alongside energy storage devices; this encouraged their entry to the electricity market. These technologies can function as stand-alone sources or as part of hybrid systems or distributed generation (DG) connected to a microgrid/national grid. Of all these renewable alternative approaches, solar and wind energy had been given immense recognition and government support, providing an economically-viable framework for realizing better incursion of such environmentally benign sources in the energy market. Although these sources are more beneficial than the conventional means of energy generation from various points of view, the main disadvantage being the total dependency on the climatic conditions such as; variation in wind speed, and solar radiation, temperature. This has made these technologies fully unreliable to satisfy a specific load demand variation at any point when considered alone. The variability in their operation has brought about the use of energy storage systems and/or backup sources to ensure continuity of electricity supply. Even with this storage device, the system suffered the problem of high cost of energy production due to oversizing and many more problems. The desire for the reliability enhancement of these renewable energy technologies has led to their combination to form a hybrid scheme.

A renewable hybrid system is regarded as a combination of RE sources operating in a synchronized and independent manner (C. Wang, 2006). Furthermore, a survey of literature on rural electrification showed that hybrid RE systems are the most efficient

solution to supply electricity to rural areas located far from the national grid (Dihrab & Sopian, 2010; Kusakana & Vermaak, 2013). The combination of different energy sources enables improvement on the system efficiency, consistency of the energy supply and reduces the energy storage needs, compared to systems with single-source RE supply (Nandi & Ghosh, 2010b). A typical hybrid renewable energy system integrates two or more energy sources, such as wind turbine, solar photovoltaic (PV), small hydro turbine and any other conventional energy system e.g diesel generator/microturbine as the case may be. In addition, it includes power electronics device, for energy conversion and energy storage devices such as batteries, super capacitor and flywheel. The use of the hybrid system that combines different RE sources with other conventional backup sources, and energy storage devices decreases the limitation of each of the energy sources and opens markets for investments (Rajashekara, 2005).

Hybrid systems employ the best features of each of complimentary energy resources on the system. For example, with solar and wind energy resources hybrid power systems having storage banks, there is a highly reliable supply which is idea for electrical loads that needed higher reliability due to the complementary nature of these two energy resources (Zhou, Lou, Li, Lu, & Yang, 2010). Solar energy supplies electricity during sunny hours of the day, while on cold and windy days characterized by cloudiness, the wind turbine supplies power in stand-alone or grid-connected applications. This complementary advantage have made the two technology widely employed in hybrid RE power systems. Furthermore, hybrid system applications exhibit higher reliability and lower the cost of generation in the absence of the grid, leading to a rapid technological advancement. Table 2.4 present the summary of benefit of the hybrid system to the single source system.

In recent times, hybrid systems that combines conventional and RE sources are being proposed to supply power to isolated loads in order to reduce CO_2 emission in the surrounding environment and complement the inherent deficiencies of each energy source. The potential of the RE sources in a specific location and the availability of diesel fuel for the conventional source determine the type of hybrid system that will be adopted for any application at such a location. Various configurations can be employed in the design hybrid systems towards effective utilization of the available RE sources, and to serve the load demand at any instant. Any combination of renewable sources with an optional backup and /or storage device is possible. The list of various hybrid system configurations available through the literature is presented in Table 2.5.

Table 2. 4: Benefits of hybrid system to single source system

Metrics	**Single source (Renewable Energy)**	**Single source (Conventional)**	**Hybrid system**
Dependency on natural resources	Very high	Independent	Partial
Load demand	Most appropriate for loads having low kWh/day	Most appropriate for consistently high kWh/day loads	Most appropriate to all kinds of loads
Capital cost/kW	High	Low	Moderate
O & M cost	Low	High	Moderate
Fuel requirements	No fuel	Relative to electrical loads	Less fuel requirement due complementary nature.
Frequency of maintenance and repair	Less frequent	Frequent	low
Reliability	Dependent on the availability of natural resources	Dependent on availability of fuel, and repair experts	Highly reliable due to complementary nature of the resources
Environmental impact	Low	high	moderate

It can be observed from Table 2.5, that solar PV and wind energy played a vital role in hybrid renewable system configuration; this is because they are highly abundant and easily accessible. However, despite the rapid growth in their implementation, there are

series of challenges faced by the system, among which are a problem of integration due to variable nature of the energy sources. In addition, the system behaviour is usually affected by switching on and off the different connected components, which can cause the system instability(X. Li, Song, & Han, 2007). Therefore, in order to select the most appropriate configuration for a specific site, a feasibility study based on meteorological data and life cycle-cost analysis is required. In addition, technical and socio-cultural considerations have to be taking while making the decision for implementation. All these issues need to be addressed to maintain reliable electricity delivery and supply.

Table 2. 5: Summary of hybrid system configurations

s/n	Hybrid system configuration	Reference
1	Wind/battery system	(Elhadidy & Shaahid, 1999; Roy, Kedare, & Bandyopadhyay, 2010; Singh & Chandra, 2009).
2	PV/battery system	(Lu & Shahidehpour, 2005; Nandi & Ghosh, 2010a; W. Wang et al., 2013)
3	PV/Microturbine	(Kalantar & Mousavi G, 2010)
4	Wind/fuel cell system	(Iqbal, 2003; Onar, Uzunoglu, & Alam, 2006)
5	Wind /Microturbine system	(Colson, Wang, Nehrir, Guda, & Li, 2007; Saha, Chowdhury, Chowdhury, & Gaunt, 2009)
6	Microturbine/Fuel cell system	(Entchev, 2004; Massardo, McDonald, & Korakianitis, 2002)
7	Wind/Diesel/Battery System	(Xu Liu et al., 2008)
8	PV/Wind/Battery system	(Nandi & Ghosh, 2010a; Zhou et al., 2010)
9	PV/wind/diesel system	(Pan, Gao, & Muljadi, 2009; Rehman, Mahbub Alam, Meyer, & Al-Hadhrami, 2012; Shaahid et al., 2010)
10	PV/Diesel/Battery	(Rehman & Al-Hadhrami, 2010; Shaahid & El-Amin, 2009)
11	PV/Fuel cell/electrolyzer/battery system	(Elbaset, 2011; Vosen & Keller, 1999)
12	PV/Fuel cell/Super Capacitor system	(Payman et al., 2009; C. Wang, 2006)

Optimal sizing of the components can reduce the cost of hybrid systems. Therefore, one of the objectives of this study is to optimally size the hybrid system comprising PV, wind, diesel and battery using cost-effective optimization algorithm. The PV and wind were chosen due to enormous potential solar and wind energy in the selected sites. The battery serves as energy storage for compensating fast transient and ripple power, while the diesel generator is employed to provide reliable backup.

2.7.1 Hybrid systems topologies

Since all renewable energy technologies (RETs) have different operating characteristics, it is important to select a standard means to integrate them into a hybrid system. There are various schemes to integrate different RE power sources to form a hybrid system. These schemes can be classified into three general categories; (i) dc-coupled, (ii) ac-coupled, and (iii) hybrid ac/dc-coupled (Nehrir et al., 2011). However, the optimal choice between ac and dc coupling depends on the type of generation, type of energy storage and eventually the load requirement. These methods are briefly discussed in the following sub-sections:

2.7.1.1 DC-Coupled

In a dc-coupled scheme shown in Figure 2.10, different RE sources are connected to the DC bus through an appropriate power electronic converters. DC sources could be linked directly to the DC bus or via a DC/DC boost converter if desired. DC loads could also be connected to the DC bus directly or through a boost converter in order to achieve required voltage for the DC loads. The system can supply power to AC loads or be interfaced to a utility grid through a converter, designed to allow bidirectional flow of power. The DC-coupling is simple, and no synchronization is required to integrate the energy sources.

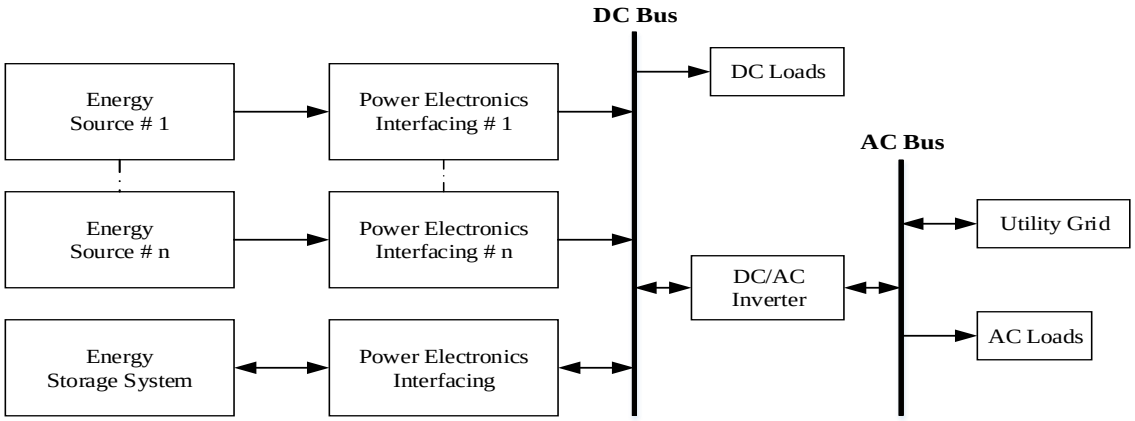

Figure 2. 10: Hybrid energy system integration: DC coupling

2.7.1.2 AC-Coupled

The schematic of a power frequency AC-coupled system is shown in Figure 2.11. In this configuration, various energy sources are integrated through their respective power electronic interfacing circuits to a power frequency ac bus. Coupling inductors could be used between the power electronic circuits and the AC bus to achieve desired power flow management (Cha & Enjeti, 2003). In this configuration, DC power can be obtained via AC/DC converter.

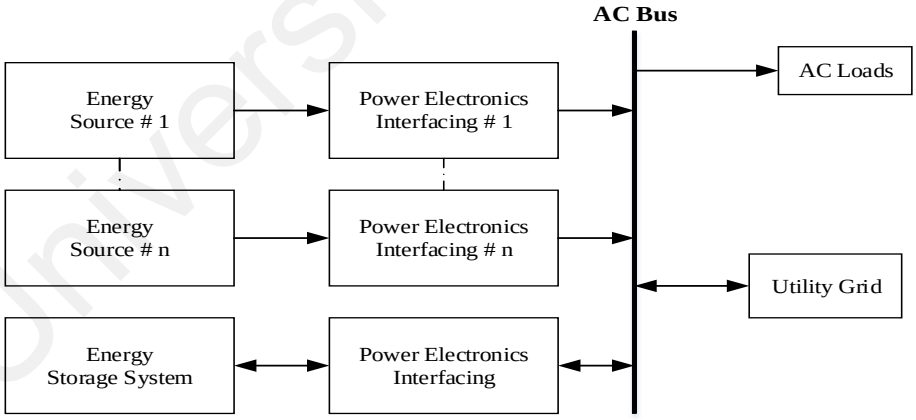

Figure 2. 11: Hybrid energy system integration: AC coupling

2.7.1.3 Hybrid AC-DC Coupled

In this configuration, different distributed generators (DG) can be linked to the DC or AC bus via appropriate converter. Figure 2.12 shows a hybrid-coupled system, where DGs are connected across the DC bus and/or AC bus. In this scheme, several energy

sources can be connected directly without extra interfacing circuits. Therefore, the system tends to offer higher energy efficiency and at the same time cost-effective. Conversely, system control and energy management in this configuration are more complex than in DC and AC-coupled systems. Table 2.6 summarizes the advantages and disadvantages of each coupling scheme.

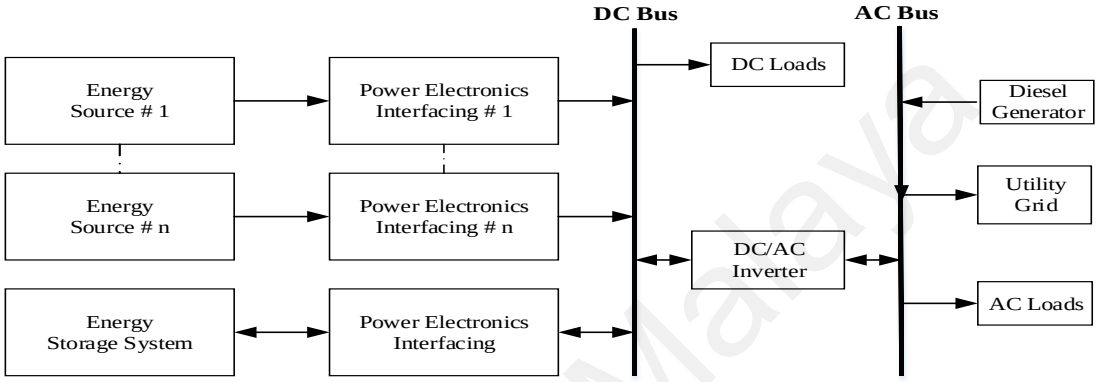

Figure 2. 12: Hybrid-coupled hybrid energy system

Table 2. 6: Summary of HRES coupling scheme

Configuration	Advantage	Disadvantage
DC Coupled (Farret, 2006)	• Simple and require no synchronization. • Has less transmission losses, hence applicable to long distance transmission; • Single-wired approach	• Problem of voltage compatibility • Prevalence of resting of the DC electrodes. • Failure of DC/AC inverter lead to entire system failure, hence no supply to the load
AC Coupled (Nehrir et al., 2011)	• Highly reliable: ease of isolation of any failed energy sources • Grid-connection friendly • Modularity of structure • Support multi-voltage and multi-terminal matching	• Require synchronism for ac bus matching to connected generators • Require power factor and THD correction • Unsuitable for long distance transmission
Hybrid AC-DC coupled (Chauhan & Saini, 2014)	• Highly efficient and low system cost • Low conversion losses	• Complex system control and energy management

2.8 Hybrid system sizing and optimization

Optimum sizing of the constituent generating units and other associating component in the hybrid energy system is vital for efficient and economic utilization of RE resources. This will help guarantee lowest-cost investments with full-scale utilization of renewable energy resources while reliably meeting the load requirement and maintaining cleaner environment. Optimal resource matching in a hybrid system is essential in realizing a cost-effective and reliable system (Bilal, Sambou, Ndiaye, Kébé, & Ndongo, 2010). However, the two issues; cost-effectiveness and reliability looks contradictory. Therefore, a trade-off between the two is desirable during the planning stage of any hybrid renewable energy project, since oversizing the system may lead to increasing overall system cost, while under sizing may lead to an unreliable system.

2.8.1 Criteria for optimum sizing and cost optimization

In order to select best combination of hybrid system component that meets the load demand, the criteria is generally categorized into two, namely; (i) power supply reliability and (ii) system economic.

2.8.1.1 Power supply reliability

Due to the variability in the characteristic of renewable energy resources, usually caused by changes in weather conditions and often affect the energy production, power supply reliability assessment must be carried out at the planning stage of the project. The following are major criteria usually employed in power supply reliability assessments;

(a) *Loss of Power Supply Probability (LPSP):* This is probability that energy deficiency will result whenever hybrid renewable energy resources (HRES) are unable to meet the load demand. It is mathematically represented as (Bahramara, Moghaddam, & Haghifam, 2016);

$$LPSP = \frac{\sum_{t=1}^{T} LPS(t)}{\sum_{t=1}^{T} P_L\,(t)\Delta t} \tag{2.10}$$

where, $LPS(t)$ is loss of power supply at hour t, $P_L(t)$, is the load demand at hour t. In a PV/wind/diesel/battery hybrid system, $LPS(t)$ at any hour t can be calculated as;

$$LSP(t) = \left[P_L(t) - \left(P_{PV}(t) + P_{WT}(t) + P_{DG}(t) + P_{batt\_dch}(t)\right)\right] \tag{2.11}$$

where, $P_{PV}(t), P_{WT}(t)$, $P_{DG}(t)$, and $P_{batt\_dch}(t)$ are PV power output, wind power output, diesel generator power output and battery discharge capacity respectively.

(*b) Expected energy not supplied (EENS):* this is the expected energy not supplied to the load due to load exceeding the power generation. It is usually measured in kWh, and can be computed as (Bilal et al., 2010);

$$EENS = \sum_{k=1}^{8760} L \times D \tag{2.12}$$

where, L is annual average demand (kW) and D, the duration during which the load could not be met (h).

(c) Level of Autonomy (LA): This represents the fraction of time under which the load is not met. That is duration of unmet load (H_{LOL}) and the total number of hours of system operation (H_{Total}). Mathematically given as (Celik, 2003);

$$LA = \frac{H_{LOL}}{H_{Total}} \tag{2.13}$$

2.8.1.2 System economic

The following are major economic criteria for evaluating the suitability of a hybrid renewable system;

(a) Annualized cost of the system (ACS): Annualized cost is sum of the annualized capital cost, replacement cost and maintenance cost of the constituents' hybrid system components. Mathematically represented as (Bilal et al., 2010);

$$C_{ann} = C_{ann,cap.} + C_{ann,rep.} + C_{ann,O\&M} \tag{2.14}$$

(b) Net present cost (NPC): Also known as life-cycle cost. It is total present value of a time-series cash flow; that is, the investment cost and the discounted present value of all future cost during the project lifetime. This comprised capital cost, replacement cost over the project life as well as operation and maintenance cost of all system components. It is mathematically represented as (Kaldellis, Zafirakis, Kaldelli, & Kavadias, 2009);

$$NPC_{Tot} = \frac{C_{ann,Tot}}{CRF} \tag{2.15}$$

where, CRF is capital recovery factor, and can be evaluated in terms of interest rate (i) and project lifetime (n) as;

$$CFR = \frac{i(1+i)^n}{(1+i)^n - 1} \tag{2.16}$$

(c) Levelised cost of energy (LCOE): It is an economic analysis tool for assessing the cost of energy production in the hybrid system. This includes both recurring and non-recurring cost throughout the project lifetime. It is defined as a ratio of total annualized cost of the system ($C_{ann,Tot}$) to the annual electricity produced (E_{Tot}). Mathematically represented as (Bilal et al., 2010);

$$COE = \frac{NPC_{Tot}}{P_L\,(kW)/(\frac{8760h}{yr})} \times CRF \tag{2.17}$$

From the above formulation, it is vivid that optimum sizing of hybrid system components is vital for both technical and economic reasons. In literatures, several

researchers have optimized NPC, ACS and LCOE under various system constraints, including; numbers of solar panel, wind turbine, diesel generator, battery state of charge, renewable energy fraction, system reliability and so on. While the decision variables considered include; numbers of wind turbine, numbers of PV panel, numbers of batteries, tilt angle of PV panel, wind turbine hub height and many more.

2.8.2 Optimization and sizing methodologies

In hybrid system sizing, problem formulation is done to determine the optimum system configuration as well as type and sizes of the constituent system's components that meet the load demand at minimum cost. Various studies on optimization approaches to economic feasibility as well as modeling of hybrid system components, including PV, wind, battery and diesel generator used in providing electricity for different applications can be found in literature. This approaches includes; probabilistic (Borowy & Salameh, 1996), graphical construction (Karaki, Chedid, & Ramadan, 1999), deterministic methods (El-Hefnawi, 1998), iterative methods (Kaldellis, Simotas, Zafirakis, & Kondili, 2009), linear programing (Chedid & Rahman, 1997), artificial intelligence methods(Sinha & Chandel, 2015) as well as commercial available software (Sinha & Chandel, 2014) as shown Figure 2.13.

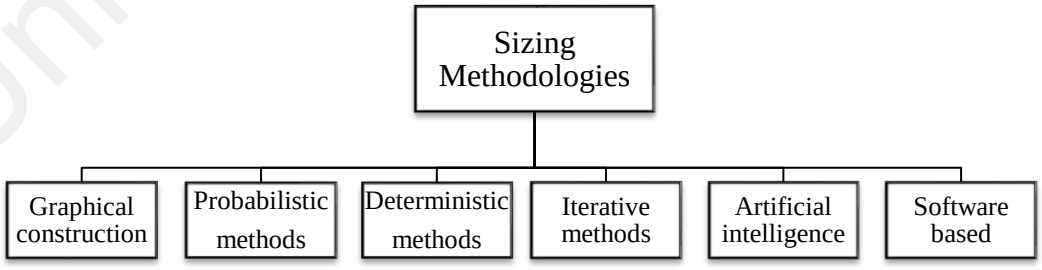

Figure 2. 13: Optimal sizing methodologies in hybrid renewable energy system

Most commonly considered objectives for optimal sizing of a hybrid system are economic and reliability of the system. The choice among these approaches is dependent

on its intended application; such as components sizing, operating strategy, type of hybrid system and number of parameter to optimize. Table 2.7 presents the summary of various optimal sizing approaches available in literature.

Table 2. 7: Summary of optimization techniques in hybrid system sizing

Optimization Techniques	**Optimized variables**	**Reference**	**Remarks**
Graphical construction approach	PV, wind, battery	(Borowy & Salameh, 1996; Markvart, Fragaki, & Ross, 2006)	Based on long term solar radiation and wind speed data
Probabilistic approach	PV,wind, battery	(Karaki et al., 1999; Tina, Gagliano, & Raiti, 2006)	Based on statistical approach of data collection
Deterministic approach	PV, wind, diesel battery	(Bilal et al., 2010; El-Hefnawi, 1998; Mahmoud & Ibrik, 2006)	Based on simple equations for determining specific values using a constant parameters
Iterative approach • Hill climbing • Dynamic Programming • Linear Programming	PV, wind, battery	(Kellogg, Nehrir, Venkataramanan, & Gerez, 1996; J. Li, Wei, & Xiang, 2012) (De & Musgrove, 1988) (Chedid & Rahman, 1997; Daud & Ismail, 2012; Kaldellis, 2004)	Based on loss of power supply probability (LPSP) to find possible combination of solar-wind combination
Artificial Intelligence • Artificial Neural Network	Hybrid PV, diesel system with/without battery	(Mellit, Menghanem, & Bendekhis, 2005)	Based on evolution techniques. Has ability to learn from previous scenarios, and once trained, can search for optimum sizing/configurations..
Software based • HOMER • Hybrid2 • HOGA • RETScreen	PV, wind, diesel battery, fuel cell, hydropower, biomass etc.	(Connolly, Lund, Mathiesen, & Leahy, 2010; Sinha & Chandel, 2014)	Selects the optimum system configuration based on the comparison of performance and energy production cost of various system configuration

In recent times, several commercial software tools have proven their efficiencies in optimizing hybrid renewable energy systems for techno-economic feasibility analysis, prominent among is Hybrid Optimization Model for Electric Renewables (HOMER), a software developed by National Renewable Energy Laboratory (NREL), United States (NREL, 2009).

In this study, the techno-economic and environmental analyses of the HRES are evaluated with HOMER by comparing the hybrid systems with those of single source systems (i.e. PV-only and diesel-only). This analyses, and results will be useful in planning and decision-making purposes on the proposed renewable power supplies in the selected rural healthcare facilities. Detailed description of the HOMER software employed in this study is presented in the next section.

2.8.2.1 Hybrid Optimization Model for Electric Renewables (HOMER)

HOMER is a computer model that can evaluate various design options for both standalone and grid-connected energy systems. HOMER performs three main tasks; simulation, optimization, and sensitivity analysis as represented (Lambert, Gilman, & Lilienthal, 2006). Fig. 2.14 shows the conceptual relationship between the three tasks.

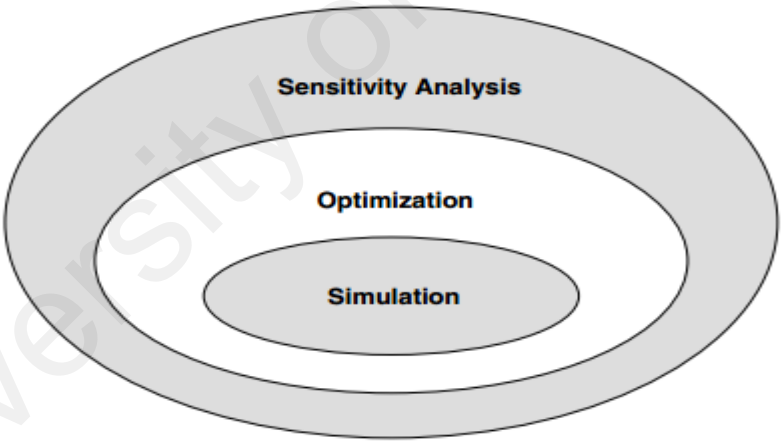

Figure 2. 14: HOMER's functions

In the simulation process, HOMER modeled the performance of each component of the proposed hybrid system on an hourly basis to ensure best possible matching between the load and the supply as well as determination of techno-economic feasibility of each system configuration. In the optimization process, the software simulate various system configurations to determine the configurations that satisfy the technical constraints and meet the load demand at minima life-cycle cost. HOMER does this by creating a list of feasible system sorted according to the least NPC. In the sensitivity analysis part,

HOMER performs multiple optimization with different input variable range, to determine the effect of changes in the input parameters on the selected system configuration.

HOMER simulates various system configurations over a preselect range of values and creates a list of a feasible system according to the specified components in the hybrid system. HOMER simulates the system operation by making energy balance calculations on an hourly basis for the entire period of the year under consideration. The flow of energy from one component to another in the hybrid system is calculated according to the difference between the available energy resources and the load demand. For systems with fuel-powered generators and/or batteries, HOMER decides for each hour, how to operate the generator and whether to charge or discharge the batteries. The software selects the optimum system configuration based on the comparison of performance and energy production cost of various system configurations. HOMER gives room for utilization of various energy resources such as; photovoltaic (PV), wind turbines, hydro turbines, diesel and fuel cell. The software requires initial inputs such as; energy resource's data, (solar radiation, wind speed, temperature and stream flow), economic and technical constraints, energy storage and system control strategies as shown in Figure 2.15.

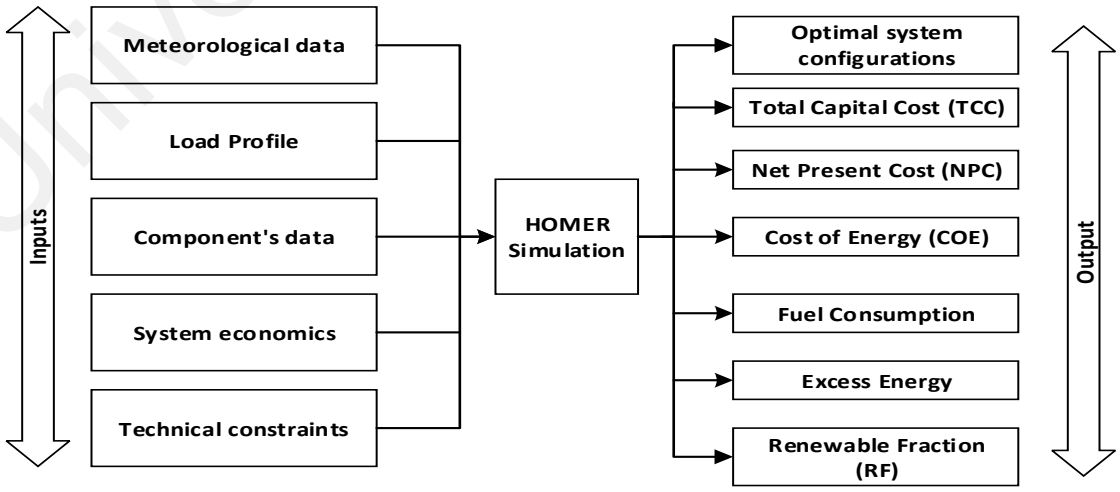

Figure 2. 15: HOMER architecture

However, in a situation where hourly measured data are not available as input, HOMER has the capability to generate synthetic hourly solar data from monthly averages. The models employed for the synthetic generation of hourly data from monthly averages for solar radiation and wind speed are discussed as follows:

(a) ***Generating synthetic hourly solar radiation data from monthly averages***

HOMER synthesizes hourly solar radiation data based on algorithm proposed by V.A. Graham (Graham & Hollands, 1990). In this algorithm, monthly mean clearness index ($\overline{K}_T$) defined in terms of monthly mean global solar radiation incident on the horizontal surface ($\overline{H}$) and monthly mean extraterrestrial radiation ($\overline{H}_o$) is represented by (Duffie & Beckman, 2013);

$$\overline{K}_T = \frac{\overline{H}}{\overline{H}_o} \tag{2.18}$$

For each month, there exist an ordered set of hourly values of clearness index values (k_T). Based on this set of hourly clearness index values, a corresponding set of ordered extraterrestrial radiation ($\overline{H}_o$) can be found, hence the hourly values of global solar radiation incident on the horizontal surface. For a given location and a date in a month, every set k_T has a unique value for $\overline{K}_T$.

The main purpose of this model is to obtain a mechanism for performing the inverse operation for finding the set $\{k_T\}$ from the knowledge of $\overline{K}_T$, and this can be perform based on the concept of stochastic disaggregation(Graham & Hollands, 1990). In doing this, a method of calculating the set $\{k_T\}$ considering both the clear and cloudy skies months is needed. For cloudy sky, a random fluctuation in k_T need to be introduced. Therefore, the model for variation in k_T events consists of two components. i.e ; a mean component of k_T and a random component given as;

$$k_T = k_{Tm} + \alpha \tag{2.19}$$

The mean component k_{Tm} represent the clearness index when the presence of radiation attenuators are evenly distributed over the day of the month, while the random component α incorporates the effect of unpredictable disturbance in the radiation attenuators owning to varying cloud cover. The disaggregation require identification and characterization of the set $\{k_{Tm}\}$ and $\{\ \alpha\ \}$ for all possible value of $\overline{K}_T$. The mean component k_{tm}, could be expressed as :

$$k_{Tm}(t) = \lambda + \epsilon exp(km) \tag{2.20}$$

where the parameters ϵ and k are the unique functions of clearness index $(\overline{K}_T)$ for the month in question, which can be obtained from the following relations;

$$\lambda(\overline{K}_T) = \overline{K}_T - 1.167K_T^3(1 - \overline{K}_T) \tag{2.21}$$

$$\epsilon(\overline{K}_T) = 0.979(1 - \overline{K}_T) \tag{2.22}$$

$$k(\overline{K}_T) = 1.141(1 - \overline{K}_T)/\overline{K}_T \tag{2.23}$$

Therefore, in order to generate synthetic hourly solar data in HOMER, it is expected to enter either the average clearness index or the average daily radiation for each month of the year, then HOMER applies equations (2.18 -2.23) to estimate the values of k_T for a given value of $\overline{K}_T$. The algorithm is found to produce realistic hourly data, and it is easy to use because it requires only the latitude and the twelve monthly average values. The algorithm creates synthetic solar data with certain statistical properties that reflect global averages. Literature have shown that synthetic solar data produce virtually the same simulation results as real data, however, little differences in key performance output variables like annual PV array production, fuel consumption, generator run time, and battery throughput are observed (typically less than 3%). Differences in key economic output variables like total net present cost and levelized cost of energy are also typically less than 2% (Bahramara et al., 2016; NREL, 2015).

(b) ***Generating synthetic wind data from monthly averages***

HOMER's synthetic hourly wind speed data synthesis algorithm requires users to enter a few parameters, from which it generates statistically reasonable time series data. The algorithm produces data that mimic the characteristics of real wind speed data, including strong and sustained gusts, long lulls between windy periods, and seasonal and diurnal patterns. HOMER uses the monthly average wind speeds, plus the four parameters in Table 2.8 to synthesize wind data for simulation (NREL, 2015).

Table 2. 8: Wind Data Parameters

S/N	Parameter	Description	Default
1	Weibull (*k)*	Reflect the breadth of the distribution of wind speed over a year	2.0
2	1-hour autocorrelation factor (r_1)	Reflects how strongly the wind speed in one time step tends to depend on the wind speed in the previous time step	0.85
3	Diurnal pattern strength (δ)	Reflects how strongly the wind speed depends on the time of the day	0.25
4	Hour of peak wind speed (φ)	The average hour of the day that tends to be windiest	15

HOMER followed the following processes in synthesizing one-year of time series wind speed data (NREL, 2015):

1. Generate a sequence of autocorrelated numbers, one for each time step of the year, using the first-order autoregressive model:

$$Z_t = a.Z_{t-1} + f(t) \tag{2.20}$$

where Z_t and Z_{t-1} are the autocorrelated value in time step *i*, and *i-1* respectively. While a is the autoregressive parameter and *f(t)* is a white noise function that return a random number drawn from normal distribution with mean 0 and standard deviation 1.

In HOMER, the autoregressive parameter (a) is set to be equal to one-time step autocorrelation coefficient (r_1), where $r_1 = exp[In(r_k/k)]$, $r_k = r_1^k$ is the one-hour autocorrelation factor, and k is the number of time steps that fit in one hour $k = 60/t$.

2. Create a full year data by piecing the desired average diurnal wind speed profile repeated every day. Since the average wind speed varied monthly, the average diurnal wind speed profile scales to a different values each month, but with repeated diurnal pattern for each month.
3. Perform a probability transformation on the sequence of numbers generated in step 2, to check its conformance with the normal distribution sequence generated in step 1.
4. Add the generated sequences in step 1 and 3, check if resulting sequences conforms to a normal distribution, and exhibit the desired degree of autocorrelation.
5. Finally, HOMER performs a probability transformation on the sequence generated in step 4 to ensure it conforms to the desired Weibull distribution.

In order to demonstrate the accuracy of this algorithm, the results of the synthetic wind data generation using the algorithm, is compared with available hourly measured wind speed data for a particular location in US as shown in Figure 2.16 (NREL, 2015). The first DMAP shows the measured wind speed data for the site, while the second shows the synthetic wind speed data that HOMER generated from the monthly average wind speeds and the four wind data parameters measured from the real data. The results obtained as seen in the figures justified that HOMER is capable of synthesizing one-year time series wind speed data from monthly averages.

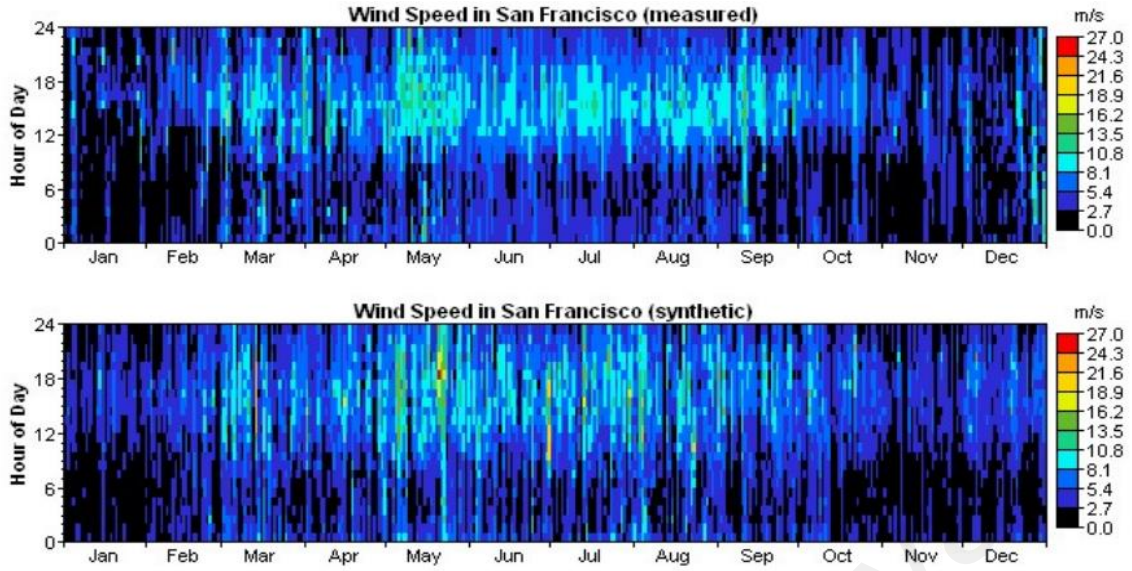

Figure 2.16: Comparison of HOMER's synthetic hourly wind speed data with measure data

2.9 Chapter summary

This chapter first addressed the energy status in Nigeria with the potentiality of renewable energy in meeting the energy demand of the country. In particular, a review of previous studies on wind and solar application in Nigeria was presented, with discovery that no study has been channeled to its application in rural healthcare facilities in the country considering the importance of reliable electric power supply in rural healthcare development.

Also presented is the review of solar energy conversion system, including previous approaches to solar radiation prediction as well as PV array performance prediction. Followed by, the reviews of wind energy conversion system with various wind turbine performance and behaviour prediction models. The review on solar and wind power density prediction shows the competency of soft computing methodologies in accurately estimating solar radiation and wind power density based on the available metrological data. The basic notion behind soft computing methodologies is to collect input/output

data pairs so that the proposed network can learn from these data. In this study, soft-computing methodology named; adaptive neuro-fuzzy inference system (ANFIS), that merges the learning power of ANNs with the knowledge representation of fuzzy logic has been proposed to predict solar radiation and wind power density in the selected sites, and the results will be compared with empirical models. Each of the reviewed approaches in PV performance predictions models has its own specific features, for example; none of earlier studies gives value of PV model parameters such as ideality factor that globally covers the solar radiation levels. Therefore, in this thesis, a simple iterative methodology to determine ideality factor for diffident radiation levels in the selected sites is developed using MATLAB. While on wind turbine performance prediction, various available wind turbines with different power output performance curve, have been reviewed with the aim to select best one according to wind speed regime at the considered sites.

The need for hybrid system configurations where single-sources renewable energy is unsuitable owing to variability of resource's output, high system cost and low reliability are also enumerated. A review of hybrid renewable energy system topologies conducted with the conclusion that the optimal choice between ac and dc coupling depends on the type of generation, type of energy storage (if any) and eventually the load requirement. However, hybrid AC-DC coupling is considered the best configuration, since it offers lower cost and higher efficiency as compared with DC and AC coupled configuration. Finally, reviews of optimum sizing methodologies in a hybrid system for purpose of efficient and economic utilization of renewable energy resources were conducted. This has shown HOMER (software-based model) as preferred optimization tool. Hence, HOMER has been considered for optimal sizing, techno-economic and environmental analyses of the proposed hybrid renewable energy system in this study.

CHAPTER 3: METHODOLOGY

3.1 Introduction

In this thesis, a complete standalone PV/Wind/diesel hybrid renewable energy system with battery energy storage for rural healthcare applications where the grid extension is not feasible is proposed. Therefore, this chapter presents the methodology employed in the thesis. Figure 3.1 summarize the step-to-step of the methodology.

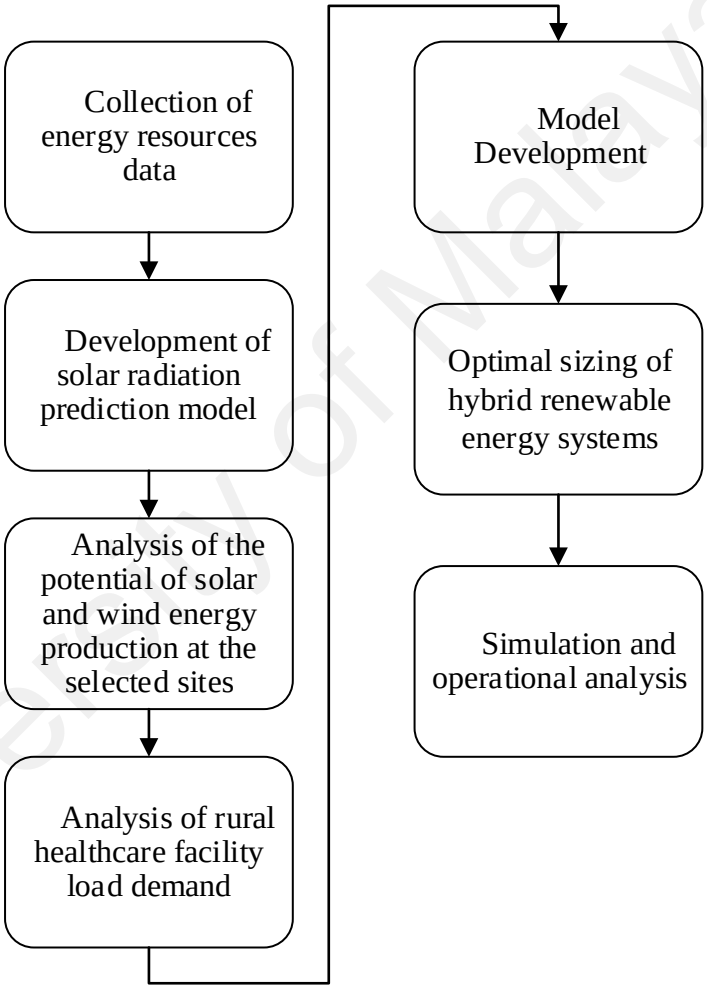

Figure 3. 1: Methodology flowchart

3.2 Data collection

The availability of RE resources at any particular place varies largely from one location to another. This is important for the development of the hybrid renewable energy system. The potentials of RES such as, solar and wind are influenced by the

geographical location and climatic conditions. Therefore, the meteorological data, including; wind speed, solar radiation, sunshine hours and ambient air temperature used for the analysis on the potential of wind and solar energy resources in this study were obtained from the Nigerian Metrological Agency (NIMET, 2014). These data were measured at respective meteorological stations located at each site with geographic information presented in Table 3.1. The sites of the hypothetical rural health clinic considered in this study are selected to reflect different geographic and climatic conditions in Nigeria. The selected locations are from each of the six climatic zones across the country which is; Iseyin (South-West), Sokoto (North-West), Maiduguri (North-East), Jos (North-Central), Enugu (South-East) and Port-Harcourt (South-South) as shown in Figure 3.2.

Table 3. 1: Geographic information of the selected locations

Location	Zone	Latitude (ºN)	Longitude (ºE)	Altitude (meters)	Climate type
Iseyin	Southwest	7.96	3.78	330	Tropical
Sokoto	Northwest	12.28	4.13	220	Tropical dry
Maiduguri	Northeast	11.83	13.15	353.8	Hot semi-arid
Jos	North central	9.92	8.9	1217	Tropical
Enugu	Southeast	6.45	7.5	247	Humid
Port Harcourt	Southsouth	4.78	7.0	465	Equatorial

According to the agency (NIMET, 2014), the wind speed data ranging between 28 and 39 years were daily captured at 10m height and 3-hour interval by a cup-generator anemometer at all the selected locations, while measured global solar radiation data on horizontal plane ranging between 18 and 31 years, were recorded with Gunn-Bellani radiometer. This instrument produces a time-oriented parameter of solar radiation falling on a black body by measuring the volume of a liquid distilled in the calibrated tube (Ajayi et al., 2014).

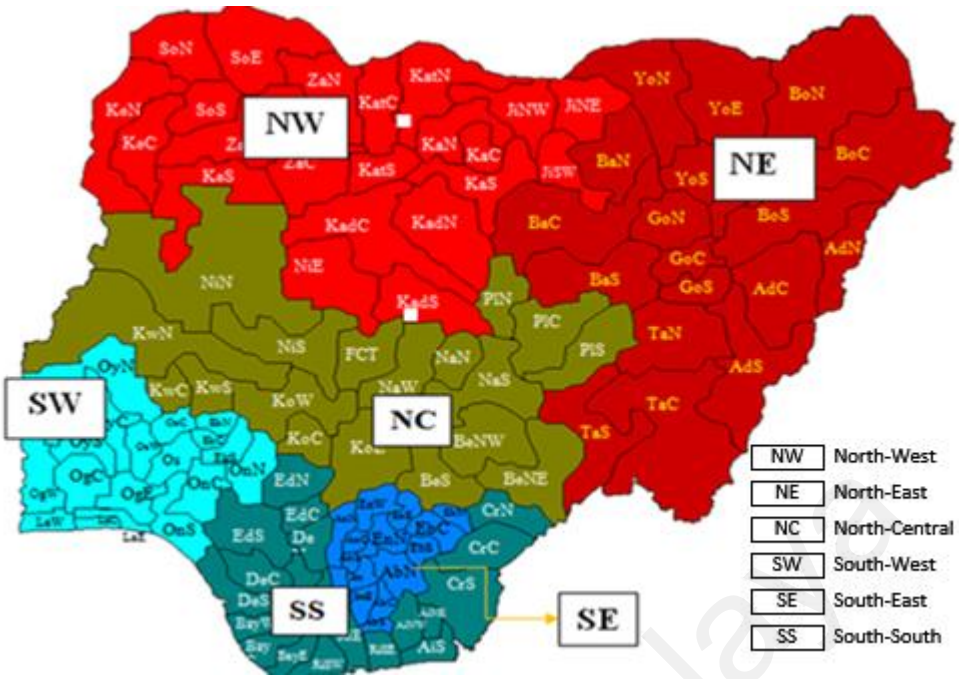

Figure 3. 2: Map of Nigeria representing the six-selected locations

The solar radiation measured in millimeters is converted into MJ/m2/day by applying a conversion factor of 1.1364 as proposed by (A. Sambo, 1986). A Campbell-Stokes recorder was used in measuring sunshine duration. Additionally, maximum and minimum temperatures at the selected station were measured using minimum and maximum dry-bulb thermometers. However, in some places where the collected data are insufficient due to days or months without records, possibly due to the improper instrument calibration, a solar prediction model and algorithms have been developed with soft computing methodologies to replace for the missing data.

3.3 Solar radiation prediction

In this section, the accuracy of a soft computing techniques are investigated for predicting solar radiation based on a series of measured meteorological data including; sunshine duration, minimum temperature and maximum temperature obtained from meteorological stations located in the considered sites. The soft computing techniques investigated are; artificial neural network (ANN), genetic programming (GP) and adaptive neuro-fuzzy inference system (ANFIS). The process was developed with these

three methods and comparisons were made. The ANFIS and ANN network has three neurons in the input layer and one neuron in the output layer. The inputs are monthly mean maximum temperature(T_{max}), monthly mean minimum temperature (T_{min}), and monthly mean sunshine duration ($\bar{n}$). These input parameters were selected due to the following reasons: they are widely available in most locations; they strongly correlate with global solar radiation, and the fact that their measurement is quite simple and the cost of equipment required is low. The motivation behind this investigation was the significance of reliable solar radiation data in the assessment and prediction of solar system energy output. The choice of the ANFIS method was made for the following reasons: it is simple, reliable, has efficient computational capability, it can be easily adapted to optimization and other adaptive techniques, and its adaptability in handling complex parameters. While the other methods were choose for comparison purpose only.

3.3.1 Correlation between meteorological data

Different regression correlations that relate the clearness index ratio ($\overline{K}_T = \overline{H}/\overline{H}_o$) to the relative sunshine duration ($\bar{n}/\bar{N}$) and air temperature ($\overline{T}_{max}, \overline{T}_{min}$) is found in (Besharat et al., 2013), where $\overline{K}_T$ is the ratio of monthly mean daily solar radiation on the horizontal surface ($\overline{H}$) to the monthly mean daily extraterrestrial solar radiation ($\overline{H}_o$); ($\bar{n}/\overline{N}$) is the ratio of monthly mean sunshine hours ($\bar{n}$) to monthly daylight hours ($\bar{N}$). The mathematical expressions for $\overline{H}_o$ and $\bar{N}$ are as follows (Allen, Pereira, Raes, & Smith, 1998):

$$\overline{H}_0 = \frac{24}{\pi} I_{sc}(w_s sin\varphi sin\delta + cos\varphi cos\delta sinw_s) d_r \tag{3.1}$$

$$\bar{N} = \frac{2}{15} w_s \tag{3.2}$$

where

$$\delta = 23.4\sin\left\{\frac{360(284+d)}{365}\right\} \tag{3.3}$$

$$w_s = \cos^{-1}(-\tan\varphi\tan\delta) \tag{3.4}$$

$$d_r = \left(1 + 0.033cos\frac{360d}{365}\right) \tag{3.5}$$

I_{sc} is the solar constant (4.921 MJ/m^2/day), φ is the latitude of the site under consideration, d_r is the inverse relative distance of the sun to earth, δ is the solar declination, w_s is the hour angle and d is the day number from 1 (January 1st) to 365 or 366 (December 31st).

Extraterrestrial radiation (H_0), relative sunshine duration ($\bar{n}/\overline{N}$) and clear-sky radiation ($\overline{H}_{so}$) serve as indicators for data quality control. H_{so} is the fraction of extraterrestrial radiation falling on the earth's surface on clear-sky days ($\bar{n} = \overline{N}$), expressed as (Allen et al., 1998);

$$\overline{H}_{so} = (0.75 + 2 \times 10^{-5}z)H_0 \tag{3.6}$$

where z is the site altitude in meters as contained in Table 3.1

Since temperature-based models is considered useful in situations where sunshine duration data is limited, therefore, Hargreaves-Samani model (Hargreaves & Samani, 1982), which gives preference to ambient temperature is also considered. This is expressed as;

$$\overline{H} = a\Delta T^{o.5}\overline{H}_o \tag{3.7}$$

where ΔT is the difference between monthly mean maximum ($\overline{T}_{max}$) and minimum temperature ($\overline{T}_{min}$) in ^{o}C, and a is an empirical value that varies according with locations.

3.3.2 Artificial neural networks (ANN) for solar radiation prediction

Artificial neural network (ANN) is a mathematical model that performs a computational simulation of the behavior of neuron in the human brain by replicating the brain's pattern to produce results based on the learning of a set of training data (Izgi, Öztopal, Yerli, Kaymak, & Şahin, 2012). The multilayer feed-forward network with a back-propagation learning algorithm is one of the most popular neural network model. Naturally, a neural network comprises of three layers: (1) an input layer; (2) an output layer; and (3) an intermediate or hidden layer (Schalkoff, 1997). The input vectors are $\in R^n$ and $D = (X_1, X_2, \dots, X_n)^T$; the outputs of q neurons in the hidden layer are $Z = (Z_1, Z_2, \dots, Z_n)^T$; and the outputs of the output layer are $Y \in R^m$, $Y = (Y_1, Y_2, \dots, Y_n)^T$. Assuming that the weight and the threshold between the input layer and the hidden layer are w_{ij} and y_j respectively, and that the weight and the threshold between the hidden layer and output layer are w_{jk} and y_k respectively, the outputs of each neuron in a hidden layer and output layer are (Behrang, Assareh, Ghanbarzadeh, & Noghrehabadi, 2010);

$$Z_j = f\left(\sum_{i=1}^{n} w_{ij} X_i - \theta_j\right) \tag{3.8}$$

$$Y_k = f\left(\sum_{j=1}^{q} w_{kj} Z_j - \theta_k\right) \tag{3.9}$$

where $f(\,)$ is a transfer function, which is the rule for mapping the neuron's summed input to its output, and by a suitable choice it is a means of introducing a non-linearity into the network design. One of the most commonly used functions is the sigmoid function, which is monotonic increasing and ranges from 0-1(Benghanem et al., 2009).

In this study, a typical feed-forward neural network consisting of three inputs, one hidden layer with seven neuron and one output layer is used to validate the performance

of the proposed model. The structure of the neural network is shown in Figure 3.3, while Table 3.2 summarizes the parameters of the model.

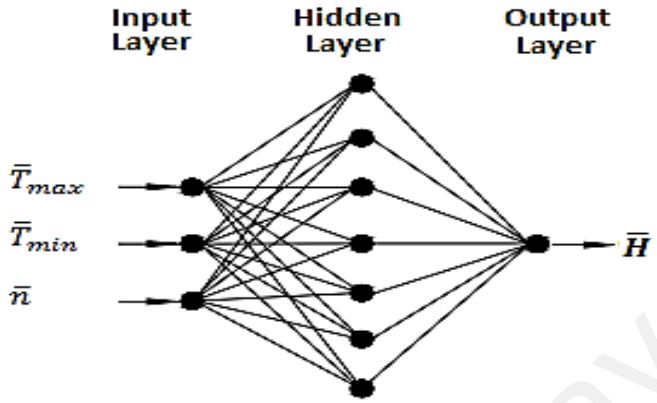

Figure 3. 3: ANN Model structure

Table 3. 2: ANN user-defined parameters

Learning rate	Momentum	Hidden node	Number of iteration	Activation function
0.2	0.1	1	1000	Continuous Log-Sigmoid function

3.3.3 Genetic programming (GP) for solar radiation prediction

Genetic programming (GP) is a systematic and domain-independent technique based on Darwinian theories of natural selection and survival to approximate the equation in symbolic form (Koza, 1992). The algorithm considers an initial population of randomly generated programs, derived from the random combination of input variables, random numbers and functions, which include arithmetic operators$(+,-,\times,\div)$, mathematical functions (sin, cos, exp, log), and logical/comparison functions, which have to be appropriately chosen based on some understanding of the process. This population of potential solutions is then subjected to an evolutionary process and the 'fitness' of the evolved programs is evaluated. Individual programs that best fit the data are selected from the initial population. The programs that represent the best fit are selected to replace part

of the information to produce better programs through 'crossover' and 'mutation', which mimics the natural world's reproduction process. Replacing the parts of the best programs with each other is called crossover, and randomly changing programs to create new programs is called mutation. The programs that do not fit the data well are discarded. This evolution process is repeated over successive generations and is driven towards finding symbolic expressions describing the data, which can be scientifically interpreted to derive knowledge about the process. The parameters of the GP used in this work are summarized in Table 3.3.

Table 3. 3: GP model parameters

Parameters	**Values**
Population size	512
Function set	$+, -, *, /, \sqrt{}, x^2, \ln(x), e^x, a^x$
Chromosomes	20-30
Head size	5-9
Number of genes	2-3
Linking functions	Addition, subtraction, arithmetic, Trigonometric, Multiplication
Fitness function error type	RMSE
Mutation rate	91.46
Inversion rate	108.53
Crossover rate	30.56
Homologues crossover rate	98.46
One-point recombination rate	0.2
Two-point recombination rate	0.2
Gene recombination rate	0.1
Gene transposition rate	0.1

3.3.4 Adaptive neuro-fuzzy inference system for solar radiation prediction

ANFIS is a hybrid intelligent scheme that merges the learning power of ANNs with the knowledge representation of fuzzy logic (Jang, 1993). This methodology has been observed to exhibit good learning and prediction capabilities when used in various engineering systems (Petković, Ćojbašić, & Lukić, 2013; Talei, Chua, & Quek, 2010; Wu, Chau, & Fan, 2010). The fuzzy inference system (FIS) is the core of ANFIS. FIS is based on expertise expressed in terms of 'IF–THEN' rules, thus it can be used to predict

the behaviour of many uncertain systems. One benefit of FIS is that it does not require knowledge of the main physical process as a pre-condition for operation. Thus, ANFIS integrates FIS with a backpropagation learning algorithm of a neural network.

The fuzzy inference system employed in this study uses three inputs, *x*, *y* and *z* and one output, f. Where *x*, *y* and *z* represents monthly mean maximum temperature (T_{max}), monthly mean minimum temperature (T_{min}), and monthly mean sunshine duration ($\bar{n}$) respectively, while *f* is the solar radiation. A first-order Sugeno fuzzy model with two fuzzy *if-then* rules is used as follows(Sugeno & Kang, 1988):

$$Rule\ 1: if\ x\ is\ A\ and\ y\ is\ C\ and\ z\ is\ E\ then\ f_1 = p_1x + q_1y + r_1z + s \tag{3.10}$$

$$Rule\ 2: if\ x\ is\ B\ and\ y\ is\ D\ and\ z\ is\ F\ then\ f_2 = p_2x + q_2y + r_2z + s \tag{3.11}$$

The ANFIS model with three inputs (x, y and z) consists of five layers is presented in Figure 3.4. In this FIS, the output of each rule is linear combination of input variables added by a constant term. The output of the i^{th} node in layer *1* is designated as $O_{1,i}$. The first layer i.e the fuzzy layer comprises input variable membership functions (MFs) and provides the input values to the next layer. Every node *i* is an adaptive node with the following node function:

$$\left.\begin{array}{ll} O_{1,i} = \mu_{Ai}(x), & for\ i = 1,2, \quad or \\ O_{1,i} = \mu_{Ci-2}(y), & for\ i = 3,4, \quad or \\ O_{1,i} = \mu_{Ei-4}(z), & for\ i = 5,6 \end{array}\right\} \tag{3.12}$$

where x or y or z is the input to node i, and A_i or B_{i-2} or E_{i-4} is a related linguistic label (e.g. 'small' or 'large'). In other words, $O_{l,i}$ is the membership grade of a fuzzy set A and C and E $(= A_1, A_2, C_1, C_2, E_1, E_2)$, which specifies how much the specified

input x or y or z satisfies the quantifier A, C or E. In this case, the membership function may be any appropriate parameterized membership function. Membership functions are denoted by $\mu_{Ai}(x), \mu_{Ci-2}(y), \mu_{Ei-4}(z)$. The generalized bell function is employed here, because it has the best abilities for nonlinear parameter generalization (Shamshirband, Petković, Hashim, & Motamedi, 2014).

$$\mu_{Ai}(x) = \frac{1}{1 + \left(\frac{x - c_i}{a_i}\right)^{2b_i}} \tag{3.13}$$

where $\{a_i, b_i, c_i\}$ is the variable set. The bell-shaped function varies according to the values of the variables changes, thereby showing different types of membership functions for fuzzy set A. The variables in the first layer are known as premise variables.

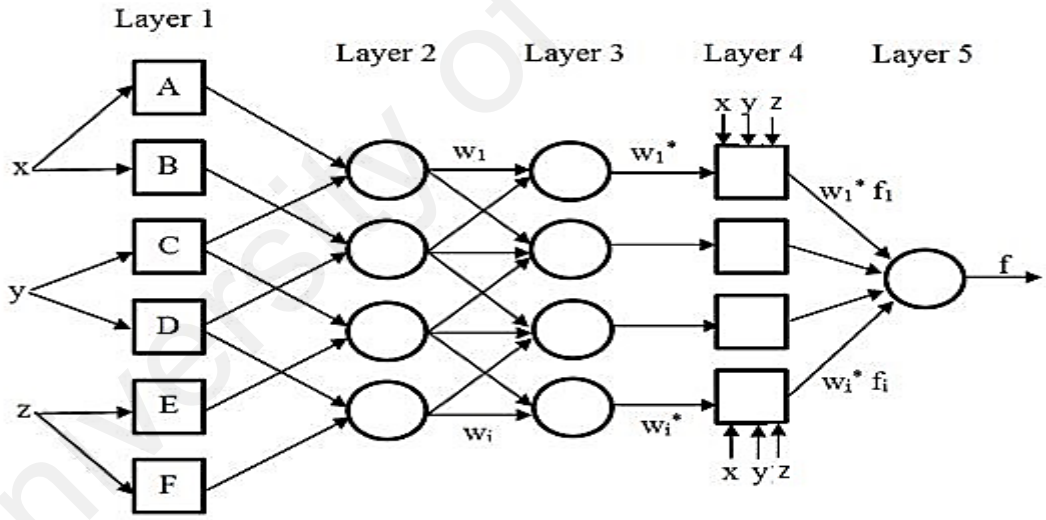

Figure 3. 4: ANFIS structure with three inputs, one output and two rules

The second layer is the product layer, which multiplies the incoming signals from the first layer to generate an output. Each node in the second layer is a fixed node and its output is the resultant of all incoming signals.

$$O_{2,i} = w_i = \mu_{Ai}(x)\mu_{Ci-2}(y)\mu_{Ei-4}(z), \qquad i = 1,2 \tag{3.14}$$

The third layer is the normalized layer and it is a non-adaptive layer. In this layer, every node *i* calculates the ratio of the rule's firing strength to the sum of all rules' firing strengths. The outputs of this layer are known as normalized weights or normalized firing strengths given by;

$$O_{3,i} = w_i^* = \frac{w_i}{w_1 + w_2}, \quad i = 1,2 \tag{3.15}$$

The fourth layer is the defuzzification layer. This layers delivers the output values resulting from the inference of rules based on the consequent parameter, where every node *i* is an adaptive node.

$$O_{4,i} = w_i^*.f_i = w_i^*(p_i\mathrm{x} + q_i\mathrm{y} + r_i) \tag{3.16}$$

where $\{p_i, q_i, r_i\}$ is the consequent parameter (Petković, Issa, Pavlović, Pavlović, & Zentner, 2012):

The fifth layer is the output layer. It combines all inputs from the defuzzification layer and transforms the fuzzy classification leading to a crispy output. The node in this layer is non-adaptive and estimates the overall output of all incoming signals.

$$O_{5,i} = \sum_i w_i^*.f_i = \frac{\sum_i w_i.f_i}{\sum_i w_i}, \tag{3.17}$$

ANFIS requires a training dataset of desired input and output pairs (x, y z, f) indicating the target system to be a model. Thereafter, ANFIS mapped the inputs to the output adaptively via the membership functions (MFs), while the rule base and related parameters emulate the given dataset.

In this study, the input data are; monthly mean maximum temperature (T_{max}), monthly mean minimum temperature (T_{min}), and monthly mean sunshine duration ($\bar{n}$), while the output is solar radiation. The monthly mean daily values of these data were divided in

two sets for the purpose of training and testing. The purpose of training process in ANFIS model is to minimize the error between the actual target and the ANFIS output. Based on the literature on ANN, the percentage of training data must be higher than testing data for effective learning of the system before the system can produce good result. The percentage of data selected for training and testing has been carefully tested based on the minimal error obtained in the statistical indicator. Initially the ratio 50/50 were tested, follow by 60/ 40, then 70/30 and finally 80/20. In all this tests, we found out the 70/30 produce least error. Therefore, 70% of data were used for sample training and the remaining 30% for testing.

The descriptive statistics of the input datasets for the selected locations (minimum value, maximum value, mean, standard deviation and variation coefficient) is presented in Table 3.4. The standard deviation in the table indicates the distribution of the data around the mean, signifying the degree of consistency of the data.

Table 3. 4: Descriptive statistics of the input datasets

Site	**Input parameter**	**Min**	**Max**	**Mean**	**Standard Deviation**	**Variation coefficient**
Iseyin	$\bar{n}$	1.30	8.40	5.50	1.44	2.08
	$\bar{T}_{\min}$	18.0	33.7	21.7	1.31	1.72
	$\bar{T}_{\max}$	22.8	37.1	31.6	2.84	8.07
Sokoto	$\bar{n}$	1.40	9.90	7.80	1.60	2.50
	$\bar{T}_{\min}$	13.9	29.0	22.6	3.30	11.2
	$\bar{T}_{\max}$	28.5	42.2	35.4	3.20	10.1
Maiduguri	$\bar{n}$	4.40	10.8	8.31	1.28	1.63
	$\bar{T}_{\min}$	9.20	28.1	20.3	4.72	11.8
	$\bar{T}_{\max}$	28.0	42.6	35.2	3.43	22.3
Jos	$\bar{n}$	3.10	10.7	7.33	1.86	3.45
	$\bar{T}_{\min}$	7.20	24.8	15.8	2.98	8.88
	$\bar{T}_{\max}$	22.6	33.3	27.8	2.33	5.41
Enugu	$\bar{n}$	2.50	8.30	5.60	1.30	1.80
	$\bar{T}_{\min}$	17.8	26.0	22.5	1.30	1.60
	$\bar{T}_{\max}$	28.0	38.3	32.1	2.20	4.60
Port Harcourt	$\bar{n}$	1.30	7.20	4.10	1.40	2.10
	$\bar{T}_{\min}$	14.9	28.5	22.7	1.30	1.80
	$\bar{T}_{\max}$	24.6	35.8	31.3	1.90	3.50

The ANFIS network is implemented in MATLAB and the Simulink block diagram for the prediction using the ANFIS network is shown in Figure 3.5. The Simulink block diagram facilitates rapid estimation of solar radiation for any input combination.

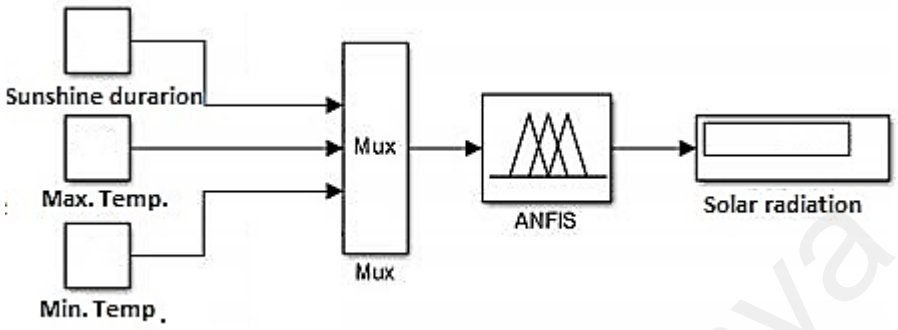

Figure 3. 5: Simulink block diagram for solar radiation estimation

To generate the fuzzy IF-THEN rule, first-order Sugeno fuzzy model was employed with three inputs. The hybrid-learning algorithm is used to determine the parameter of the model, and the consequent parameters identified by the least squares estimate. In the forward pass of this algorithm, functional signals proceed up to the defuzzification layer, while in the backward pass, the error rates propagate backwards and the premise parameters updated by gradient descent method. Linear fuzzy memberships function (MFs) are used, since it makes the subsequent computation easier. Furthermore, the proficiency of ANFIS in solar radiation prediction is compared with other methodologies earlier described.

3.3.5 Model performance evaluation metrics

In order to compare the performance of the developed soft-computing prediction models with actual measurement values, the following statistical indicators were selected (Willmott & Matsuura, 2005):

a) Mean absolute percentage error (MAPE)

$$MAPE = \frac{1}{n}\sum_{i=1}^{n}\left|\frac{Q_i - P_i}{Q_i}\right| \times 100 \quad (3.18)$$

b) Root-mean-square error (RMSE)

$$RMSE = \sqrt{\frac{\sum_{i=1}^{n}(Q_i - P_i)^2}{n}} \quad (3.19)$$

c) Coefficient of determination (R^2)

$$R^2 = \frac{[\sum_{i=1}^{n}(Q_i - \bar{Q}_i).(P_i - \bar{P}_i)]^2}{\sum_{i=1}^{n}(Q_i - \bar{Q}_i).\sum_{i=1}^{n}(P_i - \bar{P}_i)} \quad (3.20)$$

d) Correlation coefficient (r)

$$r^2 = \frac{\sum_{i=1}^{n}(Q_i - \bar{Q}_i).(P_i - \bar{P}_i)}{\sqrt{\sum_{i=1}^{n}(Q_i - \bar{Q}_i).\sum_{i=1}^{n}(P_i - \bar{P}_i)}} \quad (3.21)$$

where P_i and O_i are known as the experimental and predicted values, respectively, while $\overline{P_i}$and $\overline{Q_i}$ are the mean value of P_i and O_i respectively and n is the total number of test data. The MAPE shows the mean absolute percentage deviation between the predicted and experimental values. The RMSE value provides infomation on the short term performance of the correlation by comparing the extent of deviatiaon of the predicted value from the actual mearsured value, R^2 and r is a measure that allows one to determine the level of linear relationship between the predictions and the actual value. The smaller the value of RMSE and MAPE the better the performance model and vice versa in the case of R^2 and r.

3.4 Renewable energy resources assessment

Various analyses have been conducted in order to ascertain the potential of the two proposed energy sources; wind and solar in the selected sites. The potentials of solar energy resources at the selected sites were assessed based on certain key solar resource's

parameters, including monthly and annual global solar radiation (GSR), beam radiation, diffuse radiation, and clearness index. The optimal tilt angle for south facing solar collector orientation was also determined. On the other hand, wind energy potentials were examined based on monthly mean daily wind speed data. This section thus, presents the methodology together with the mathematical model employed in the assessment.

3.4.1 Solar energy

Characteristics of solar energy resources at selected sites are analyzed based on average monthly global solar radiation and monthly clearness index, monthly average daily diffuse and beam radiations. These parameters are vital for the purpose of efficient design and performance evaluation of solar energy applications. For all the sites considered in this study, the available daily data were averaged to obtain the monthly and annual mean values. However, certain precautions were taken into consideration prior to utilization of the dataset in the analysis; this is done to enhance the quality of the dataset. For example, to ensure the reliability of the solar radiation data; firstly, the daily clearness index (K_T) was computed and the values observed to be out of range ($0.015 < K_T < 1$) were eliminated. Secondly, in a case where there is month with few missing or unreliable data values, the missing data are substituted with the predicted values obtained from the ANFIS prediction model earlier discussed.

For the monthly analysis, monthly mean clearness index ($\bar{K}_T$) defined in terms of monthly mean global solar radiation incident on the horizontal surface ($\bar{H}$) and monthly mean extraterrestrial radiation ($\bar{H}_o$) (Duffie & Beckman, 2013)

$$\bar{K}_T = \frac{\bar{H}}{\bar{H}_o} \tag{3.22}$$

where ($\bar{H}_o$) is computed from the experesion earlier presernted in Equation 3.1

3.4.1.1 Total solar radiation on horizontal surface

The total monthly solar radiation on horizontal surface is a composite of monthly mean beam ($\bar{H}_b$) and diffuse radiation incident on horizontal surfaces ($\bar{H}_d$).

$$\bar{H} = \bar{H}_b + \bar{H}_d \tag{3.23}$$

Where the monthly mean diffuse radiation on horizontal surfaces ($\bar{H}_d$) is estimated based on the correlation proposed in (Erbs, Klein, & Duffie, 1982):

$$\frac{\bar{H}_d}{\bar{H}} = \begin{cases} 1.391 - 3.560\bar{K}_T + 4.189\,\bar{K}_T^2 - 2.137\,\bar{K}_T^3, for\ w_s \leq 81.4^0\ and\ \ 0.3 \leq \bar{K}_T \geq 0.8 \\ 1.311 - 3.022\bar{K}_T + 3.427\,\bar{K}_T^2 - 1.821\,\bar{K}_T^3, \quad for\ w_s \geq 81.4^0\ and\ \ 0.3 \leq \bar{K}_T \geq 0.8 \end{cases} \tag{3.24}$$

3.4.1.2 Total radiation on tilted surface

For the purpose of solar energy design and performance calculation, it is often necessary to estimate the solar radiation on the tilted surfaces, from the measured global solar radiation data. Solar radiation on tilted surface is a composite of the beam and diffuse radiation on tilted surface; including ground reflected radiation. Numerous models have been suggested by researchers to determine the global solar radiation on tilted surface (Hay & Davies, 1980; Klucher, 1979; Reindl, Beckman, & Duffie, 1990). The most prominent is the isotropic model proposed by Hottel and Woertz (Hottel & Woertz, 1942), and later modified by Liu and Jordan (B. Liu & Jordan, 1961) as expressed in Equation (3.25).

$$\bar{H}_T = \bar{H}_b\bar{R}_b + \bar{H}_d\bar{R}_d + \bar{H}\rho_g\left(\frac{1 - cos\beta}{2}\right) \tag{3.25}$$

where β is the tilt angle of the solar collector whose optimum value is to be determined as shown in Figure 3.6, while ρ_g is the ground albedo factor taken as 0.2 in this study. $\bar{R}_b$

is the ratio of the monthly beam radiation on inclined surface to the horizontal surface expressed (Duffie & Beckman, 2013):

$$\bar{R}_b = \frac{\cos(\varphi-\beta)\cos(\delta)sin(w_s') + (\pi/180)w_s'\sin(\varphi-\beta)\sin(\delta)}{\cos(\varphi)\cos(\delta)\sin(w_s) + (\pi/180)w_s\sin(\varphi)\sin(\delta)} \quad (3.26)$$

w_s' represent the sunrise hour angle on tilted surface, given as;

$$w_s' = min\begin{Bmatrix}\cos^{-1}(-tan\varphi tan\delta)\\ \cos^{-1}(-\tan(\varphi-\beta)tan\delta)\end{Bmatrix} \quad (3.27)$$

$\bar{R}_d$ is ratio of monthly mean diffuse solar radiation on the tilted surface to the measured global radiation on horizontal surface. The Hay-Davies model (Hay & Davies, 1980), which takes into account the circumsolar components of diffusion (anisotropy index), is adopted in this study to determine the value of $\bar{R}_d$.

$$\bar{R}_d = \frac{\bar{H}_b}{\bar{H}_o}\bar{R}_b + \left(1-\frac{\bar{H}_b}{\bar{H}_o}\right)\left(\frac{1+cos\beta}{2}\right) \quad (3.28)$$

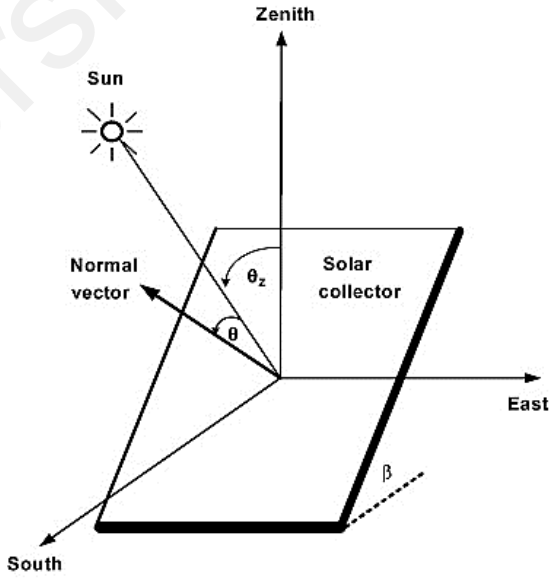

Figure 3. 3: The schematic view of solar collectors with the characteristic angles

The optimum tilt angle β_{opt} , is the angle of inclination that produced maximum monthly mean global radiation according to Equation 3.25. It is function of geographical latitude and local climatic condition of the sites under consideration. The optimum value is estimated separately for each of the sites considered in this study. This varies between 0^0 and 90^0; a code developed in MATLAB was used to determine the optimum value for each respective months in all the selected sites.

The two prevailing seasons available in Nigeria; dry and rainy seasons were adopted for the seasonal optimal angle. The rainy season months range between April and September in the northern part of the country, and between April and October in the south region. On the other hand, dry season months extend from October to March in the northern region, and November to March in the south. The amount of energy gain due to optimal tilt orientation of solar collector, compared to solar collector positioned in the horizontal plane is also considered in this analysis. The percentage of solar energy gain (SEG) due to optimal tilt for each month of the year and the whole year is obtained from Equations (3.29) and (3.30) respectively.

$$SEG_{mon} = \frac{\bar{H}_T - \bar{H}}{\bar{H}} \times 100 \tag{3.29}$$

$$SEG_{Ann} = \frac{\sum_{i=1}^{12} \bar{H}_T - \sum_{i=1}^{12} \bar{H}}{\sum_{i=1}^{12} \bar{H}} \times 100 \tag{3.30}$$

3.4.2 Wind energy

For the estimation of the expected power output of the wind turbine for the proposed hybrid system wind resources at the selected sites, the wind energy potential of the site needed to be analyze. Thus, this section presents the methodology employed in the wind energy potential assessment.

3.4.2.1 Wind speed distribution

Over the years, several statistical models such as normal, lognormal, Weibull and Rayleigh's distributions are widely utilized for wind data analysis(Chang, 2011; Morgan, Lackner, Vogel, & Baise, 2011). Among these statistical distributions, two-parameter Weibull probability distribution function was widely adopted for wind data assessments because it provides a good match with experimental data when compared to the other statistical models (O. Ohunakin, Adaramola, & Oyewola, 2011). It is flexible and requires only two parameters to estimate. It is a special case of generalized gamma function commonly used in describing wind speed frequency distribution as well as the estimation of wind power density (Gökçek et al., 2007). In this study, Weibull distribution function (WDF) earlier expressed in Equations (2.4) and (2.5) are employed to describe the monthly wind speed variation and seasonal changes occurring in the selected sites as well as the estimation of wind power density. The Weibull shape (k) and scale (c) parameters are estimated from standard deviation (SD) method expressed as (Chang, 2011) ;

$$k = -\left(\frac{\sigma}{\bar{v}}\right)^{-1.086} \qquad for\ 1 \leq k \leq 10 \tag{3.31}$$

$$c = \frac{\bar{v}}{\Gamma(1 + 1/k)} \tag{3.32}$$

where, $\bar{v}$ is the average wind speed in (m/s), σ is the standard deviation which shows degree of variation of wind speed and $\Gamma(x)$ is the gamma function which is given by:

$$\Gamma(x) = \int_{o}^{\infty} \exp(-u)u^{x-1}dx \tag{3.33}$$

3.4.2.2 Extrapolation of wind speed at different hub height

Wind speed at a specific hub height is of interest in wind power application, hence in this study; exploration of wind speed at different hub height as a function of reference

height obtained using the relation presented in Equation (2.6). However, the surface roughness coefficient is obtained from the following expression(Ucar & Balo, 2009);

$$\alpha = [0.37 - 0.088In(v_0)] \Big/ \left[1 - 0.088In\left(\frac{h_0}{10}\right)\right] \tag{3.34}$$

Alternatively, the Weibull probability density function earlier discussed can be employed for the extrapolation. Since the boundary layer development and ground surface effects are non-linear with respect to the wind speed, the scale (c) and shape parameter (k) of Weilbull will change as a function of hub height, expressed as;

$$c(h) = c_0 \left(\frac{h}{h_0}\right)^n \tag{3.35}$$

$$k(h) = k_0 \left[1 - 0.088In\left(\frac{h_0}{10}\right)\right] \Big/ \left[1 - 0.088In\left(\frac{h}{10}\right)\right] \tag{3.36}$$

where c_0 and k_0 are the scale and shape parameter respectively at reference hub height (10m in this study). The exponential value *n* is given as;

$$n = [0.37 - 0.088In(c_0)] \Big/ \left[1 - 0.088In\left(\frac{h_0}{10}\right)\right] \tag{3.37}$$

3.4.2.3 Wind power and energy density

Wind power density gives an insight to the wind energy potential of any particular site. It expresses the average wind power per square meter (W/m^2). It can be determined from measured wind speed data and probability density function. In the first instance, the wind power is proportional to the cube of the wind speed as shown in Equation 2.1. Conversely, with the two-parameter Weibull distribution (equations 2.5 and 2.6), the expression of wind power estimation is given by (Sathyajith, 2006):

$$P_d = \frac{P(v)}{A} = \frac{1}{2}\rho \int_0^{\infty} v^3 f(v) dv = \frac{1}{2}\rho c^3 \Gamma\left(1 + \frac{3}{k}\right) \quad (3.38)$$

where $P(v)$ is the wind power in (Watts), P_d is the wind power density (W/m^2), A is the swept area of the wind turbine rotor (m^2) and ρ is the air density of the selected sites. In this study, ρ is taken to be 1.225 kg/m^3 in all sites. The corresponding mean energy density of the wind is obtained by multiplying Equation (3.38) with period of time (T) under consideration (Tchinda, Kendjio, Kaptouom, & Njomo, 2000):

$$E_d = \frac{1}{2}\rho c^3 \Gamma\left(1 + \frac{3}{k}\right) T \quad (3.39)$$

The annual energy output is given in as:

$$\bar{E}_{d,ann} = \sum_n^{12} \bar{E}_{jm} \quad (\text{kWh/m}^2/\text{year}) \quad (3.40)$$

where, $\bar{E}_{jm}$ is the extractible mean monthly energy output given by $24x10^{-3}P_d xT$, with P_d given by Equation (3.38) and T is the number of day in the month considered.

3.5 Energy demand assessment of a rural health clinic

The energy needs assessment is an important factor in energy intervention planning and design as it gives information concerning the various types of electrical appliances, their power rating and the time of operation within the day. Therefore, a thorough assessment of energy demands of a healthcare facility is critical to the selection of the most suitable energy resources. For instance, a health post, which is the most basic health facility available in remote villages, is usually characterized with medical services such as: (i) treatment of minor illnesses or injuries, (ii) child deliveries and provision of basic immunization services. The energy need of such facilities is considered relatively low, due to limited availability of medical equipment. On the other hand, a health clinic that offers a wider range of medical services than health post, and possesses equipment that

allows more medical diagnoses can be considered high in energy demands. According to United States Agency for International Development (USAID, 2014), healthcare facility can generally be categorized into three. The first (Category I), is applicable to the rural setting and characterized with limited medical services and staff. In this category, electricity is often required for lighting during evening hour's operations and to support limited surgical procedures such as suturing, refrigeration for maintenance of cold-chain vaccines and other medical supplies. Basic equipment in this facility may include a centrifuge, hematology mixer, microscope, incubator and hand-held power aspirator. The estimated load demand for this category range between 5-10kWh/day. The second category (Category II), contains medical equipment that is similar to the first category, but can as well accommodate sophisticated medical diagnostic equipment with frequent usage when compared to facility in the first category. Additional energy-consuming device that can be obtained in this category includes: refrigerators often used for food/blood bank storage, communications equipment to communicate with medical expert in referral centers. The estimated energy demand in this category is in the range of 10-20kWh/day. The third (category III) usually serves as a primary referral center, because it can coordinate communication between several smaller facilities and major hospital in large towns. This could also contain sophisticated diagnostic equipment such as; x-ray machine and CD4 counters. demanding additional power. Daily typical energy demand of this facility is in the range of 20-30kWh.

The listing of various device's inventories commonly found in major health facilities is provided in appendix B. The range of energy requirements signifies the peak power demand expected in a facility when most of the devices are operating simultaneously. However, some of the devices that required high-energy demand could be used intermitted while others are on stand-by power mode. All this need to be considered while estimating average daily energy demand of any facility, most especially if the facility is

equipped with battery-powered storage, for storing excess energy from the generator or RE sources to be used in the later time.

A standard rural healthcare facility located in Iseyin district area of Oyo state, Nigeria has been used to create the load profile for five other hypothetical rural health clinics distributed across different climatic zones of Nigeria as earlier mentioned. This healthcare facility is made up of an emergency room, a doctor's consulting room, nurse/injection room, one male ward, one female ward, an operating room, a delivery room, and a laboratory. The total number of bed space in the clinic is 10. In this facility, electricity is required for: (1) Lighting for night hour's operations to support limited surgical procedures (such as; suturing and cesarean section) and to provide illumination in the surroundings at night. (2) Refrigerators, to keep cold chain vaccines, blood bank and other perishable medical supplies at desire temperature. (3) Basic laboratory equipment, including centrifuge, microscope, incubator, hematology mixer and hand-held power aspirator. Other appliances that require electrical power include; ceiling/wall fans, TV set, VCR, desktop computer and VHF radio communication equipment to aid communication with nearby referral centers. This rural clinic can be classified as category II rural health facility. The load descriptions and estimated demand of each facility are presented in Table 3.5.

Load profile data for the intended application have been studied and analyzed. Accurate analysis of system load profile is necessary for the design of a reliable and efficient system. The optimal sizing and modeling of the energy storage device also depend on the load profile. This includes the calculation of the power demand of each equipment expected to be used at the clinic, followed by the estimation of the lighting load and other miscellaneous load. This is done to determine the daily watt-hour demand of the health center.

Table 3. 2: The load description and estimated demand of the rural health clinic

Load Description	Quantity	Rated Power(W)	Total Power (W)	Daytime hour (h/d)	Night hours (h/d)	Total on-time (h/d)	Total Energy (kWh/d)
Lighting- CFL (indoor)	8	15	120	2	6	8	0.96
Lighting-CFL (outdoor)	6	40	240		12	12	2.88
Ceiling/wall fan	7	60	420	4	4	8	3.36
Blood bank refrigerator	1	70	70	12	6	18	1.26
Vaccine Refrigerator	1	60	60	12	6	18	1.08
Small Refrigerator	1	300	300	5	5	10	3.00
Centrifuge	1	242	242	3	-	3	0.73
Microscope	2	20	40	6	-	6	0.24
Hematology Mixer	1	28	28	4	-	4	0.11
Hematology Analyzer	1	230	230	4	-	4	0.92
Lab Autoclave	1	1500	1500	2	-	2	3.00
Incubator	1	400	400	5	-	5	2.00
Oxygen Concentrator	1	270	270	2	-	2	0.54
Ultrasound machine	1	800	800	2	-	2	1.60
Vacuum Aspirator	1	40	40	2	-	2	0.08
Suction Apparatus	1	100	100	2	-	2	0.20
Desktop Computer	1	150	150	5	-	5	0.75
TV set	1	80	80	4	2	6	0.48
VCR	1	20	20	2	2	4	0.08
Mobile Charger	4	20	80	2	4	6	0.48
VHF Radio Receiver:							
Standby	1	2	2	24	12	36	0.07
Transmitting	1	30	30	2	2	4	0.12
Total			4,442			121	23.94

3.5.1 Criteria for selection of the appropriate energy system for the load

The following attributes were considered during the selection of the appropriate hybrid energy system for the healthcare facility load;

1) *Peak power capacity:* The amount of electricity supplied in watts is the peak capacity that the system can provide. Various appliances use up different amount of electricity, ranging from a few watts to several kilowatts. Likewise, the various power generating equipment generates different quantities of electricity. The generating capacity should be adequate to support the available electrical load. Therefore, the use of more energy-efficient lighting and medical equipment is critical to optimizing available peak power supply in healthcare facilities.

2) *Daily energy capacity:* The proposed power supply must be able to meet the daily energy demand of a typical rural health clinic. The various usage of different appliances in healthcare facility could be categorized as; continuous (e.g refrigerators and space heating), intermittent such as in laboratory equipment, periodic for evening/early-morning lighting or just once or twice a day, such as the operation of autoclaves for instrument sterilization. The estimated daily energy capacity needed for the healthcare facilities considered for this study is presented in Table 3.5.

3) *Evening peak hours supply:* Evening hours are times when many patients, including pregnant women, may arrive for treatment at the clinic to avoid wasting time during their daytime jobs. In the evening time, the demand for electricity supply across all consumer sections of rural areas such as; households, commercial shops and street lighting is typically considered high. Availability of power supply in healthcare facility in the evening and during the night hours where there is no referral clinic nearby is considered important for quality healthcare delivery. Electric power supply in the evening is vital to enable medical health personnel feel secured and enhance their productivity during night shifts. Therefore, the power supply is designed to suits the expected nighttime load demand.

4) *Duration of supply:* The period of power supply in any healthcare facility depends on size and types of healthcare services rendered. Electricity supply should be available to support all equipment required to enhance quality medical services delivery at all times, most especially maternal healthcare and childbirth services or other emergency services. Some equipment, such as; laboratory equipment for testing of samples collected during the day and analyzed in a batch are used intermittently. However, other appliances such as refrigerators may require

continuous operation to keep the medical supplies at desire temperature irrespective of the clinic operating time.

5) *Reliability:* Reliability in this context refers to the probability of occurrence of power supply failure. Unexpected interruptions can arise due to failure of any components of the hybrid energy system. For the purpose of ensuring efficient healthcare services delivery during power disruptions, health facility is expected to be provided with backup power generators. Backup generators may not provide sufficient electricity for all the equipment; nevertheless, it can serve to support priority applications such as lighting, refrigerators and other critical equipment. Frequent unscheduled power interruptions of long duration can have severe impacts on health services. For instance, reliable power supply is vital for anesthesia machines and oxygen concentrators, and outages could affect patient's life as well as damage equipment, vaccines, blood and medicines. Therefore, reliability of the power supply is given important attention while designing the power system.

6) *Environmental health and sustainability:* It is expected that energy supply to any healthcare facility should not lead to environmental hazard. Environmental impart such as air pollution, water pollution and noise pollution in any quantities that could further deteriorate the health of patients, affect the medical staff or people living at the health facility premises should be avoided. Reduction of CO_2 emission per kWh of power generated will lead to environmental sustainability. To this aim, more priority is given to utilization of RE sources than the diesel generator source in providing power supply to the rural healthcare facilities considered for this study, hence the need for high renewable faction. Renewable fraction (RF) is the total amount of power generated by the renewable energy

sources compared to total power generation from the hybrid system. This can be express as;

$$RF = \left(1 - \frac{\sum P_{diesel}}{\sum P_{RE}}\right) \times 100\% \tag{3.41}$$

where P_{diesel} is the power output of the diesel generator and P_{RE} is the power output of the connected renewable energy sources, solar PV and wind in this case.

3.6 Mathematical modeling of hybrid system components

Mathematical modeling of various components of the proposed hybrid system is essential for effective analysis of the entire system; hence, this section provides basic information on method adopted in modeling of each component.

3.6.1 PV model

Modeling of the PV cell is a mathematical description of the PV output current-voltage (I-V), and power-voltage (P-V) relations. This represents an important task in the entire PV system pre-installation procedure. A general equivalent circuit that represents the operation of PV is illustrated in Figure 2.6; however, a more detailed model is a two-diode model presented in Figure 3.7. Many authors usually depend on the manufacturer's data to determine the values of both series and shunt resistance. However, the ideality factor, saturation current as well as photon current need to be determined since these parameters are not often provided by many manufacturers.

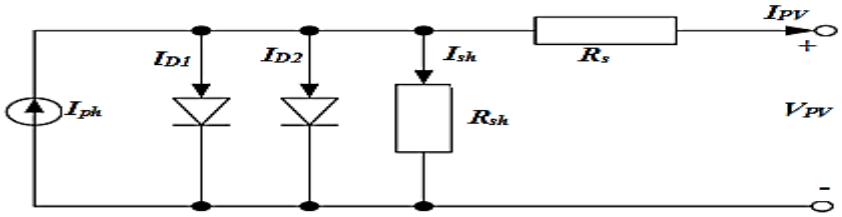

Figure 3. 4: Two-diode PV equivalent circuit

Based on the equivalent circuit represented in Figure 3.7, the PV panel output current is given as:

$$I_{PV} = I_{ph} - I_{D1} - I_{D2} - \left[\frac{V_{PV} + I_{PV}R_s}{R_{sh}}\right] \tag{3.42}$$

where;

$$I_{D1} = I_{01}\left[\exp\left(\frac{V_{PV}+I_{PV}R_s}{\alpha_1 V_{T1}}\right) - 1\right], \quad I_{D1} = I_{02}\left[\exp\left(\frac{V_{PV}+I_{PV}R_s}{\alpha_2 V_{T2}}\right) - 1\right]$$

I_{ph} is the photon current from the incident light, I_{01} and I_{02} are the reverse saturation currents of each diode. While α_1, α_2, V_{T2} and V_{T2} are each diode ideality constants and thermal voltages respectively (Sandrolini, Artioli, & Reggiani, 2010). Considering single PV module, the diode thermal voltage is given as;

$$V_{T1} = V_{T2} = N_s\frac{KT}{q} \tag{3.43}$$

where, N_s is the number of series cell per module, K, the Boltzmaan constant ($1.38 \times 10^{-23}J/K$), q is the electron charge ($1.602 \times 10^{-19}C$) and T the diode p-n junction temperature in Kelvin. Although greater accuracy can be achieved using two-diode model compared to the single diode model, the main demerit of this model is that it requires the computation of seven parameters, namely; I_{ph}, I_{01} , I_{02}, α_1, α_2, R_s and R_{sh}. Some of these parameters can be assumed arbitrarily to reduce the number of unknown, thereby less complexity and reduction in computation time. In an attempt to reduce the computation time, the proposed model neglects the series and shunt resistances; therefore, equation (3.42) is reduced to:

$$I_{PV} = I_{ph} - I_{01}\left[\exp\left(\frac{V_{PV}}{\alpha_1 V_{T1}}\right) - 1\right] - I_{02}\left[\exp\left(\frac{V_{PV}}{\alpha_2 V_{T2}}\right) - 1\right] \tag{3.44}$$

where the unknown parameter are now; $I_{ph},\ I_{01}\ ,\ I_{02},\ \alpha_1, \alpha_2$. All these parameter can be estimated from manufacturer datasheet as highlighted in the following section.

3.6.1.1 Determination of model parameters

(a) Photon current I_{ph}

The value of photon current I_{ph}, is dependent on the solar radiation and temperature of a particular location, thus expressed as (Sandrolini et al., 2010);

$$I_{ph} = [I_{SC-STC} + K_i(T - T_{STC})]\frac{G}{G_{STC}} \tag{3.45}$$

where, I_{SC} is the short circuit current at standard test conditions (STC), i.e solar radiation, G_{STC} =1000W/m^2 and temperature, T_{STC} = 25^{o}C. While K_i is short circuit current temperature coefficient obtained from the manufacturer datasheet.

(b) Reverse saturation current (I_{01}, I_{02})

The reverse saturation current of the diode I_{01} and I_{02} can be found from the relation (Villalva & Gazoli, 2009):

$$I_{01} = \frac{I_{SC-STC} + K_i(T - T_{STC})}{\left[\exp\left(\frac{V_{oc-STC} + K_v(T - T_{STC})}{\alpha_1 V_{T1}}\right) - 1\right]} \tag{3.46}$$

where, K_v is the voltage temperature coefficient of PV module(V/^{0}C) obtained from manufacturer datasheet, and V_{oc-STC}, the open circuit voltage at standard test conditions. The value of I_{02} can be obtained from I_{01} based on the relation below (Gupta, Tiwari, Fozdar, & Chandna, 2012):

$$I_{02} = \left(\frac{T^{\frac{2}{5}}}{3.77}\right) I_{01} \tag{3.47}$$

c) Ideality constant (α_1, α_2)

In this study, ideality constant of the PV module has been estimated by a simple iterative code developed in MATLAB. For this purpose, two PV operation conditions are taken in to consideration.

i. Open circuit condition ($V_{PV} = V_{oc}$)

ii. Maximum power point (MPP) condition (V_{mp}, I_{mp})

Under the first condition, $I_{PV} = I_{oc} = 0$, hence equation (3.44) becomes;

$$0 = I_{ph} - I_{01}\left[\exp\left(\frac{V_{oc}}{\alpha_1 V_{T1}}\right) - 1\right] - I_{02}\left[\exp\left(\frac{V_{oc}}{\alpha_2 V_{T2}}\right) - 1\right]$$

On simplification, α_2 can be expressed in terms of α_1 as;

$$\alpha_2 = \frac{V_{oc}}{V_{T2}\, In\left(\frac{I_{ph} - I_{01}\left(\exp\left(\frac{V_{oc}}{\alpha_1 V_{T1}}\right) - 1\right)}{I_{02}} + 1\right)} \tag{3.48}$$

The procedure for the evaluation is as follows;

(1) Input the available parameter from datasheet ($V_{oc}, I_{oc}, V_m, I_m, K_i, K_v, N_s$)

(2) Increment the value of α_1 and obtain the corresponding value of α_2

(3) Evaluate I_{PV} (equation 3.44) for voltage range ($O < V < V_{oc}$) and calculate $P_{max,cal}$ based on the earlier obtained parameters.

(4) Calculate maximum current ($I_{max,cal} = P_{max,cal}/V_{mp}$)

(5) Increment α_1 until error between $I_{max,cal}$ and I_{mp} is within the tolerance value.

The flowchart of MATLAB program is shown in Figure 3.8.

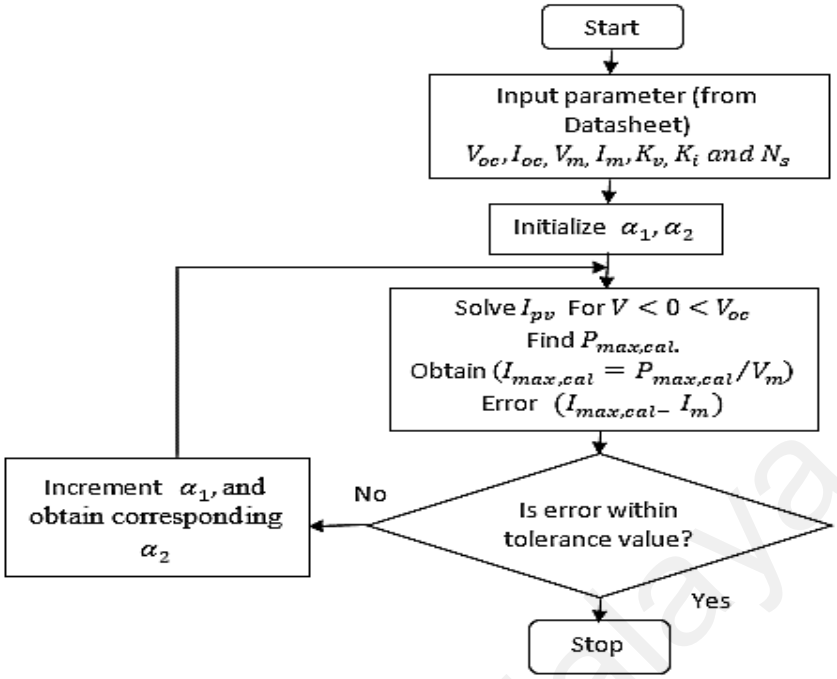

Figure 3. 5 Matching flowchart of ideality constant determination

A mono-crystalline PV module (Solex- SK37) has been considered in this study for the evaluation of the proposed techniques. Table 3.6 present the specification of the PV module (Solex, 2014).

Table 3. 3: PV module specifications

Parameter	Value
Model name	Solkar- SK37
Type	Mono-crystalline
$I_{sc}\ (V)$	2.55
$V_{oc}\ (V)$	21.24
$I_{mp}(V)$	2.25
$V_{mp}\ (V)$	16.56
$P_{mp}\ (W)$	37.26
$K_v\ (V/°C)$	-0.310
$K_i(A/°C)$	0.0017
N_s	36

Equation (3.44), has no unique solution, since module output voltage (V_{PV}) and current (I_{PV}) are interdependent. Therefore, a numerical approach such as Newton-Raphson can be used to obtain the I-V and P-V characteristics of the module for entire current range (0 to I_{sc}), and for voltage range (0 to V_{oc}). The PV module current that

satisfies this equation at a specific module voltage and certain values of other variables and constant is solved numerically with Newton-Raphson method as follows;

$$h(I_{PV}, V_{PV}) = I_{PV} - f(I_{PV}, V_{PV}) = 0 \tag{3.49}$$

$$I_{PV_{n+1}} = I_{PV_n} - \left(\frac{h(I_{PV},\ V_{PV})}{\frac{dh(I_{PV},\ V_{PV})}{dI_{PV}}} \right)_{at\ I_{PV} = I_{PV_n}} \tag{3.50}$$

where, I_{PV_n} and $I_{PV_{n+1}}$ are the present and next value of the parameter respectively. The PV module current is computed iteratively and number of iteration determine such that the absolute error between the present calculated and the previous one is less than a certain specified tolerance (i.e 0.001).

3.6.1.2 I-V and P-V characteristics of PV module

A typical I-V and P-V curves can be drawn from the computed PV module current (I_{PV}) for different voltages ($V_{PV} = 0, V_{mp}\ and\ V_{oc}$) at different solar radiation levels ($G = 200, 400, 600, 800\ and\ 1000 W/m^2$) and different temperature levels (i.e $T = 25, 50, 75\ ^0$C) using equation (3.45).

Three main points is of interest in this curve are:

1) The short circuit point: this is the point at which PV module voltage is zero and current maximum ($I_{SC} = I_{max}$)
2) Maximum power point (MPP): this is a point where the product of current and voltage peaks.
3) Open circuit point: This occurs where the PV current is zero and voltage maximum ($V_{oc} = V_{max}$).

The correct estimation of these points for other conditions is the central objective of any modeling technique. At instances, where PV manufacturer's datasheet do not show I-V and P-V curves at different solar radiation and temperature levels, equations (3.51 to 3.54) can be considered to calculate the value of short circuit current and open circuit voltage at different radiation and temperature levels (Chouder et al., 2012).

$$I_{SC}(G,T) = I_{SC-STC}\,(G/G_{STC}) + K_i(T - T_{STC}) \tag{3.51}$$

$$V_{oc}(G,T) = V_{oc-STC} - K_v(T - T_{STC}) + \alpha V_T In\ (G/G_{STC}) \tag{3.52}$$

$$I_{mp}(G,T) = I_{mp-STC}\,(G/G_{STC}) \tag{3.53}$$

$$V_{mp}(G,T) = V_{oc-STC} - K_v(T - T_{STC}) \tag{3.54}$$

where, K_v and K_i are the open circuit voltage and short circuit current temperature coefficient respectively.

3.6.1.3 Modeling and simulation of PV operation with MATLAB-Simulink

Modeling and simulation of PV in MATLAB involves the use of equation earlier presented in the previous sections. Figure 3.9 shows the Simulink block diagram of PV model developed in MATLAB.

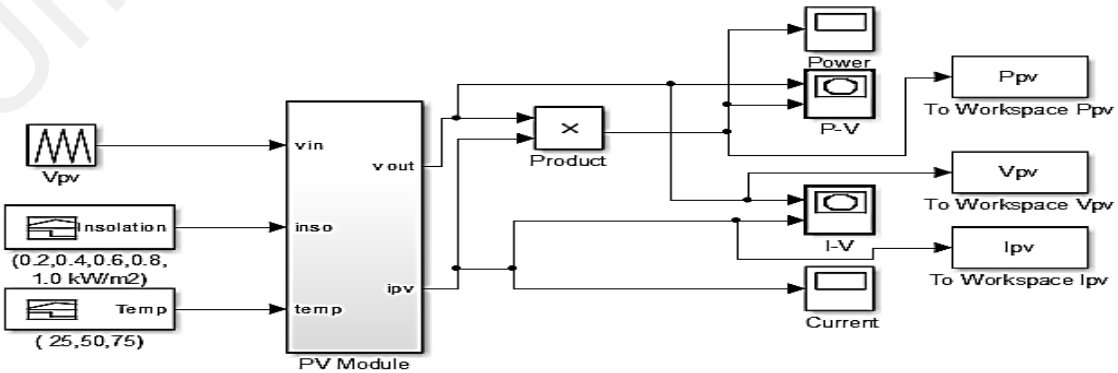

Figure 3. 6: Block diagram of PV model in MATLAB-Simulink

Inputs to this model are global solar radiation and temperature. Additional data are obtained from manufacturer's datasheet. The PV model is developed to obtain the I-V and P-V characteristic curve for validation purposes.

3.6.1.4 PV module output power

The system efficiency and output of a PV system vary for different day and different seasons of the year due to the changing local meteorological conditions. Therefore, adequate information on the daily and seasonal pattern of these meteorological data will enable energy planners to have a better understanding of the performance of a PV system. The PV output current at any solar radiation and temperature can be determined from equation (3.53), where I_{mp-STC} is the PV module maximum power point at standard test conditions. This is obtained from manufacturer datasheet. Since the PV output voltage and current are independent, the Newton-Raphson iteration method earlier described can be used to compute the output voltage if the output current is known.

The PV panel output power can be calculated as follows while considering the effect of solar radiation and temperature;

$$P_{PV-gen} = P_{mp-STC} \times (G/G_{STC})\,[1 + K_T(T_{cell} - T_{STC})] \tag{3.55}$$

where, P_{mp-STC}, G_{STC} and T_{STC} are respectively the module rated power, solar radiation and temperature at standard test conditions obtained from manufacturer's datasheet. *G* is the solar radiation on inclined surface (W/m^2), while K_T is the module power temperature coefficient. T_{cell} is the PV module cell temperature given as(Ismail, Moghavvemi, & Mahlia, 2013);

$$T_{cell} = T_{amb} + \left[\frac{(NOCT - 20}{800}\right] \times G \tag{3.56}$$

where, T_{amb} is the ambient temperature (^{0}C) and *NOCT* is the normal cell temperature (^{0}C) usually specified in manufacturer datasheet.

The overall generated power output of PV panels is obtained by multiplying panel output power (P_{pv-gen}) by the numbers of panel (N_{pv}) considered.

$$P_{pv(t)} = P_{pv-gen} \times N_{pv} \tag{3.57}$$

PV module performance usually degrades annually due to moistures and shading effects. The degradation rate is dependent upon the type of the module and the manufacturers. An annual degradation rate of 0.01 percent is suggested in (Bortolini, Gamberi, Graziani, Mora, & Regattieri, 2013) . In this study, annual incremental factor for the size of the PV array is proposed to compensate the degradation effect. To obtain the size of PV array in any particular year (n), the size in the previous year (n-1) will be added to the PV size at same year multiplied by the degradation rate, mathematically represented as;

$$P_{pv-sys(n)} = P_{pv-sys(n-1)} + DR \times P_{pv-sys(n-1)};$$

$$for\ n = 2, 3 \ldots \ldots project\ lifetime \tag{3.58}$$

where n is year under consideration and DR is the degradation rate.

3.6.2 Wind turbine model

Accurate modeling is vital in the design of an optimal system. Wind speed distribution at the selected sites, hub height and power output curve of chosen wind turbine, are important factors in determining the performance of wind turbines; therefore, all these factors have been properly accounted for in modeling the wind turbines.

3.6.2.1 Wind turbine energy output performance

Optimum operation of WECS at any particular sites depends upon its rated power, cut-in and cut-out wind speed with respect to the sites wind characteristics. For effective maximization of energy output of wind energy conversion system, it is very important to adequately select these parameters. The performance of a wind turbine at any particular sites can be examined by computing the amount of mean power produced over a period of time and the conversion efficiency (capacity factor) of the wind turbine.

Capacity factor is one of the important performance parameters of wind turbines and can be defined as the ratio of mean power output to the rated electrical power of the wind turbine given as(Mathew, 2006);

$$C_f = \frac{P_{e,ave}}{P_{eR}} = \left(\frac{e^{-\left(\frac{v_c}{c}\right)^k} - e^{-\left(\frac{v_r}{c}\right)^k}}{\left(\frac{v_r}{c}\right)^k - \left(\frac{v_r}{c}\right)^k} - e^{-\left(\frac{v_f}{c}\right)^k} \right) \tag{3.59}$$

where, $P_{e,ave}$ and P_{eR} are mean power output and rated power of the wind turbine respectively, while v_c, v_r and v_f are cut-in, rated and cutt-off wind speed respectively. High value of capacity factor reflects the effectiveness of the wind turbine in harnessing the wind energy potential at any particular place. In other word, for the purpose of cost effectiveness in wind power generation, the capacity factor should not be less than 0.25 (Mathew, 2006)

Therefore, the resultant energy output of wind turbine is given as;

$$E_{out} = C_f E_{rated} \tag{3.60}$$

Since the objective of this thesis is to utilize the available renewable energy resources (wind and solar) at the selected sites to supplement the conventional diesel generator and battery energy storage system in providing reliable electricity to the rural clinics, five (5)

small commercial wind turbine model with rated power ranging from 1 to 5kW is considered in this study. The selected wind turbine model and their specifications are given in Table 3.7 (Wood, 2010).

Table 3. 4: Specification of the five selected wind turbines

Parameter	**Type 1**	**Type 2**	**Type 3**	**Type 4**	**Type 5**
Model name	ABS 1000	FDQ 3.0-	Windera	Wind Cruiser	SNT-50
Rated output (kW)	1	1	3	3	5
Rated wind speed	12	9	11	12	11
Cut-in speed (m/s)	2.5	2	3	2	2.5
Cut-off speed (m/s)	25	25	25	25	25
Rotor diameter (m)	1.8	3	4	4	4.26
Hub Height (m)	17	17	12.5	17	18
Number of blade	5	3	3	3	3

For each sites, the yearly energy output and the capacity factor of each wind turbine based on Weibull distribution parameter are determined by Equations (3.35, 3.36, 3.37, 3.59 and 3.60).

3.6.3 Diesel generator model

Renewable energy systems are characterized by intermittent output and are therefore integrated with conventional power sources to ensure delivery of continuous power output. Diesel generator (DG) is a steady source of power in various HRES. The DG systems are designed to supply the load and also charge the battery energy storage system, if the renewable energy source along with battery is unable to supply the load. Proper energy balance is required for optimum system operation as the consumption of fuel is proportional to the power being supplied by the DG. The fuel consumption of the diesel generator, F_G (l/h) is modeled as dependent on the DG output power as (Dufo-López & Bernal-Agustín, 2008):

$$F_G = B_G \times P_{G-rated} + A_G \times P_{G-out} \tag{3.61}$$

where $P_{G-rated}$ is the nominal power of the diesel generator, P_{G-out} is the output power, while A_G and B_G represents the coefficients of fuel consumption curve as defined by the user (l/kWh).

The main concerns in optimization of diesel generator operation include; avoidance of partial loading, insufficient run-time to attain operating temperature as well as avoidance of excessive operation. The optimum diesel generator operating range should be 70-89% (Torres & Lopes, 2013). A single-phase diesel generator, with capacity for both manual and induction starting, including self-regulation with the use of a governor to supply precise fuel quantity at different load requirement is considered in this study. The governor works to keep the generator speed approximately constant at any load level. Figure 3.10 shows the main component of the diesel generator control.

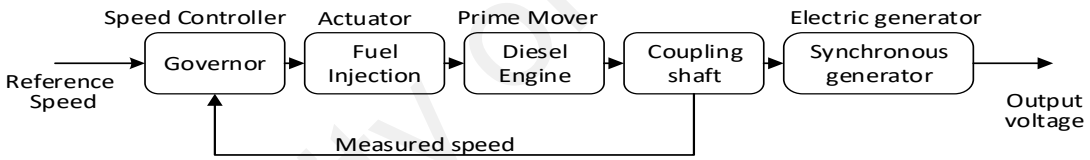

Figure 3. 7: Main component of a typical diesel generator control

3.6.4 Battery energy storage

Due to random behaviors of renewable energy resources (varying weather condition), battery capacity changes constantly in hybrid system. At any time *t*, the battery capacity dependent on its previous state of charge (SOC), available energy from the RE sources in the HRES and the system load demand. The charging process of the battery occurs, whenever the energy output of PV modules and wind turbines is greater than the load demand. The battery charge capacity at this period can be described as (Diaf, Diaf, Belhamel, Haddadi, & Louche, 2007);

$$C_B(t) = C_B(t-1).(1-\sigma) + \left[P_T(t) - \frac{P_L(t)}{\eta_{inv}}\right] \times \eta_{Batt} \quad (3.62)$$

where $P_L(t)$ is the load demand, σ is the battery self –discharging rate, η_{inv} and η_{Batt} are the inverter and battery efficiency respectively. While, $P_T(t)$ is the total power generated by the RE sources in the hybrid system at time *t* , given as:

$$P_T(t) = N_{pv}P_{pv} + N_{wt}N_{wt} \quad (3.63)$$

Where P_{pv} is the power output of PV panel, P_{wt} is output power of the wind turbine, N_{pv} and N_{wt} are number of PV module and wind turbine respectively.

On the other hand, whenever the total power generated by the RE sources is insufficient to meet the load demand the battery bank is in discharge mode. Therefore, the nominal capacity of battery and the charge quantity of the battery bank at this period can be respectively model as:

$$C_{Batt}(Wh) = \frac{P_L(t) \times AD}{\eta_{Batt} \times \eta_{inv} \times DoD} \quad (3.64)$$

$$C_B(t) = C_B(t-1).(1-\sigma) + \left[\frac{P_L(t)}{\eta_{inv}} - P_T(t)\right] / \eta_{Batt} \quad (3.65)$$

where *DoD* is battery depth of discharge while, *AD* is the chosen number of days of autonomy. During this process, the battery discharge efficiency (η_{batt_disch}) is equal to 1, while it varies between (0.65–0.85) during charging period depending on the charging current. At any time *t,* the battery charge capacity is subject to the following constraints:

$$SOC_{min} \leq C_B(t) \leq SOC_{max} \quad (3.66)$$

where SOC_{max} and SOC_{min} are the maximum and minimum allow battery state of charge respectively. At this point, the maximum charge quantity of battery bank (SOC_{max}) takes

the value of nominal capacity of battery bank (C_{Batt}) and the minimum charge quantity of battery bank (SOC_{min}) is determined by the maximum depth of discharge.

$$SOC_{min} = (1 - DOD)C_{Batt} \tag{3.67}$$

The operational lifetime of battery can be prolonged if *DOD* is set within the range (30–50) % depending on the manufacturer's specifications.

3.7 Hybrid system optimal sizing

In this study, HOMER has been employed in the simulation, optimal sizing, sensitivity analysis as well as techno-economic evaluation of the proposed hybrid renewable energy system in the selected sites. The entire process in HOMER is divided into three parts; simulation, optimization and sensitivity analysis. In the simulation process, HOMER modeled the performance of each component of the proposed hybrid system on an hourly basis to ensure best possible matching between the load and the supply as well as determination of techno-economic feasibility of each system configuration. In the optimization process, the software simulate various system configurations to determine the configurations that satisfy the technical constraints and meet the load demand at minima life-cycle cost. HOMER does this by creating a list of feasible system sorted according to the least NPC. In the sensitivity analysis part, HOMER performs multiple optimization with different input variable range, to determine the effect of changes in the input parameters on the selected system configuration.

Inputs to the software include; site's load profile, renewable energy resource's data, fuel price, system controls parameters, constraint parameter as well as component's technical and economics details. The optimal sizing of hybrid system component involves different combination of PV array, wind turbine, diesel generator, converter, batteries, that meets the load demand of the selected rural healthcare facilities.

Stand-alone diesel system, hybrid PV–diesel system with battery, hybrid wind–diesel system with battery, PV–wind–diesel system with battery configurations were analysed in this study. The economic feasibility of each configuration is based on the net present cost (NPC); two other parameters, including levelized cost of energy (COE) and renewable fraction (RF) were also employed as performance criteria for the selection of the optimum configuration. CO_2 emissions (tons/yr.) and diesel consumption (l/yr.) were considered for the analysis of environmental friendly solution. All the input parameters are fed into the HOMER to determine the optimal system from the various configurations. The amount of power generated by each configuration, were compared to the annual load demands to ensure it meets the load demands. A comprehensive framework of optimal sizing and selection of different configurations of energy resources in each of the selected locations is shown in Figure 3.11.

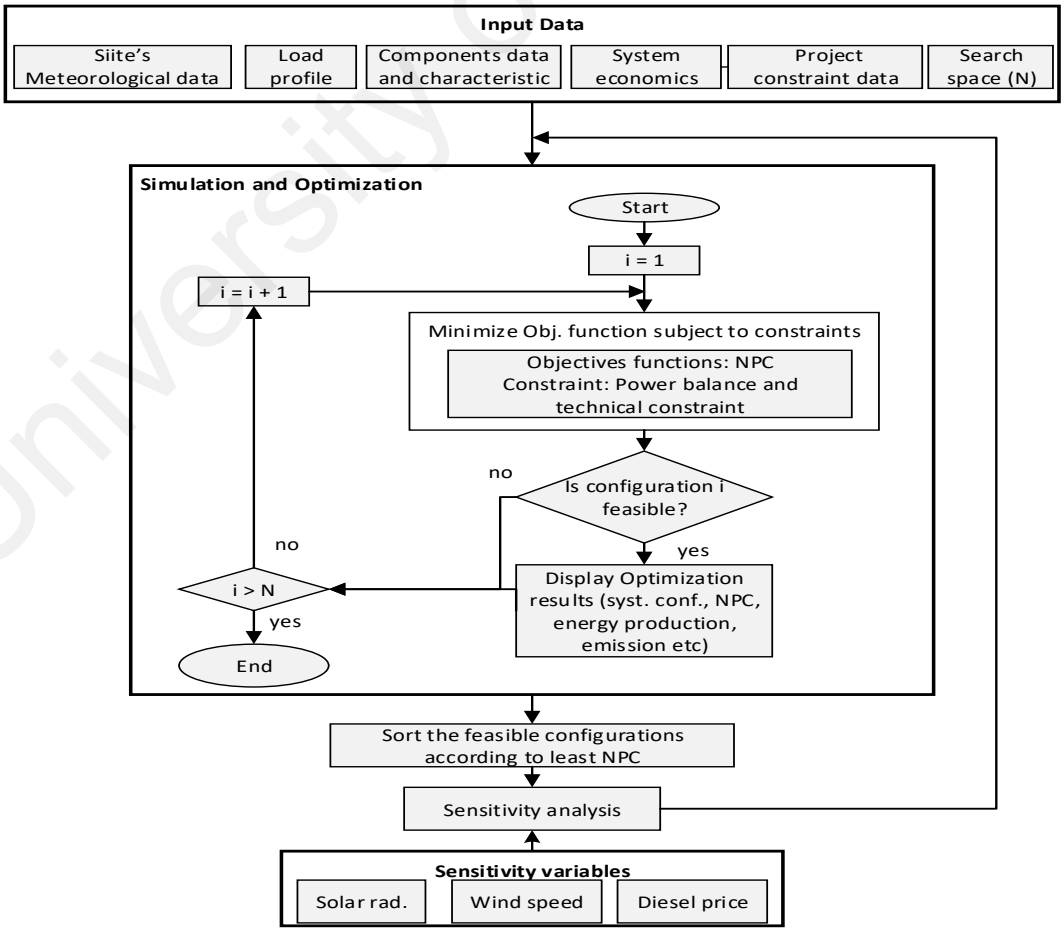

Figure 3. 8: Comprehensive framework of HOMER optimal sizing procedure

3.7.1 HOMER input data

Six types of data are required by HOMER for simulation and optimization. These include meteorological data, load profile, equipment characteristics, search space, economic and technical data. The following subsections described them in details.

3.7.2 Meteorological data

Hourly values of global solar radiation, wind speed and temperature data obtained are not available at the selected sites, however the available monthly averages were synthesis to hourly data based on the algorithm earlier described for its conversion in HOMER. These data serve as energy resources input to the software. HOMER utilized these data to compute power output of solar PV array and wind turbines. Table 3.8 present the monthly mean hourly data of solar radiation, wind speed and temperature of the respective sites inputted into the HOMER software, while figure 3.12 and 3.13 respectively represent the synthetic hourly solar radiation and wind speed data obtained from the monthly averages using the earlier described algorithm.

Table 3. 5: Monthly mean hourly solar radiation, wind speed and temperature data of the selected sites

Sites	**Meteorological data**	**Jan**	**Feb**	**Mac**	**Apr**	**May**	**Jun**	**Jul**	**Aug**	**Sep**	**Oct**	**Nov**	**Dec**
Iseyin	Sol. Rad (kWh/m^2/d)	4.66	5.07	5.29	4.93	4.72	4.26	3.36	2.94	3.77	4.43	5.15	4.92
	Wind Speed (m/s)	4.21	4.36	4.54	4.71	4.33	4.35	4.20	4.26	3.94	3.61	3.48	3.91
	Temperature (^{0}C)	27.3	28.8	29.2	27.7	27.0	25.8	24.6	24.1	25.0	26.0	27.4	27.2
Sokoto	Sol. Rad (kWh/m^2/d)	5.00	5.61	5.96	6.03	5.63	5.43	4.73	4.45	5.12	5.51	5.36	5.02
	Wind Speed (m/s)	8.95	8.63	7.35	7.59	8.70	9.03	7.94	6.23	5.81	6.02	7.50	7.86
	Temperature (^{0}C)	25.3	27.8	31.4	33.6	32.8	30.6	28.1	27.3	28.3	29.6	27.9	25.5
Maiduguri	Sol. Rad (kWh/m^2/d)	5.24	5.80	6.19	6.30	5.93	5.47	5.13	4.80	5.53	5.82	5.56	5.05
	Wind Speed (m/s)	4.94	5.90	6.10	5.80	5.81	6.06	5.66	4.62	4.49	4.55	5.10	4.68
	Temperature (^{0}C)	22.0	24.7	29.1	32.5	32.9	31.1	28.3	26.9	28.2	28.6	26.0	22.7
Jos	Sol. Rad (kWh/m^2/d)	5.70	6.15	6.09	5.34	4.82	4.64	4.20	4.04	4.64	5.03	5.71	5.66
	Wind Speed (m/s)	9.15	9.15	9.15	9.15	9.15	9.15	9.15	9.15	9.15	9.15	9.15	9.15
	Temperature (^{0}C)	19.7	21.6	24.1	24.6	23.6	22.0	20.9	20.7	21.7	22.1	20.7	20.1
Enugu	Sol. Rad (kWh/m^2/d)	4.60	5.12	4.80	4.62	4.71	4.34	3.61	3.46	4.15	4.77	5.24	4.93
	Wind Speed (m/s)	5.62	5.66	6.30	6.22	5.35	5.21	5.48	5.44	4.85	4.56	4.12	4.95
	Temperature (^{0}C)	27.5	29.0	29.5	28.6	27.5	26.6	25.9	25.7	26.2	26.6	27.4	26.9
Port Harcourt	Sol. Rad (kWh/m^2/d)	4.76	5.14	4.74	4.76	4.54	4.13	3.35	3.53	3.71	4.24	4.56	4.82
	Wind Speed (m/s)	3.40	3.89	3.90	3.98	3.71	3.67	3.67	3.93	3.64	3.19	2.91	2.86
	Temperature (^{0}C)	27.0	28.1	28.3	28.2	27.4	26.6	25.8	25.8	26.1	26.6	27.1	26.8

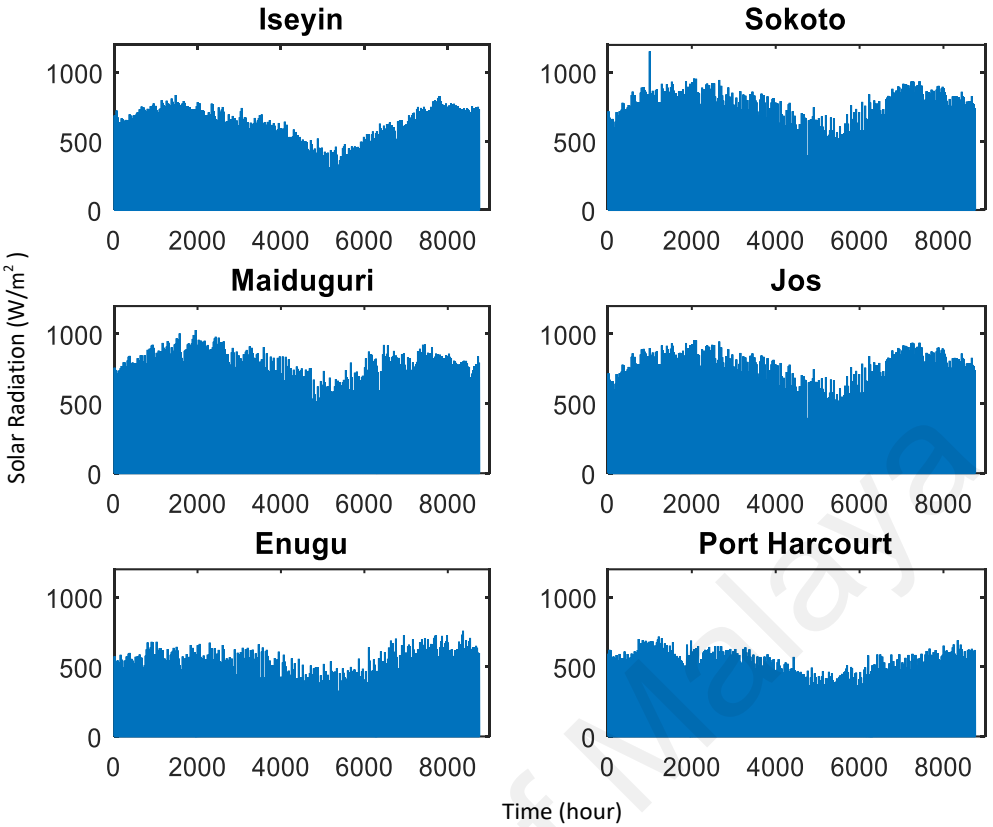

Figure 3.12: Synthetic hourly solar radiation data for the selected sites

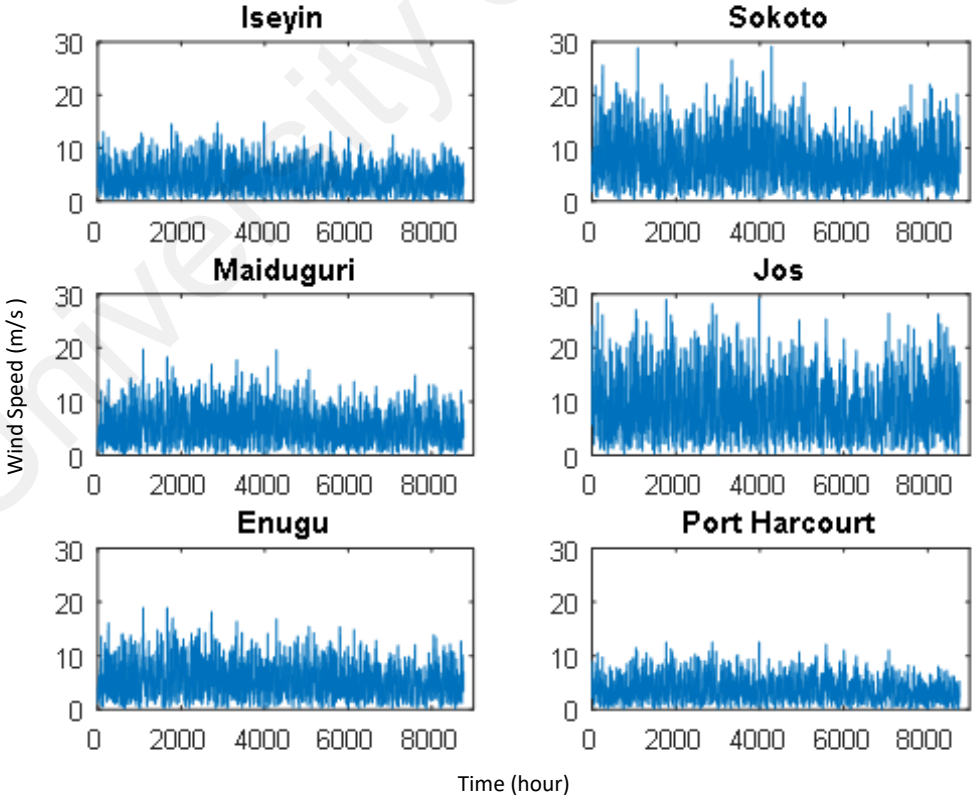

Figure 3.13: Synthetic hourly wind speed data for the selected sites

3.7.2.1 Clinics load profile

The load profile of the respective rural health clinic in the considered sites is an essential input parameter to the HOMER model, since optimal sizing of different energy sources and the battery storage device depends on the load profile. As earlier mentioned, each of the rural healthcare facilities considered for this study is classified as a category II rural health clinic according to United States Agency for International Development (USAID, 2014), hence assumed to have identical load profile.

Therefore, the computation of the energy demand of each equipment presented in Table 3.5 with their expected operating hours known as watt-hour demand is shown in Figure 3.14 for the rural health facilities in the selected sites. Based on this profile, average daily energy demand and the peak load are found to be approximately 21.9kWh and 3.75kW respectively.

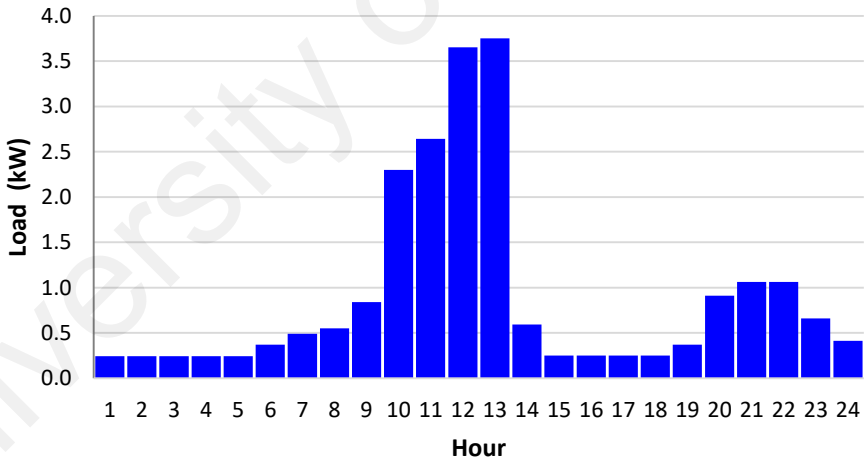

Figure 3. 14: Daily load profile of the selected healthcare facilities

It should be noted that, all the equipment presented in Table 3.5 are not expected to operate simultaneously, because each has specific daily hours of operation. Major load occurs during the daytime (9am to 1pm) and nighttime (7-10pm). This is due to the nature of the rural settings where the dwellers visit the clinic in the morning/late night after the day work. Based on this variation, a day-to-day random noise of 10% and hour-to-hour random variability of 15% is specified in HOMER. This is done to check the effect of the

daily and hourly load variation on the hybrid system configuration to avoid underestimating the peak load demand of the proposed system.

3.7.2.2 Hybrid system components data

Assumptions regarding components pricing and sizing as adopted in the proposed hybrid system, are expressed below:

a) A 36-cell mono-crystalline PV module with rated capacity 250W_p, manufactured by Canadian Solar Company was selected for simulation. The current PV module price in Nigeria's market is $3,160/kW, while the installation cost is $40/kW (Ngpricehunter). Therefore, the capital cost and replacement cost of 1kWp PV array were taken as $3200 and $3200 respectively. The lifetime of PV arrays was taken as 25 years. The de-rating factor that accounts for losses due to temperature effects, dirt from the PV module's surface and wiring losses was considered as 80%, and the ground reflection of the modules were taken as 20%. Different sizes of PV arrays were considered to obtain the optimal size for each site.

b) Three different wind turbine model (1kW, 3kW and 5kW) with technical specifications given in Table 3.7 is considered for the hybrid system configurations in each site. The initial cost, replacement cost and cost of maintenance for each type are specified in the Table 3.7. In order to find an optimal size, different sizes of each model were analyzed. The operational lifetime of the turbines varies between 15 to 20 years.

c) The initial cost of a 1kW AC diesel generator is $200, with a replacement cost of $200 and maintenance cost of $0.05/hr (Ngpricehunter). Two different sizes (5kW and 7.5kW) of diesel generator was considered. The operating lifetime

of a diesel generator was taken as 15,000 hours with a minimum load ratio of 25%.

d) A bi-directional converter is added to maintain the flow of energy between the alternating current (AC) and direct current (DC) components. It functions as a rectifier when it converts AC to DC, and as an inverter on the other way around. The initial capital and replacement cost of the converter used for this study were taken as $245/kW and $245/kW respectively (Ngpricehunter). The operational and maintenance cost is taken as $10/year (Ismail et al., 2013). The efficiency of the converter is 90% and 85% for the rectifier, while the lifetime was taken as 10 years(mygadgetsmall). Different sizes of converters were considered during the analysis.

e) Trojan L16P type battery with rated 6V nominal voltage, 2kWh nominal capacity, 1,075 throughput, 85% round trip efficiency and 30% minimum state of charge is considered for this study. The initial cost of one unit is $330 (Ngpricehunter). Replacement and operational maintenance costs were assumed as $300 and $10/year respectively (Adaramola, Paul, et al., 2014). In order to find an optimal configuration, the battery bank was assumed to contain a different number of batteries. Each battery string contains 10 batteries, and the lifetime energy of each battery is 1,075kWh throughput(Ngpricehunter).

3.7.2.3 System economic parameters

In HOMER, the system life-cycle cost is represented by total net present cost (NPC). The NPC is a composite of system component's initial capital cost, replacement cost, annual operating and maintenance cost as well as fuel costs as earlier discussed in section 2.8.1.1. However, in a PV/wind/diesel/battery hybrid system, total annualized cost of the entire hybrid system can be represented as;

$$C_{ann,Tot} = \sum_{N=1}^{N_{pv}} C_{ann,pv} + \sum_{N=1}^{N_{wt}} C_{ann,wt} + \sum_{N=1}^{N_{batt}} C_{ann,DG} + \sum_{N=1}^{N_{batt}} C_{ann,bat} + \sum_{N=1}^{N_{conv}} C_{ann,conv} \quad (3.68)$$

where, N_{pv}, N_{wt}, N_{DG}, N_{bat}, and N_{conv} are numbers of PV modules, wind turbine, diesel generator, battery and converter respectively. While $C_{ann,pv}$, $C_{ann,wt}$, $C_{ann,DG}$, $C_{ann,bat}$ and $C_{ann,conv}$ are total annualized cost for each components (PV modules, wind turbine, diesel generator battery and converter) as compute using Equation (2.14).

In this study, the project lifetime is considered 25 years and the current annual interest rate in the Nigeria is 11%, while the inflation rate stand at 15.1%. These economic parameters are needed to compute the CRF given in Equation (2.16). Thereafter, HOMER uses the CRF to compute the NPC for various system configurations. HOMER aim is to minimize the total net present cost (NPC) and cost of electricity (COE) by finding the optimal system configuration that matches the load demand and satisfies these constraints. It should be noted that all economic factors considered in HOMER are calculated in constant dollar (US$) terms. As at the time of this research work, USD1 is equivalent to N282.25 Nigeria's naira.

3.7.2.4 System technical constraints

Constraints are pre-determined conditions the systems must fulfil in HOMER to ensure realistic optimal solution; otherwise, HOMER neglects those systems that do not content the defined constraints. In this study, the maximum renewable fraction (RF) ranges from 0-100% are considered, while maximum unserved energy is assumed to be 0%. In addition, 0% maximum annual capacity shortage was considered in the simulation. The maximum allowable capacity shortage factor is a ratio of the total capacity shortage and the total annual electric load, which represent the amount of time to which the system

could not meet the load demand and its reserves. However, this is not the case in this system due to the nature of the load and the intended application which requires 100% reliability. Hourly load variation of 10% is considered in the simulation with operating reserve accounting for sudden spikes in the system. In the case of PV panel's output, 25% reserve is considered this is due to its inherent dependence on solar irradiance leading to unpredictable output.

3.7.2.5 System control/energy management

System control parameter defines how the system models the operation of battery and generators in the hybrid system. A dispatch strategy is a set of rules that controls the operations of the diesel generator and the battery bank. Two types of dispatch strategies are available in HOMER, namely; load following and cycle charging. In the load-following strategy, a generator produces power that is sufficient only to serve the load and does not charge the battery bank. Conversely, in the cycle-charging strategy, the generator operates at its maximum rated capacity to serve the load and charges the battery bank with the excess power. In the proposed system, cycle-charging strategy has been considered. This means that HOMER will simulate each system using this dispatch strategy and subsequently determine the optimal configuration.

In a multi-source hybrid energy system, an overall control/energy management system to manage the energy flow within the various connected energy source and the load is essential. To this aim, an energy management/control system has been designed for the optimization of the energy flows among the various energy sources and the load. The control strategy is designed to operate in different modes according to the flowchart in Figure 3.15.

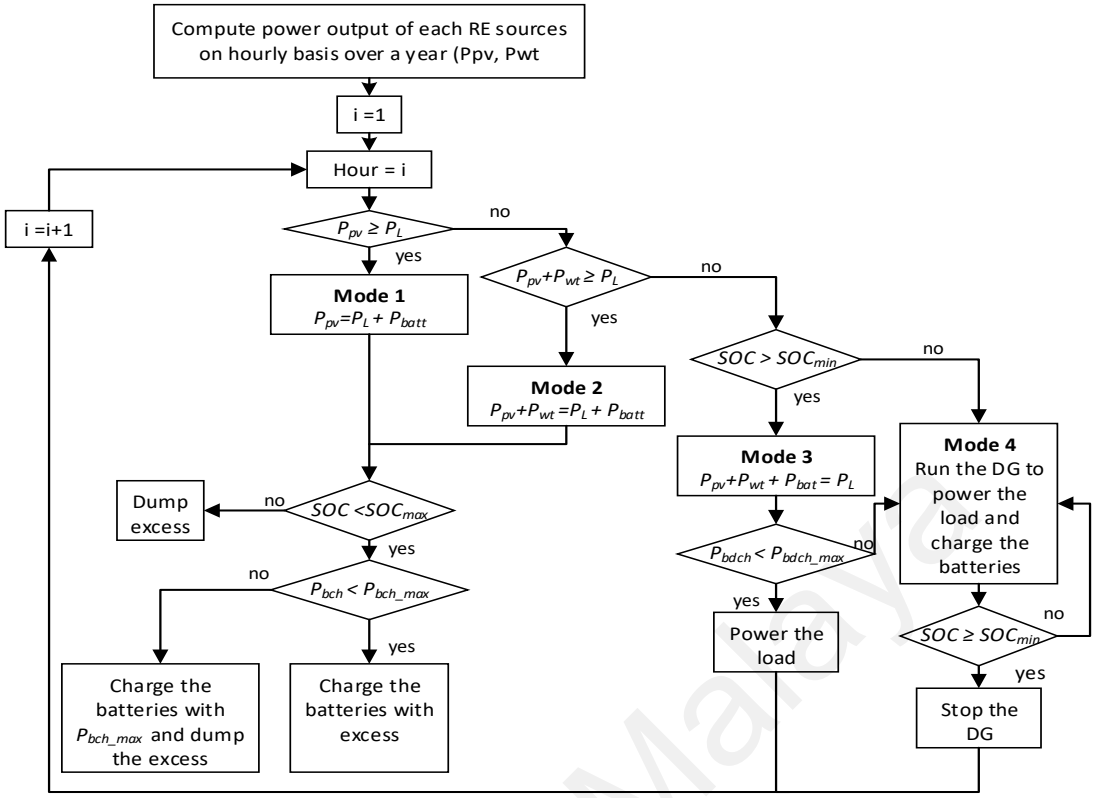

Figure 3. 9: Flowchart of the energy management system adopted in HOMER

In this control system, priority is given to RE sources to supply the load, that means, under normal operating condition the power output of solar PV (P_{pv}) and wind turbine (P_{wt}) will supply the load while excess energy will be used to charge the battery until maximum state of charge (SOC_{max}) is reached. Any further excess energy can be used by dump load. In the case of insufficient energy from either the RE sources or the battery to supply the load, a conventional diesel generator will be operated automatically to supply the load and charge the battery. The supervisory control is responsible for switching from one operating mode to another depending on the atmospheric conditions, the load demand, and the battery SOC. The decision to operate any of the energy sources and to charge/discharge the battery takes place every hours upon the energy balance computation.

The summaries of the techno-economic details and system constraints utilized in the modeling proposed hybrid system is presented in Tables 3.9 and 3.10 respectively.

Table 3. 6 Techno-economic details of proposed hybrid system components

Components	Parameters	Value
PV module	Rated capacity (W_p)	250
	Efficiency at STC (%)	13
	Derating factor (%)	80
	Capital cost ($/W)	3.2
	Replacement cost ($/W)	3.2
	Operating and maintenance cost ($/yr.)	10
	Lifetime (yr.)	25
Wind turbine	Rated capacity (kW)	1 , 3, 5
	Rotor diameter (m)	3, 4, 4.26
	Cut-in wind speed(m/s)	2, 2, 2.5
	Cut-off wind speed (m/s)	25, 25, 25, 25, 25
	Rated wind speed (m/s)	9, 12, 11
	Capital cost ($)	2034, 3095,15016
	Replacement cost ($)	1104, 1857, 7038
	Operating and maintenance cost ($/yr.)	50, 60, 100
	Lifetime (yr.)	20, 15, 20
Diesel generator	Rated capacity (kW)	5kW, 7.5kW
	Minimum load ratio	30
	Fuel curve ratio(l/hr/kW)	0.33
	Fuel curve intercept (l/hr/kW)	0.05
	Fuel price($/L)	1.1
	Capital cost ($/kW)	200
	Replacement cost ($/kW)	200
	Operating and maintenance cost ($/hr)	0.5
	Lifetime (hr.)	15000
Battery	Model	Trojan L16P
	Nominal voltage (V)	6
	Nominal capacity (kWh)	2
	Minimum state of charge	30
	Round trip efficiency (%)	85
	Battery per strings	10
	Capital cost ($/unit)	330
	Replacement cost ($/unit)	300
	Operating and maintenance cost ($/yr)	10
	Lifetime throughput	1,075
Converter	Rated Power(kW)	5
	Efficiency (%)	85-90
	Initial capital cost($/kW)	245
	Replacement cost($/kW)	245
	O & M cost ($/yr.)	10
	Operational lifetime(yr.)	10

Table 3. 7: Model system economic, control and technical constraints

Parameters	Values
Simulation time step (min)	60
Dispatch strategy	cycle charging
Project lifetime (yr)	25
Annual interest rate (%)	11
Infulation rate(%)	15.1
Diesel price ($)	0.75
Maximum renewable fraction (%)	100
Maximum unserved energy(%)	0
Maximum annual capacity shortage(%)	0

3.7.3 Optimization

Assessment of optimal system configurations is carried out by optimizing the objective function of total life-cycle cost of the entire hybrid system represented in Figure 4.16. Optimal value of decision variable is determined during the optimization process. The decision variables considered for this study are based on the available resources and the load demand. This includes; size of PV panel, number of wind turbine, number of battery and the size of converter. The objective function is given as:

Minimize:

$$C_{ann} = \sum_{j} (C_{ann,cap.} + C_{ann,rep.} + C_{ann,O\&M}) \tag{3.69}$$

where *j* is the number of units of the system component (solar panel, wind turbine, diesel generator, battery and converter). $C_{ann,cap.}$, $C_{ann,rep.}$ and $C_{ann,O\&M}$ is the annualized capital, replacement, operating and maintenance cost of each system components. The equation can be rewrite as:

$$C_{ann}(j) = N \times \{[C_{ann,cap.} + C_{ann,rep.} \times K_j(i, L_j, y_j)] \times CRF(i,n) + C_{ann,O\&M}\} \tag{3.70}$$

where *N* is the number of components/capacity, *CFR* is capital recovery factor earlier described in Equation (2.16), where *n is* project lifetime and *i* is the real interest rate, which is a function of nominal interest rate (i_{nom}) and annual inflation rate (*f*) defined as;

$$i = \frac{i_{nom} - f}{i + f} \tag{3.71}$$

K is single payment present worth factor given as;

$$K_j(i, L_j, y_j) = \sum_{x=1}^{y_j} \frac{1}{(i+1)^{x \times L_j}} \tag{3.72}$$

where L and y are respectively the useful lifetime and the number of replacement of component during the project lifetime (n).

For each search space in the optimization process, the objective function is minimized subject to the set constraint. The constraints include; energy balance constraint (loss of power supply probability), battery charging and discharging constraints and generator technical constraints. Figure 3.16 present the schematic of the proposed hybrid system.

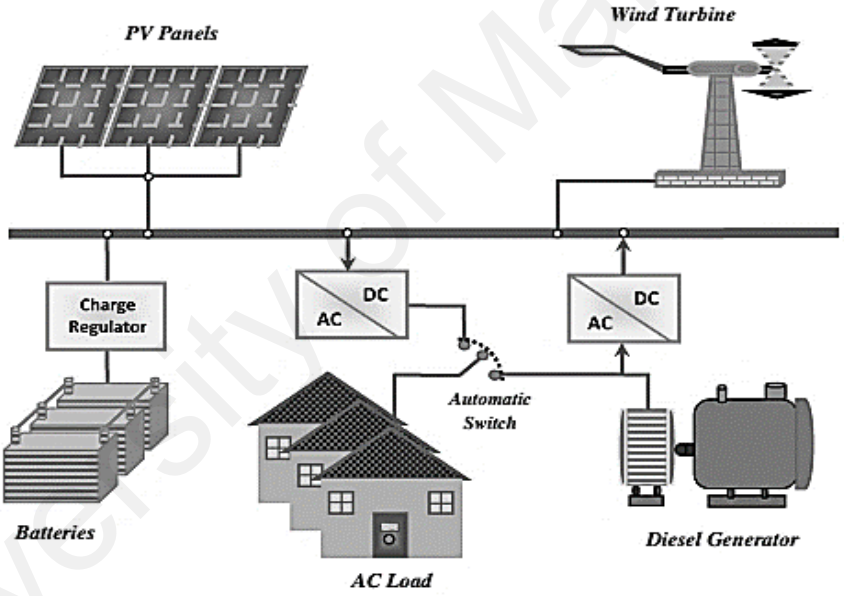

Figure 3. 10: The proposed hybrid system configuration

3.7.4 Sensitivity analysis

Sensitivity analysis helps in the exploration of the effect of the changes in the available resource and economic condition. This analysis provides the range of the variables for which it makes sense to include the renewable energy in the system design. To this aim, three most dominant input parameter of HOMER model, namely; solar radiation, wind speed and diesel price were selected and varied by $\pm$ 20% for each site. For each range of the sensitivity parameter, simulation and optimization are performed and new feasible

and optimal system configuration obtained. The sensitivity values of each parameter in the selected site are presented in Table 3.11.

Table 3. 8: Sensitivity parameter in the selected sites

Site	**Sensitivity variables**	**Variation**								
		-20%	**-15%**	**-10%**	**-5%**	**0%**	**5%**	**10%**	**15%**	**20%**
Iseyin	Sol. Radiation	3.57	3.79	4.01	4.24	4.46	4.68	4.91	5.13	5.35
	Wind Speed	3.33	3.54	3.74	3.95	4.16	4.37	4.58	4.78	4.99
Sokoto	Sol. Radiation	4.26	4.52	4.79	5.05	5.32	5.59	5.85	6.12	6.38
	Wind Speed	6.10	6.49	6.87	7.25	7.63	8.01	8.39	8.77	9.16
Maiduguri	Sol. Radiation	4.46	4.73	5.01	5.29	5.57	5.85	6.13	6.41	6.68
	Wind Speed	4.25	4.51	4.78	5.04	5.31	5.58	5.84	6.11	6.37
Jos	Sol. Radiation	4.14	4.39	4.65	4.91	5.17	5.43	5.69	5.95	6.20
	Wind Speed	6.90	7.33	7.76	8.19	8.62	9.05	9.48	9.91	10.3
Enugu	Sol. Radiation	3.62	3.85	4.08	4.30	4.53	4.76	4.98	5.21	5.44
	Wind Speed	4.25	4.51	4.78	5.04	5.31	5.58	5.84	6.11	6.37
Port Harcourt	Sol. Radiation	3.49	3.71	3.92	4.14	4.36	4.58	4.80	5.01	5.23
	Wind Speed	2.85	3.03	3.20	3.38	3.56	3.74	3.92	4.09	4.27
All sites	Diesel price	0.60	0.64	0.68	0.71	0.75	0.79	0.83	0.86	0.90

3.8 Chapter summary

This chapter begins with analysis of method of renewable energy resource's data collection for the sites considered in this study; this is followed by the prediction of meteorological data (mainly solar radiation) using soft-computing techniques to cater for the missing dataset. ANFIS that merges the learning power of ANNs with the knowledge representation of fuzzy logic has been employed as one of the soft-computing techniques, because it is seen to exhibit good learning and prediction capabilities when used in various engineering applications. Renewable energy resources and energy demand assessment was also conducted in this chapter with a view to determine the feasibility of employing solar and wind resources in the energy mix of rural healthcare facility. Also discussed in this chapter, is the methodology employed in the modeling of proposed hybrid system components for effective analysis of the entire system. For the purpose of PV module

parameter extraction and operation, an iterative code has been developed in MATLAB-Simulink, while the performance of the selected wind turbine model is evaluated based on capacity factor and energy production capacity of each wind turbine. Due to random behaviors of renewable energy resources, battery bank has been modeled to charge and discharge according to developed energy management strategies in HOMER.

Finally in this chapter, is the operational description of the optimization tool employed for sizing of hybrid system component with minima life-cycle cost while meeting the clinic load demand. Techno-economic specifications of hybrid system components as well as various system constraints in the modeling and optimization were also presented in this section. The chapter concludes with sensitivity analysis of some important inputs parameter of the HOMER software. This is done to examine the impact of variation in the values of inputs parameter on the cost of energy production in the hybrid system.

CHAPTER 4: RESULTS AND DISCUSSIONS

The chapter presents the results of various sections of the study earlier highlighted in the previous chapters. A discussion of each of these results is also included within this chapter. Foremost in this chapter is the results of solar radiation prediction with ANFIS, followed by the results of renewable energy resources assessment, results of MATLAB Simulink modeling of PV module, results on the performance of selected wind turbine and finally the results of optimal sizing of the entire hybrid system in the selected rural healthcare facilities .

4.1 Solar radiation prediction

The performance results of soft-computing techniques namely, ANFIS for predicting solar radiation for selected sites in the case study is present in this section. Initially, the ANFIS model employed for this study was trained with data measured. The ANFIS inputs were fuzzified using three bell-shaped membership functions. Following the training process, the ANFIS network was tested for determination of the solar radiation. According to the model, input parameters (monthly mean minimum temperature, monthly mean maximum temperature and monthly mean sunshine duration) and the output (solar radiation) were collected and defined as the learning technique. The percentage of data selected for training and testing has been carefully tested based on the minimal error obtained in the statistical indicator as shown in Table 4.1. Initially the ratio 50/50 were tested, follow by 60/ 40, then 70/30 and finally 80/20. In all this tests, we found out the 70/30 produce least error. Therefore, 70% of data were used for sample training and the remaining 30% for testing.

Table 4. 1: Training and testing data selection

Metrics	50/50		60/40		70/30		80/20	
	Training	**Testing**	**Training**	**Testing**	**Training**	**Testing**	**Training**	**Testing**
RMSE	1.3260	1.6527	1.2865	1.6467	1.2511	1.6217	1.2872	1.6691
MAPE	6.5679	8.5078	6.4800	8.5097	6.1730	8.2236	6.2072	8.3131

The ANFIS decision surface for solar radiation estimation using the three input parameters is illustrated in Figure 4.1.

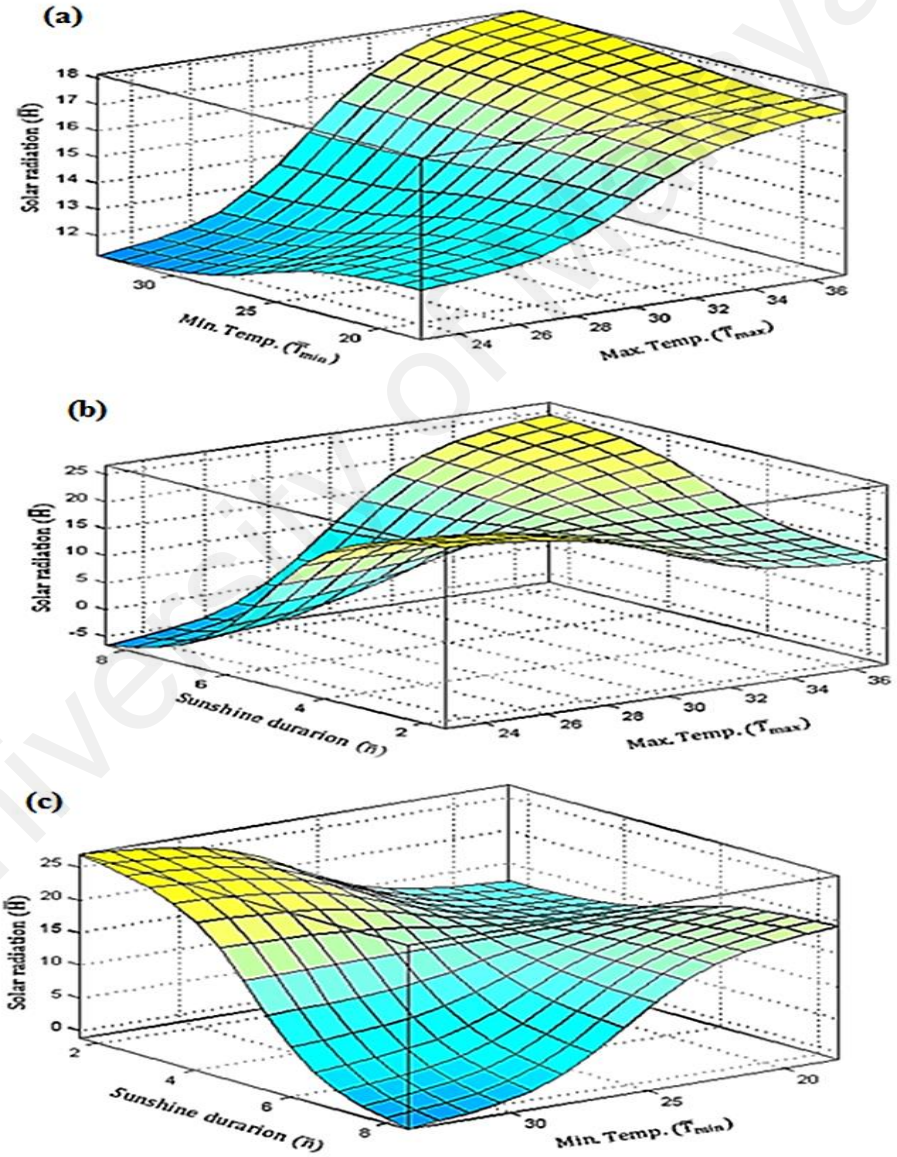

Figure 4. 1: ANFIS decision surfaces for solar radiation estimation. (a) max and min temperature (b) sunshine duration and max temperature (c) sunshine duration and min temperature

According to the decision surface, the solar radiation variation is evident in relation to the three input parameters. This figure shows the influence of the three input meteorological parameter on the solar radiation. It is worth noting that the maxima values solar radiation occurs at the maxima values of $\bar{T}_{min}$ and $\bar{T}_{max}$, while the maxima value of solar radiation occurs for the minimal sunshine duration ($\bar{n}$).

The suitability level of proposed ANFIS model is compared to ANN and GP. The estimated solar radiation is represented in Figure 4.2 in the form of a scatterplot by the three methodologies, ANFIS, ANN and GP.

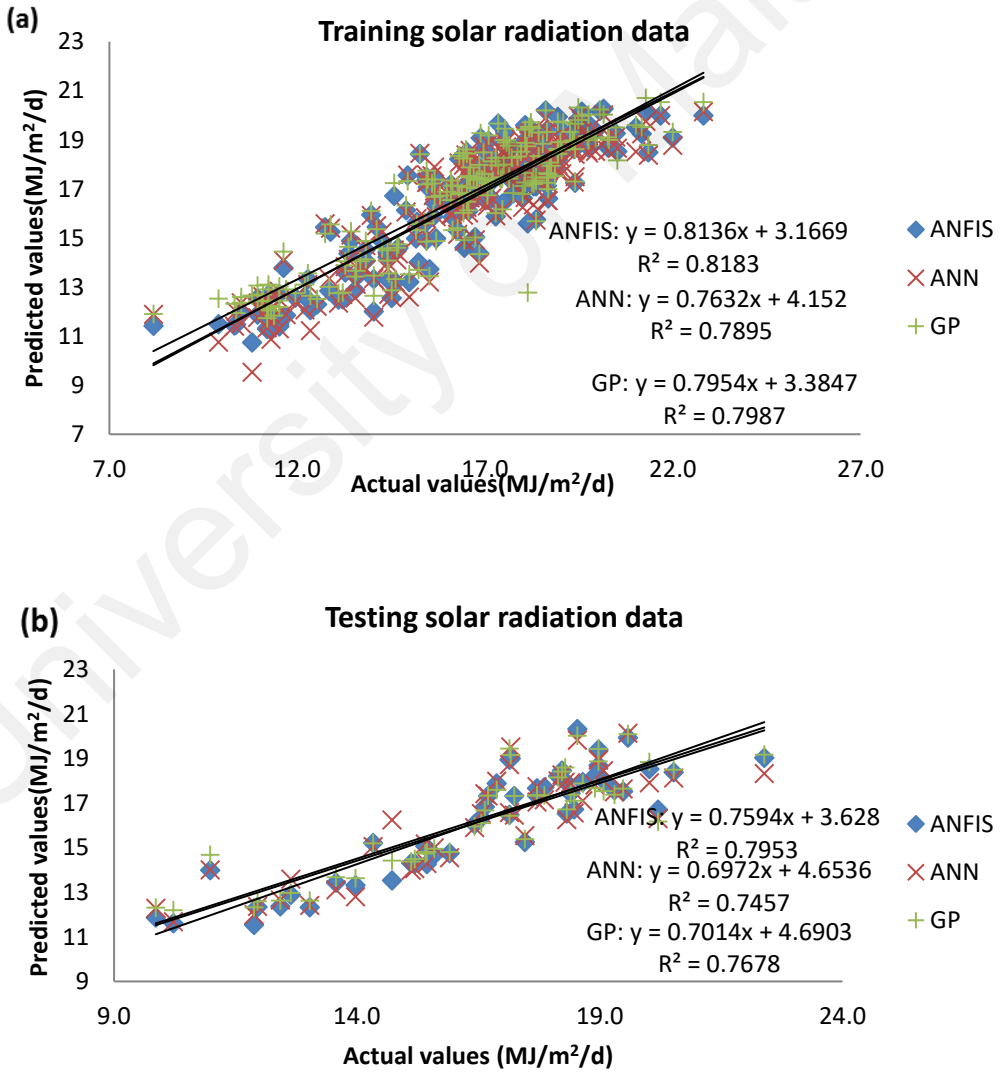

Figure 4. 2: Scatter plots of predicted and experimental data with the three machine learning models (a) Training, (b) Testing

The training data of solar radiation and predicted values are shown in Figure 4.2(a), while Figure 4.2(b) presents testing and predicted values. In addition, these show the comparisons between measured and predicted solar radiation by ANFIS, ANN and GP techniques. It can be observed that ANFIS model has better predictions ability for global solar radiation prediction than ANN and GP methods based on the obtained R^2-value.

4.1.1 Model performance analysis and comparison

Performance evaluation of the proposed ANFIS model was carried out to determine the importance of each independent input variable on the output. Root mean square error (RMSE), coefficient of determination (R^2), correlation coefficient (r) and mean absolute percentage error (MAPE) served to evaluate the differences between the predicted and actual values for all the models. According to Figure 4.2(a), the R^2 value is high; it is clear that most of the points fall along the diagonal line on the ANFIS prediction model. Consequently, it can be concluded that the prediction result has a good agreement with the measured data using this model. Figure 4.3 represents solar radiation forecasting for period of 48 months using the three model in comparison with the measured data in Iseyin site. According to this figure, the ANFIS model captures virtually all extreme solar radiation data values. The number of either overestimated or underestimated values produced is limited.

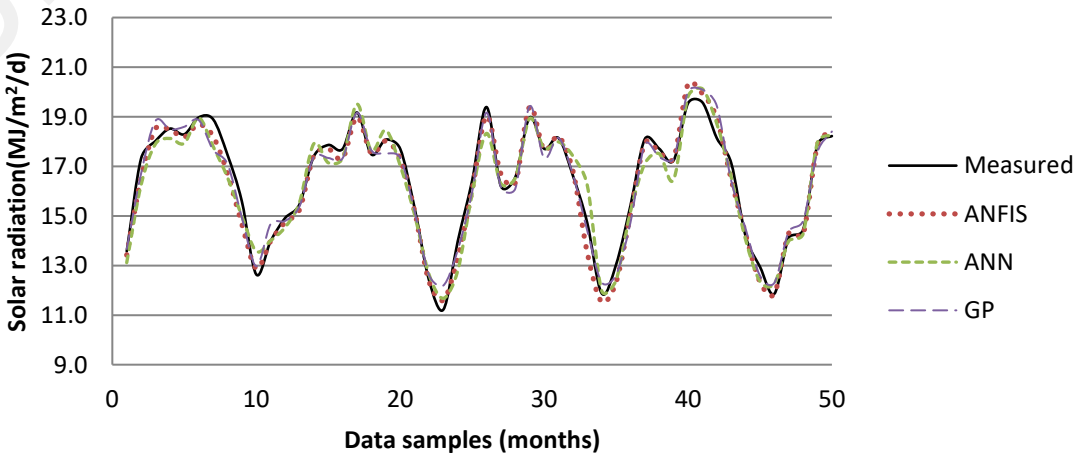

Figure 4. 3: Solar radiation prediction by ANFIS, ANN and GP

Table 4.2 compare the ANFIS model with ANN and GP models for Iseyin, Maiduguri and Jos, while Table 4.3 summarizes the results of the comparison in the three considered case studies. The results presented in Table 4.2 show that the ANFIS model has the best capabilities for global solar radiation estimation. The performance of the developed ANFIS model is different between the three considered sites, mainly due to the difference in climatic conditions. More importantly, performance of the developed model was compared to the ANN and GP models, and the achieved results revealed that ANFIS is a superior approach for solar radiation prediction among the three methods.

Table 4. 2: Model performance statistic at the selected sites

Performance metrics	Sites	ANFIS		ANN		GP	
		Testing	Training	Testing	Training	Testing	Training
RMSE	Iseyin	0.4662	0.4935	0.4801	0.5502	0.5301	0.5202
	Maiduguri	0.5357	2.4934	0.6317	2.6083	0.5522	2.5498
	Jos	0.6988	1.8661	0.7673	2.0458	0.7507	0.7678
R^2	Iseyin	0.8183	0.7953	0.7895	0.7457	0.7987	0.7678
	Maiduguri	0.8253	0.6095	0.7782	0.6334	0.7872	0.6632
	Jos	0.8024	0.5300	0.7596	0.4659	0.7619	0.5181
r	Iseyin	0.9046	0.8918	0.8937	0.8635	0.8885	0.8762
	Maiduguri	0.9084	0.8577	0.8821	0.6652	0.8872	0.8039
	Jos	0.8956	0.7280	0.8730	0.6496	0.8708	0.6899
MAPE	Iseyin	6.1754	6.2253	6.6195	6.9862	7.0605	6.4681
	Maiduguri	6.2616	13.985	6.2253	16.075	6.6035	15.685
	Jos	6.1768	11.519	6.7813	13.431	6.7813	13.209

Table 4. 3: Average model performance statistics for all sites

Model	Data set	RMSE	R^2	r	MAPE
ANFIS	Testing	0.6988	0.8024	0.8956	6.1768
	Training	1.8661	0.5300	0.7280	11.5192
ANN	Testing	0.7673	0.7596	0.8730	6.7813
	Training	2.0458	0.4659	0.6496	13.4305
GP	Testing	0.7507	0.7619	0.8708	6.9594
	Training	1.9532	0.5181	0.6899	13.2089

Furthermore, in demonstrating the precision of the developed model (ANFIS), the model was compared/correlated with several other solar radiation prediction models (Abdalla, 1994; Bakirci, 2009; Olatomiwa, Mekhilef, Shamshirband, Mohammadi, et al.,

2015; Olatomiwa, Mekhilef, Shamshirband, & Petkovic, 2015; Ramedani et al., 2014a; Yohanna et al., 2011). The result of comparison is presented in Table 4.4. The comparison indicates that the ANFIS model proposed for this study is ideal for estimating global solar radiation. The selected statistical performance indicator shows the capability of the model to produce favorable results in greater accuracy compared with other models. From these analysis, it was found that the performance of each models vary from one location to another, because the models' performances are highly dependent upon the solar radiation characteristics and weather conditions of the locations. The results showed that solar radiation estimation is totally location dependent; therefore, calibrating a general model to estimate the solar radiation for an entire region including several stations would only be possible option if the climate conditions of the region were similar. Otherwise, the amount of errors obtained may be high for some location with different weather conditions. On this basis, we conclude the proposed models can be considered an efficient technique for global solar radiation prediction with a higher degree of reliability for practical purposes in Nigeria.

Table 4. 4: Comparison between the proposed models with existing models

Reference	Model type	No. of Input	Country	R^2
(Yohanna et al., 2011)	Empirical	3	Nigeria	0.6081
Abdalla (Abdalla, 1994)	Empirical	5	Bahrain	0.7802
(Bakirci, 2009)	Empirical	3	Turkey	0.7802
(Ramedani et al., 2014a)	ANN	7	Iran	0.7990
(Ramedani et al., 2014a)	SVR-RBF	7	Iran	0.7902
(Olatomiwa, Mekhilef, Shamshirband, & Petkovic, 2015)	SVR-Poly	3	Nigeria	0.7395
(Olatomiwa, Mekhilef, Shamshirband, Mohammadi, et al., 2015)	SVM-FFA	3	Nigeria	0.8024
(Ramedani et al., 2014a)	ANFIS	7	Iran	0.8001
Present study	ANFIS	3	Nigeria	0.8541

4.2 Renewable energy resources assessment

The potentials of major renewable energy sources (wind and solar) in selected locations across the six geo-political regions of Nigeria, based on long-term daily meteorological data spanning between 18 and 39 years have been assessed, and the result obtained is discussed in the following section;

4.2.1 Monthly and yearly clearness index

The monthly mean clearness index for all the sites are shown in Figure 4.4. It varies from 0.28 to 0.56 for Iseyin, 0.42 to 0.61 for Sokoto, 0.46 to 0.63 for Maiduguri, 0.41 to 0.65 for Jos, 0.34 to 0.56 for Enugu, and 0.36 to 0.52 for Port-Harcourt. All the sites considered in this study experience different weather conditions, and the amount of solar radiations in the atmosphere as well as the characteristic of solar radiation changes from one sites to another. As a result, the monthly clearness index varies from one climatic zone to another. However, based on the obtained clearness index, it can be observed that all the sites considered enjoyed clear sky conditions throughout the year except for Port-Harcourt, Enugu and Iseyin, which had some months (July, August and September) with rain cloudy sky.

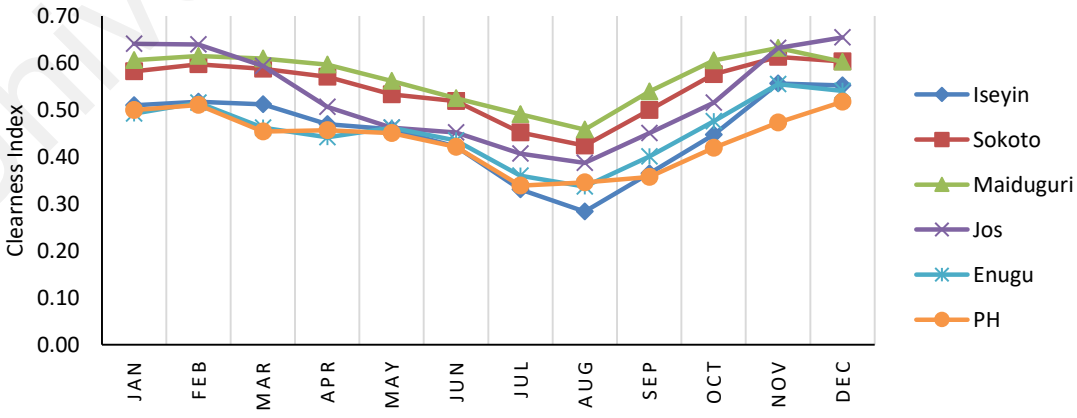

Figure 4. 4: Monthly variation in clearness index for the six locations

4.2.2 Solar radiation on horizontal, tilted surfaces and optimum tilts

The monthly mean beam ($\overline{H}_b$) and diffuse ($\overline{H}_d$) for each site were computed from measured global solar radiation ($\overline{H}$) incident on the horizontal surface based on Equations (3.23) and (3.24). These parameters are required in assessment study of any solar energy applications. Figure 4.5 shows the mean monthly radiation for each sites.

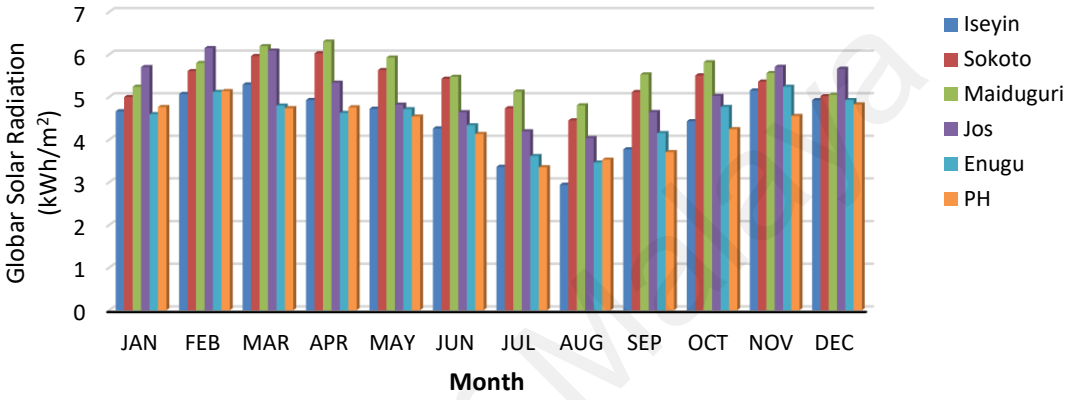

Figure 4. 5: Mean monthly radiation on horizontal plane

Maiduguri is observed to have the highest global solar radiation among the selected sites, while the least occurred at Port Harcourt. The maximum and minimum values for Maiduguri were obtained in April and August respectively, while the maximum and minimum value was obtained in December and July respectively in Port Harcourt. Values obtained for the remaining sites can be seen on the figure. It can further be observed from obtained results, that all locations have higher levels of horizontal global solar radiations during the dry season months (October to April). This shows that the dry season is the best season for solar energy harvesting. During the rainy season (April to September), the amount of total radiation reduce notably compare with others. The annual averages of these parameters are shown in Table 4.5. Values obtained for global, beam and diffuse radiation, as well as clearness index, showed that all the sites considered for this study enjoy a considerable solar energy potential suitable for solar energy conversion applications.

Table 4. 5: Annual bean, diffuse, horizontal and tilted radiation for the selected sites

Sites	$\bar{H}_0$(kWh/m^2)	$\bar{H}_d$(kWh/m^2)	$\bar{H}$ (kWh/m^2)	$\bar{H}_T$((kWh/m^2)
Iseyin	2.364	2.090	4.459	4.758
Sokoto	3.274	2.049	5.319	5.797
Maiduguri	3.544	2.023	5.568	6.060
Jos	3.122	2.045	5.167	5.640
Enugu	2.407	2.121	4.528	5.795
Port Harcourt	2,228	2.128	4.356	4.554

Monthly optimum tilt angle and the resulting solar energy gain (SEG) for the six selected locations are shown in Table 4.6. The optimal tilt angles are obtained based on the relations given in equations (3.23-3.28) and the MATLAB code for its computation is presented in Appendix A.

Table 4. 6: Monthly optimal tilt variation with corresponding solar energy gain

Site	Iseyin		Sokoto		Maiduguri		Jos		Enugu		Port Harcout	
	β_{opt} (^{0})	SEG (%)	β_{opt} (^{0})	SEG (%)	β_{opt} (^{0})	SEG (%)	β_{opt} (^{0})	SEG (%)	β_{opt} (^{0})	SEG (%)	β_{opt} (^{0})	SEG (%)
Jan	36.3	18.1	41.6	26.6	41.6	27.0	40.4	25.6	34.5	15.9	33.3	10.1
Feb	26.1	8.6	31.5	13.7	31.3	13.7	29.8	12.4	24.7	7.6	23.0	6.5
Mar	11.0	1.4	15.9	3.10	15.6	3.1	13.6	2.3	9.2	0.9	7.6	0.6
Apr	0	0.0	0	0.0	0	0.0	0	0.0	0	0.0	0	0.0
May	0	0.0	0	0.0	0	0.0	0	0.0	0	0.0	0	0.0
Jun	0	0.0	0	0.0	0	0.0	0	0.0	0	0.0	0	0.0
Jul	0	0.0	0	0.0	0	0.0	0	0.0	0	0.0	0	0.0
Aug	0	0.0	0	0.0	0	0.0	0	0.0	0	0.0	0	0.0
Sep	3.5	0.1	8.2	0.8	8.0	0.8	5.7	0.4	2.5	0.1	1.0	0.0
Oct	20.2	4.7	26.4	9.2	26.4	9.3	23.2	6.7	19.4	4.4	16.8	3.1
Nov	34.7	16.8	39.6	24.0	39.5	24.0	37.7	21.5	33.3	15.3	30.1	11.4
Dec	39.8	23.4	44.5	32.2	44.1	31.4	43.2	30.6	38.2	21.0	36.3	18.2

The adjustment of solar panels on the optimum tilt angle and orientation as reflected in Table 4.6 plays a significant role in increasing the performance of PV panels. Monthly optimum tilt angle correspond the maximum monthly solar radiation for Iseyin, Sokoto, Maiduguri, Jos, Enugu and Port-Harcourt lies respectively in the range (0-39.8^o), (0-44.5^o), (0-44.1^o), (0-43.2^o), (0-38.5^o) and (0-36.3^o). In all the considered sites, the

optimum angle is equal to 0^0 in the month of April, May, June, July and August. This implies that the solar panels can be position horizontally for all these five months and still yield an optimal result. However, due to low altitude of the Sun in January and December, the panel surface requires to be adjusted at a higher tilt angle if a higher solar gain is desired.

The results revealed that optimum tilt angle increases with increase in the latitude angle. In terms of SEG, highest values are obtained in Sokoto (32.2%), Maiduguri (31.4%), Jos (30.6%), Iseyin (23.4%), Enugu (21%), and Port-Harcourt (18.2%); all these were obtained in December. It is clearly seen that the values of SEG in some months in all the selected sites are very low. Thus, it can be concluded that if the solar panel surfaces are maintained in horizontal position between the months of March to September (rainy season) for all the sites, there would be no effect on the total SEG. Because, monthly tilt angle adjustment may be impractical owing to its financial implication, seasonal and yearly fixed adjustment strategies can be used adopted as alternative options. Table 4.7, also shows the seasonal (dry and rainy season) and yearly fixed optimum tilt angles for each site. The maximum optimal angle occurs in the dry season, while the minimum occurs in the rainy season. It was observed that the seasonal and yearly optimum tilt angles increase with an increase in the latitude angle just as obtained in monthly tilt angles.

Table 4. 7: Seasonal and annual mean optimal tilt variation with corresponding solar energy gain

Site	**Iseyin**		**Sokoto**		**Maiduguri**		**Jos**		**Enugu**		**Port Harcout**	
	$\boldsymbol{\beta}_{\mathbf{opt}}$ **(^{0})**	**SEG (%)**	$\boldsymbol{\beta}_{\mathbf{opt}}$ **(^{0})**	**SEG (%)**	$\boldsymbol{\beta}_{\mathbf{opt}}$ **(^{0})**	**SEG (%)**	$\boldsymbol{\beta}_{\mathbf{opt}}$ **(^{0})**	**SEG (%)**	$\boldsymbol{\beta}_{\mathbf{opt}}$ **(^{0})**	**SEG (%)**	$\boldsymbol{\beta}_{\mathbf{opt}}$ **(^{0})**	**SEG (%)**
Dry	29.6	11.4	34.6	16.6	34.4	16.5	32.9	15.4	28.0	10.1	26.1	7.8
Rainy	3.4	4.80	4.90	10.0	4.90	10.1	4.1	7.1	3.1	4.5	2.5	3.1
Annual	14.3	5.7	17.3	9.1	17.2	9.1	16.1	8.29	13.5	5.4	12.3	4.15

4.2.3 Wind speed frequency distribution

The annual probability density and cumulative distribution functions obtained for wind speed at the selected locations are shown in Figures 4.6 and 4.7 respectively.

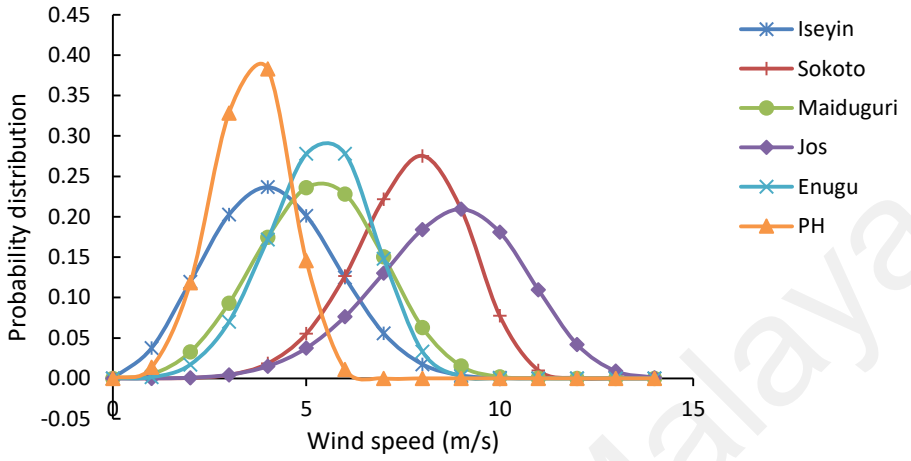

Figure 4. 6: Probability density function of the selected sites

It can be observed from Figure 4.6 that, the peak of the density functions of all the sites skewed towards the higher values of mean wind speed; the peak further indicates the most frequent velocity. The most frequent wind speeds of 9.0, 8.0 and 6.0 m/s are expected in Jos, Sokoto, and Maiduguri respectively, while the least occurs in Port-Harcourt at 3.5 m/s.

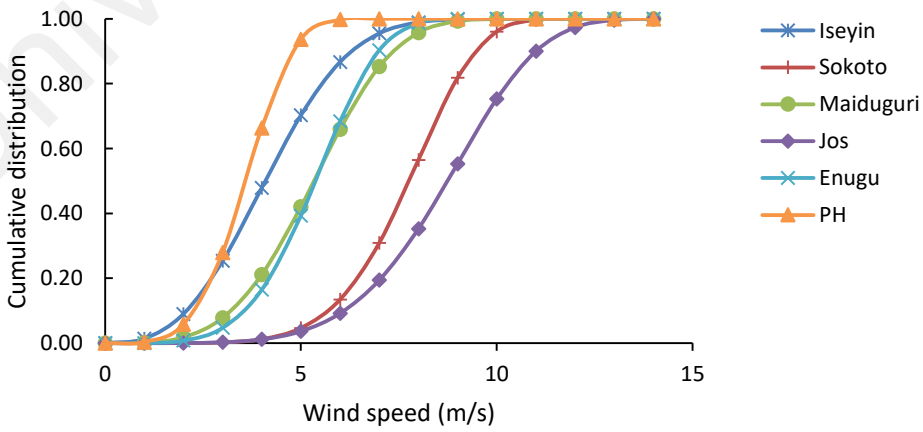

Figure 4. 7: Cumulative density function of the selected site

It can further be observed that Jos has the highest spread of wind speeds among the locations. Similar trend is observed in the cumulative probability distributions of wind

speed in all the locations as shown in Figure 4.7. For wind speeds greater or equal to 3.0 m/s cut-in wind speed, Sokoto, Jos, Enugu, Maiduguri, Port Harcourt, and Iseyin have frequencies of about 99.8, 99.7, 94.5, 90.3, 65.9 and 64.3% respectively. All the sites have monthly peak frequency range between 26 and 40.6%, and having 26, 28.5, 35.3, 37.3, 40.2 and 40.6% for Iseyin, Jos, Maiduguri, Enugu, Sokoto and Port Harcourt respectively. Iseyin has its peak frequency at 4m/s in December, Jos at 10m/s in May, Maiduguri in September at 5m/s, Enugu in October at 5m/s, Sokoto at 7m/s in August and Port Harcourt in January at 4m/s.

4.2.4 Mean wind speed and mean power density

The monthly mean wind speeds at 10m height, wind power density and Weibull parameters for the selected sites are presented in Tables 4.8 and 4.9. The monthly mean wind speed varies between 3.48 m/s in November and 4.71 m/s in April for Iseyin.

Table 4. 8: Monthly and annual Weibull parameters variation in the selected sites

Site	Iseyin		Sokoto		Maiduguri		Jos		Enugu		Port Harcout	
	k	c(m/s)	k	c(m/s)	k	c(m/s)	k	c(m/s)	k	c(m/s)	k	c(m/s)
Jan	3.182	4.702	5.262	9.719	3.185	5.517	3.496	10.17	3.485	6.248	4.185	3.741
Feb	3.257	4.864	4.264	9.486	3.587	6.549	4.730	10.00	4.860	6.175	4.633	4.256
Mar	2.504	5.117	5.459	7.965	3.764	6.753	6.602	9.694	5.742	6.807	5.439	4.227
Apr	3.005	5.274	5.734	8.202	4.251	6.377	3.944	9.882	5.090	6.767	4.977	4.399
May	3.095	4.842	9.938	9.147	3.976	6.412	7.553	9.595	4.426	5.868	4.656	4.057
Jun	2.725	4.890	9.936	9.494	3.585	6.727	5.405	9.281	4.838	5.685	4.149	4.041
Jul	2.891	4.711	6.534	8.519	3.029	6.336	7.116	9.239	5.450	5.939	3.461	4.081
Aug	2.916	4.776	7.537	6.635	3.866	5.107	6.217	8.854	3.939	6.007	4.281	4.319
Sep	2.445	4.443	5.351	6.303	4.796	4.902	4.611	7.824	4.819	5.294	4.617	3.983
Oct	2.387	4.073	3.171	6.724	3.742	5.039	4.406	8.382	5.253	4.952	3.487	3.546
Nov	2.022	3.927	3.964	8.279	3.546	5.664	4.023	9.419	3.750	4.562	3.452	3.237
Dec	3.027	4.377	5.872	8.483	3.441	5.206	4.725	10.23	3.341	5.515	2.879	3.208
Ann	2.788	5.150	6.085	9.870	3.731	6.722	5.236	11.12	4.583	6.818	4.178	4.610

The shape parameter *k* varies between 2.02 and 2.92, while the scale parameter *c* lies between 3.92 and 5.27 m/s. Power density varies between 46.48 W/m^2 in October and 89.69 W/m^2 (March).

Table 4. 9: Monthly and annual mean variation of wind speed and power density in the selected sites

Site	Iseyin		Sokoto		Maiduguri		Jos		Enugu		Port Harcout	
	V (m/s)	P (W/m^2)	V (m/s)	P (W/m^2)	V (m/s)	P (W/m^2)	V (m/s)	P (W/m^2)	V (m/s)	P (W/m^2)	V (m/s)	P (W/m^2)
Jan	4.21	61.44	8.95	494.61	4.94	99.22	9.15	603.3	5.62	140.00	3.40	28.90
Feb	4.36	67.47	8.63	469.62	5.90	159.9	9.16	544.5	5.66	127.55	3.89	41.98
Mar	4.54	89.21	7.35	271.71	6.10	173.3	9.04	488.0	6.30	169.32	3.90	40.62
Apr	4.71	88.69	7.59	296.17	5.80	142.7	8.95	538.0	6.22	167.32	3.98	44.24
May	4.33	67.82	8.70	415.45	5.81	146.7	9.01	474.1	5.35	110.60	3.71	36.34
Jun	4.35	74.12	9.03	464.55	6.06	173.3	8.56	430.1	5.21	99.60	3.67	36.44
Jul	4.20	64.29	7.94	331.25	5.66	153.2	8.65	422.9	5.48	112.65	3.67	39.11
Aug	4.26	66.75	6.23	156.81	4.62	74.55	8.23	371.9	5.44	120.89	3.93	44.29
Sep	3.94	59.35	5.81	134.79	4.49	63.90	7.15	260.8	4.85	80.43	3.64	34.40
Oct	3.61	46.48	6.02	179.97	4.55	72.12	7.64	322.5	4.56	65.44	3.19	25.60
Nov	3.48	48.18	7.50	316.03	5.10	103.8	8.54	464.1	4.12	53.50	2.91	19.52
Dec	3.91	50.54	7.86	327.40	4.68	81.31	9.36	581.1	4.95	97.52	2.86	20.35
Ann.	4.16	85.46	7.63	515.4	5.309	171.4	8.62	741.0	5.31	172.7	3.56	54.07

The annual mean wind speed and wind power density are found to be 4.16m/s and 85.64W/m^2 respectively. According to the wind power classification scheme (Elliott & Schwartz, 1993) of Pacific Northwest Laboratory presented in Table 4.10, the monthly mean and the annual mean power density for Iseyin falls into Class 1. Ths is considerd poor and may only be suitable for battery charging, water pumping and other small wind power applications.

Table 4. 10: Wind power classification

Power Class	Average wind speed (m/s) at 10m	Power density (W/m^2) at 10m	Remarks
1	0-4.4	$0 < P \leq 100$	Poor
2	4.4-5.1	$100 < P \leq 150$	Marginal
3	5.1-5.6	$150 < P \leq 200$	Fair
4	5.6-6.0	$200 < P \leq 250$	Good
5	6.0-6.4	$250 < P \leq 300$	Excellent
6	6.4-7.0	$300 < P \leq 400$	Outstanding
7	> 7.0	$400 < P \leq 1000$	Super

The minimum and maximum values of the monthly mean wind speeds are found to be 5.81 and 9.03m/s respectively for Sokoto. The monthly mean shape parameter (k) has

values between 3.17 and 9.94, while the scale parameter *c* is between 6.30 and 9.72 m/s. The monthly mean wind power density varies from 134.79 W/m^2 in September to 494.61 W/m^2 in January. However, the annual mean power density for this site stand at 515.40 W/m^2, which makes the site to ranked at Class 7 and thus suitable for grid-connected wind power applications. In the case of Maiduguri, the minimum and maximum values of the monthly mean wind speeds are 4.49 m/s (in September) and 6.10 m/s (in March) respectively. The monthly mean power density varies from 63.90 W/m^2 in September to 173.38 W/m^2 in March; with annual mean power density for 171.40 W/m^2, the site is ranked Class 3. The minimum and maximum values of the monthly mean wind speeds varied from 7.15 (September) to 9.36 m/s (December) respectively in Jos. The monthly mean shape parameter *k* ranges between 3.50 and 7.55, while the scale parameter *c* is from 7.82 and 10.23m/s. Monthly mean wind power density varies from 260.83 W/m^2 in September to 603.38 W/m^2 in January. The average annual power density stands at 741.20 W/m^2, making the site to fall in Class 7 of the wind power classification. This classification places Jos on a high potential site for large-scale grid-connected wind turbine applications.

The wind speed characteristics of Enugu and Port-Harcourt are also shown Tables 4.8 and 4.9. The minimum and maximum values of wind speed are 4.12 and 6.30m/s respectively for Enugu whereas they exist as 2.86 and 3.98 m/s in Port-Harcourt for the minimum and maximum. Considering the wind power density, the dry season is found to be the windiest season for both sites. Monthly wind power ranges from 53.50 W/m^2 in November to 169.32 W/m^2 in March at Enugu, while it varies from 19.52 to 44.29 W/m^2 in November and August respectively in Port-Harcourt. With the wind power classification in Table 4.9, Enugu falls under Class 3, and Port-Harcourt in Class 1, thereby making the Enugu to be fairly considered for wind power applications and Port-Harcourt poor.

4.2.5 Wind energy density

The result of two employed methods for the computation of energy density at Iseyin site is presented in Tables 4.11 (i.e using measured data from the site and Weibull probability density functions). Hourly measured wind data obtained from the respective meteorological stations in each site is divided into bins (0-1, 1-2, 2-3 and so on) and the duration of occurrence of the data at any particular bin is calculated from the obtained wind speed data as shown in Figure 4.8.

Thereafter, the probability density function (PDF) for each wind speed range, energy available in the wind at each range and the total energy expected in each site is calculated. The detail values of the computed parameters in each of the remain sites can be found in appendix (C1-C5).

Table 4. 11: Annual mean energy density of Iseyin site

Wind speed range (m/s)	Mid-range V(i) (m/s)	Duration (hr.)	Prob. of Occurrence f(vi)	Power (W/m^2)	Power density_ data (W/m^2)	Weibull PDF fw(vi)	Power density_ Weibull (W/m^2)	Energy density_ Weibull (kWh/m^2)	Energy density_ data (kWh/m^2)
0-1	0.5	403	0.046	0.08	0.003	0.008	0.001	0.01	0.03
1-2	1.5	1077	0.123	2.04	0.251	0.058	0.118	1.03	2.20
2-3	2.5	1499	0.171	9.45	1.618	0.130	1.229	10.77	14.17
3-4	3.5	1584	0.181	25.94	4.690	0.193	5.008	43.87	41.09
4-5	4.5	1388	0.158	55.13	8.735	0.214	11.810	103.45	76.52
5-6	5.5	1095	0.125	100.66	12.582	0.183	18.451	161.63	110.22
6-7	6.5	745	0.085	166.15	14.130	0.121	20.126	176.30	123.78
7-8	7.5	461	0.053	255.23	13.432	0.061	15.610	136.75	117.66
8-9	8.5	269	0.031	371.55	11.409	0.023	8.624	75.55	99.95
9-10	9.5	132	0.015	518.71	7.816	0.006	3.370	29.52	68.47
10-11	10.5	61	0.007	700.36	4.877	0.001	0.920	8.06	42.72
11-12	11.5	27	0.003	920.13	2.836	0.000	0.173	1.51	24.84
12-13	12.5	12	0.001	1181.64	1.619	0.000	0.022	0.19	14.18
13-14	13.5	4	0.000	1488.53	0.680	0.000	0.002	0.02	5.95
14-15	14.5	3	0.000	1844.42	0.632	0.000	0.000	0.00	5.53
15-16	15.5	0	0.000	2252.94	0.000	0.000	0.000	0.00	0.00
		8760	1.000		85.311		85.463	748.66	747.32

However, Table 4.12 presents the summary of both annual power and energy density for each site using the two methods. From these tables, we observed a good correlation between the energy and power densities values obtained using both methodologies.

Table 4. 12: Summary of annual energy density at the selected sites using the available data and Weibull function

Method	Parameter	Iseyin	Sokoto	Maiduguri	Jos	Enugu	Port Harcourt
Data	Power (W/m^2)	85.33	516.57	172.45	741.22	172.38	54.58
	Energy(kWh/m^2)	747.32	4525.14	1510.67	6393.12	1510.0	478.16
Weibull	Power (W/m^2)	85.46	515.41	171.35	741.22	172.73	54.07
	Energy(kWh/m^2)	748.66	4514.97	1510.03	6491.33	1513.1	473.44

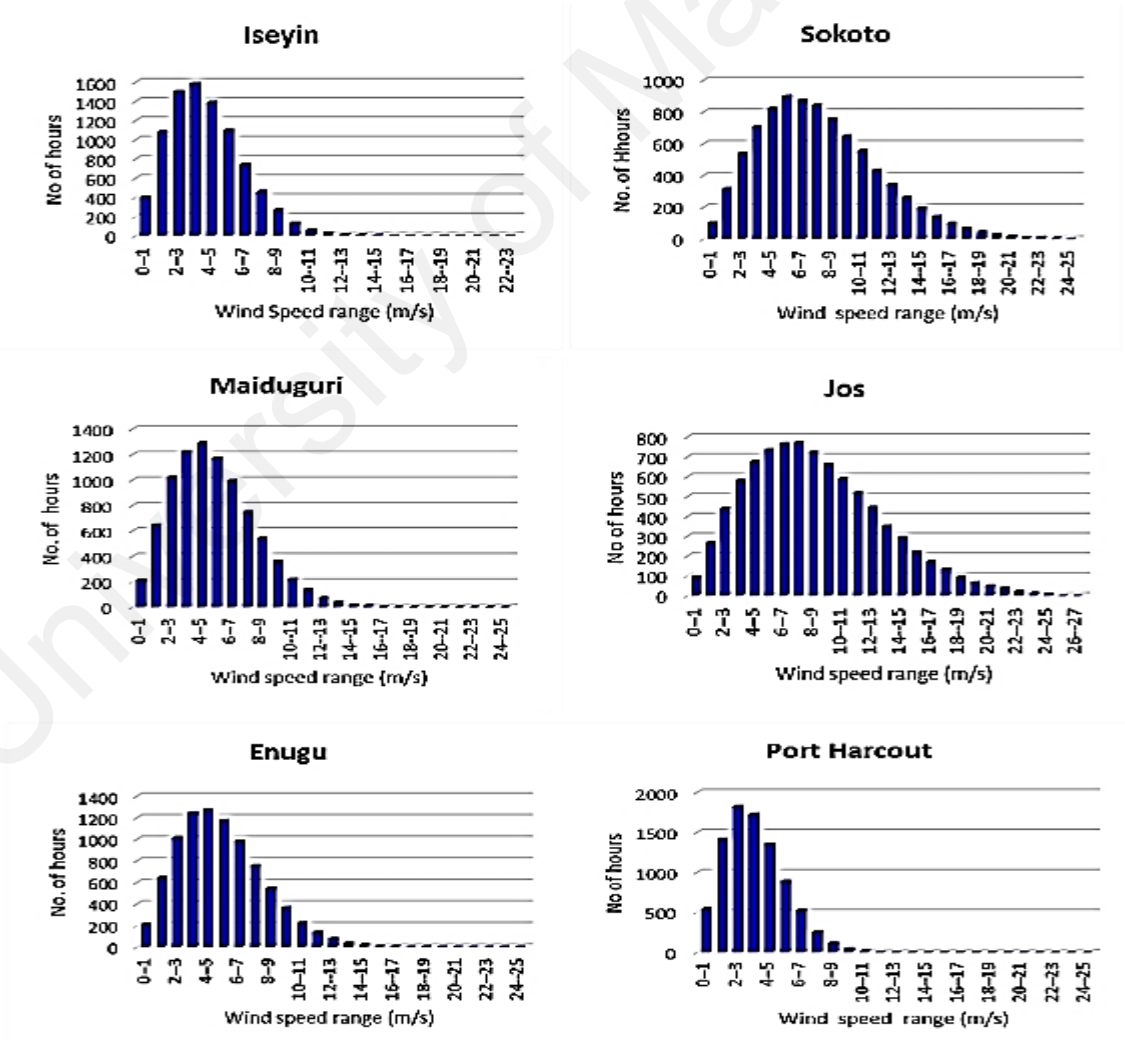

Figure 4. 8: Numbers of hours of occurrence of wind speed in each bin for the selected sites

It can be observed from Figure 4.8 that, Jos and Sokoto had the highest spread of wind speeds among the selected, this has contributed to high energy density the two sites. Annual energy density of 478.16 and 747.30 kWh observed in Port Harcourt and Iseyin site respectively. This is considered too low for profitable wind energy applications, unless for water pumping or battery charging purpose.

4.3 Hybrid system components model performance

Accurate mathematical modeling of the proposed hybrid system components is essential for effective analysis of the entire system, thus this section present the results of performance of PV and wind turbine model.

4.3.1 PV model

Various results of the performance of the developed PV model in MATLAB/Simulink using earlier mentioned equations and its validation with manufacturer data for the selected PV modules under varying solar radiation and temperature are discussed in this section. The tabulation of numerical results shows the correlation of the PV module parameters with module characteristic curve as an indicator of PV model performance.

4.3.1.1 Determination of PV model parameters

(a) Photon current

Table 4.13 presents different value of I_{ph} obtained as the solar insolation and module temperature varies. From this table, it is seen that the module photon current largely depends on the solar irradiance incident on the PV surface and slightly depend on the module temperature as modeled by Equation (3.45).

Table 4. 13: Photon current for various insolation and temperature

Value of I_{ph} (A)			
Solar Irradiance (W/m$^{2)}$	**Temperature (^{0}C)**		
-	**25**	**50**	**75**
200	0.510	0.519	0.527
400	1.020	1.037	1.054
600	1.530	1.556	1.581
800	2.040	2.074	2.108
1000	2.550	2.593	2.635

(b) Reverse saturation current

As can be seen from the model equation (3.46), PV module reverse saturation current is dependent of the module temperature. The equation is modified to consider the influence of the variation in temperature on the saturation current via short circuit current and open circuit voltage. The computation of the two reverse saturation current (I_{01}, I_{02}) based on the two-diode PV model considered in this study is presented in Table 4.14.

Table 4. 14: Reverse saturation current for various temperature

Temperature (^{0}C)	**Module reverse current**	
	I_{01}(mA)	**I_{02}(mA)**
25	2.460 x 10^{-3}	6.392 x10^{-3}
50	2.581 x10^{-3}	6.781 x10^{-3}
75	2.691 x10^{-3}	6.934 x10^{-3}

(c) *Ideality constants*

Ideality constant is one of the important parameters in PV module performance analysis. This parameter is computed using earlier described algorithm developed in MATLAB. Table 4.15 present the computed ideality constant of the considered PV module at standard test and conditions (G=1000W/m^2 and T=25^{0}C).

Table 4. 15: Computed module ideality constant @ STC

Parameter	**Computed values**
α_1	1.58
α_2	2.10

4.3.1.2 Model validation

Tables 4.16 and 4.17 presents the summary of the computed PV module parameters in comparison with manufacture data at different solar radiation and temperature levels (Solex, 2014). From the two tables, we observed a good correlation between the computed parameter and the data available from the manufacturer datasheet. The absolute error within the computation is minimal; hence prove the accuracy of the developed model. It should also be noted that, outside the standard test and conditions (G=1000W/m^2 and T=25^{0}C) the variation in the ideality constant do not have significant effect on the module short circuit current (I_{sc}), however, in the case of open circuit condition, the module voltage (V_{oc}) varies linearly with variation in the ideality constant.

Table 4. 16: Comparison of simulation result and manufacturer datasheet at different solar radiation level

Parameter	**1000W/m^2**		**800W/m^2**		**600W/m^2**		**400W/m^2**		**200W/m^2**	
	Data-sheet	Simu-lation	Data sheet	Simu-ation	Data sheet	Simu-lation	Data sheet	Simu-lation	Data sheet	Simu-lation
$I_{sc}\ (A)$	2.55	2.56	2.03	2.03	1.51	1.52	0.99	1.00	0.49	0.50
$V_{oc}\ (V)$	21.2	21.2	20. 8	20.3	20.3	20.4	19.1	19.2	17.8	17.6
$I_{mp}(A)$	2.25	2.26	1.81	1.81	1.40	1.41	0.89	0.90	0.35	0.37
$V_{mp}\ (V)$	16.6	16.5	16.2	16.2	15.9	16.0	15.4	15.5	15.1	15.0
$I_{01}\ (\mu A)$	2.46	2.45	1.98	2.00	1.46	1.47	0.87	0.87	0.35	0.36
$I_{02}\ (\mu A)$	6.93	6.92	6.21	6.22	5.32	5.34	4.88	4.90	3.45	3.46
α_1	1.60	1.58	1.43	1.45	1.30	1.35	1.20	1.21	1.12	1.13
α_2	2.20	2.21	2.10	2.11	1.81	1.81	1.63	1.63	1.52	1.54

In addition, the I-V and P-V characteristic curves of the considered PV module are shown in Figures 4.9 and 4.10 for different levels of solar radiation and temperature respectively. The computed value of PV module voltage and current are compared with manufacturer data and the value obtained proved the accuracy of the model.

Table 4. 17: Comparison of simulation result and manufacturer datasheet at different temperature level

Parameter	25^0C		50^0C		75^0C	
	Datasheet	Simulation	Datasheet	Simulation	Datasheet	Simulation
$I_{sc}\ (A)$	2.55	2.56	2.59	2.60	2.63	2.63
$V_{oc}\ (V)$	21.2	21.2	18.3	18.2	16.6	16.6
$I_{mp}(A)$	2.25	2.26	2.28	2.27	2.31	2.30
$V_{mp}\ (V)$	16.6	16.5	13.2	13.4	11.9	12.0
$I_{01}\ (\mu A)$	2.46	2.45	2.58	2.59	2.69	2.69
$I_{02}\ (\mu A)$	6.93	6.92	6.78	6.78	6.94	6.93
α_1	1.60	1.58	1.63	1.63	1.71	1.72
α_2	2.20	2.21	2.30	2.31	2.42	2.41

4.3.1.3 Effect of varying solar radiation on the PV model

Figures 4.9(a) and (b) respectively show the I-V and P-V characteristic curve of the PV solar array at different solar radiation levels and constant temperature.

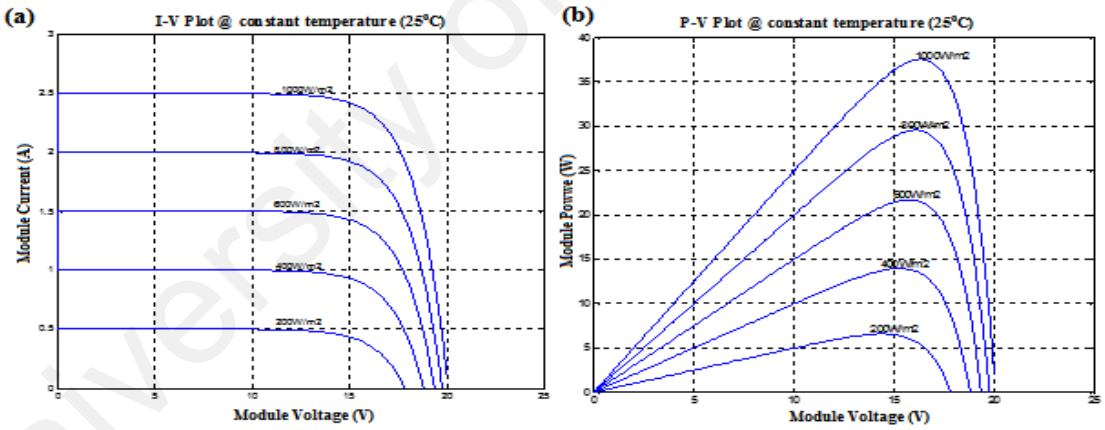

Figure 4. 9: Characteristic curve of solar module at diffent solar rasiation levels:

(a) I-V Curve (b) P-V curve

As we can see from these figures, the module current is strongly dependent on the solar radiation. Increase in solar irradiance incident on PV surfaces, lead to corresponding increase in module current as well as module voltage. Thus, resulted in more power output from the PV module.

4.3.1.4 Effect of varying temperature on the PV model

The performance of the model based on temperature variations is shown in Figures 4.10(a) and (b) representing the, I-V and P-V characteristic curve respectively under constant solar radiation at standard test condition (1000W/m^2). PV current is observed to increase slightly, while the output voltage decrease drastically with an increase in module temperature resulting in net reduction in PV power output. This observation shows the effect of the module on the PV power output.

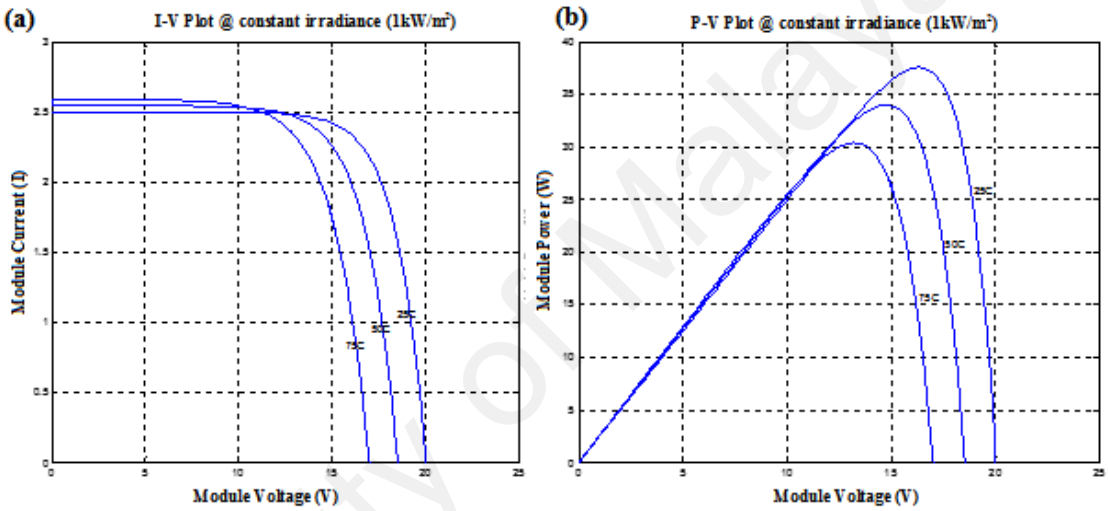

Figure 4. 10: Characteristic curve of solar module at different temperature levels: (a) I-V curve (b) P-V curve

4.3.2 Wind turbine model

The performance of the selected wind turbines at various sites in this study is presented in Table 4.18, Figures 4.11 and 4.12 in terms of annual energy production (MWh/year) and capacity factor (%).

It is seen from the figures, that irrespective of the wind turbine model, Jos and Sokoto seem to be good sites for wind turbine applications due to enormous potential of wind energy resources at the two sites compared to others. According to Table 4.18, the expected annual mean energy output of Jos site ranges from 5.68MWh/yr. with ABS 1000 to 33.7MWh/yr. with SNT-50 model wind turbine.

Table 4. 18 Annual energy output and capacity factor of the selected wind turbine at the considered sites

Model	Performance Metric	Iseyin	Sokoto	Maiduguri	Jos	Enugu	PH
FDQ-3.0-1	CF (%)	26.5	86.2	42.1	90.9	40.1	9.34
	E_{ave} (MWh/yr.)	2.32	7.55	3.75	7.97	3.52	0.82
ABS 1000	CF (%)	11.3	44.6	15.9	64.9	11.3	2.58
	E_{ave} (MWh/yr.)	0.99	3.90	1.39	5.68	1.00	0.23
Windera	CF (%)	11.4	50.9	17.6	69.4	13.0	2.73
	E_{ave} (MWh/yr.)	2.99	13.4	4.63	18.3	3.42	0.72
Wind Cruiser	CF (%)	11.7	44.6	15.9	64.9	11.3	2.65
	E_{ave} (MWh/yr.)	3.08	11.7	4.20	17.1	2.97	0.70
SNT-50	CF (%)	15.1	62.5	23.0	76.9	2.36	3.98
	E_{ave} (MWh/yr.)	6.63	27.4	10.1	33.7	7.87	1.75

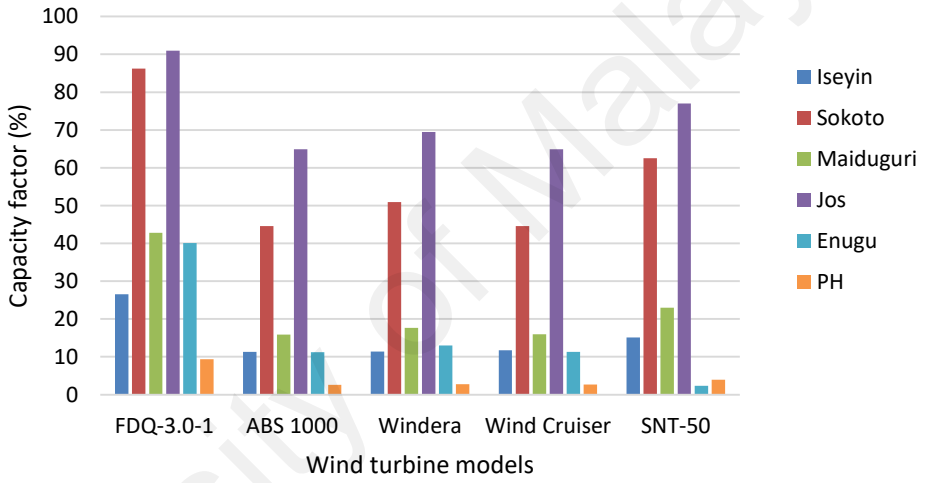

Figure 4. 11: Capacity factor of the selected wind turbine at various sites

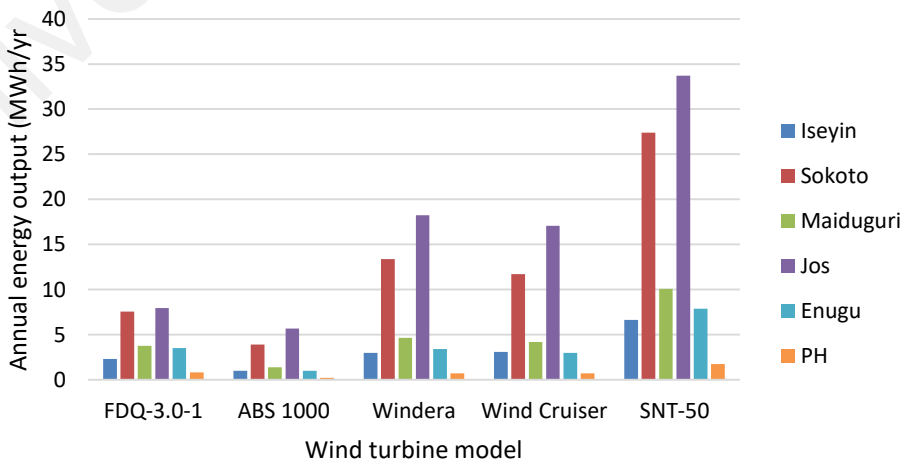

Figure 4. 12: Expected annual average energy output of selected wind turbine

In the 1kW wind turbine models category, FDQ-3.0-1 is considered the best in terms of energy production and capacity factor in all the sites; this is due to relatively low cut-in wind speed and rated wind speed compared to ABS-1000 model even though both have same hub height. In the 3kW wind turbine models category, Windera model outperformed the Wind Cruiser in all the considered sites except Iseyin, owing to its low rated speed, even though it hub height is considered lowest among all the other models.

The minimum annual energy output of 0.23 and 0.99MWh/yr. are obtained in Port Harcourt and Iseyin site respectively with ABS-1000 turbine model. While the maximum values are 1.75 and 6.63MWh/yr. respectively at Port Harcourt and Iseyin using 5kW SNT-50 model wind turbine. This value is just slightly higher than value obtained using 1kW FDQ-3.0-1 wind turbine model. Therefore, it will be more economical to employ 1kW FDQ-3.0-1 model at both Port Harcourt and Iseyin due to a low wind regime observed in these sites.

The cost-effectiveness of a wind turbine model can be measured by its capacity factor. Among the selected models, FDQ-3.0-1 has the highest capacity factor, followed by SNT-50. The value for these models is more than the recommended values of >25% at both Jos and Sokoto site; therefore, any investment on this two type of wind turbine at the sites will be considered worthwhile investment. On the other hand, since Iseyin and Port Harcourt sites is considered a low wind regime site, the capacity factor of ABS 1000 and Wind Cruiser model is seemed to be the least. Therefore, the two sites may only be applicable to small wind application such as water pumping of battery charging. However, increasing the hub height of the wind turbine will increase the capacity factor and consequently, the annual energy output of the wind turbine. Although this will lead to increase in capital cost of the wind turbine installation.

4.4 Optimum system configurations

The optimal configuration assessment for the selected rural sites, were carried out based on data collected from each site and system load profile in Figure 3.12. However, for the purpose of comparison, similar load profile obtained from Iseyin rural healthcare center is employed in all other hypothetical sites. The feasibility of hybrid renewable energy system for powering the rural health facilities is based on the availability of the energy resources in the selected sites and life-cycle cost of the configurations. In order to determine the operational characteristics (annual electricity production, annual load served, excess electricity and renewable fraction), HOMER performed an hourly time series simulation for every possible system configuration on a yearly basis. The RE sources and diesel generator were evaluated to determine the feasibility of the system. HOMER searched for optimum system configuration and component sizes that meet the load requirement at the lowest NPC, and present the results.

Table 4.19 present optimal results in the selected sites in terms of number and sizes of constituent hybrid system components in each configuration, initial capital cost, total NPC, cost of energy production, the amount of liter of fuel consumed by diesel generator and finally the renewable faction of each configuration. Based on these results, the best system configuration for Port Harcourt sites is hybrid PV-diesel-battery system, while PV-wind-diesel-battery is considered optimal for the rest locations (Iseyin, Sokoto, Maiduguri, Jos and Enugu). The optimal configuration obtained for Jos has the lowest NPC ($68,585) and COE (0.207$/kWh) of all the sites considered, followed by Sokoto site with $71,210 NPC and 0.215$/kWh COE. The lowest NPC and COE obtained from these sites is due to high solar and wind resources availability in the sites as compared to other sites.

Table 4. 19: Comparison of various system configurations in the selected sites

Sites	System Configuration	Components size					Economics			Fuel Consp (L/yr.)	RF (%)
		PV (kW)	Wind (kW)	Diesel (kW)	Batt. (no.)	Conv. (kW)	Initial cap ($)	Total NPC ($)	COE ($/kWh)		
Iseyin	PV-Wind-Diesel-Batt.	6	1	5	24	5	35,070	102,949	0.311	425	84
	PV-Diesel-Battery	6	-	5	24	5	29,345	110,717	0.334	791	71
Sokoto	PV-Wind-Diesel-Batt.	4	2	5	8	5	29,115	71,210	0.215	142	95
	Wind-Diesel -Battery	-	3	5	16	5	24,680	81,358	0.246	253	91
Maiduguri	PV- Wind-Diesel-Batt.	6	1	5	16	5	32,430	81,545	0.246	128	96
	PV-Diesel-Battery	6	-	5	24	5	29,345	90,428	0.273	307	89
Jos	PV- Wind-Diesel-Batt.	4	2	5	8	5	29,115	68,585	0.207	113	96
	Wind-Diesel -Battery	-	3	5	16	5	24,680	77,773	0.235	243	91
Enugu	PV- Wind-Diesel-Batt.	5.5	2	5	16	5	36,555	89.991	0.272	154	95
	PV-Diesel-Battery	6	-	5	24	5	29,345	109,373	0.330	758	72
Port Harcourt	PV-Diesel-Battery	7	-	5	24	5	32,545	106,870	0.323	554	80
	PV-Wind-Diesel-Batt.	7	2	5	16	5	44,240	108,920	0.329	177	94
All sites	Diesel-Battery	-	-	5	8	1	3,885	175,199	0.529	3,359	0
	Diesel alone	-	-	7.5	-	-	1,500	451,942	1.360	9155	0

Since the conventional stand-alone diesel generator is presently employed in the selected rural healthcare facilities, it is thereby considered as the base case simulation. It is selected in order to allow a comparison to be made regarding the total savings that can be made in terms of cost and emission when renewable energy sources are included for the design and implementation of the hybrid power system. This configuration (Diesel-alone system) is observed to be the worst configuration with highest NPC ($451,942) and COE (1.360$/kWh). Although it has the least initial capital cost ($1,500) among other system configurations, high fuel consumption due to longer hours of operation of the generator and its associated maintenance cost has led to it high NPC. It is also noted that the COE of a diesel-alone system is more than four times optimal configuration in all the selected sites. This observation has demonstrated that configuration with the lowest capital cost, may not necessarily be the configuration with the lowest cost of energy.

Conversely, the third optimum configuration NPC (diesel-battery system) cost 45% more than the best optimal configuration in the entire sites. Therefore, addition of

renewable energy sources (wind and solar PV) and batteries to the existing diesel-alone system in the selected sites is considered a good investment in terms of fuel savings and emission reduction.

4.5 Energy production of each component in optimal system configuration

Previous researches have demonstrated that RE system performance analysis for a year is sufficient for planning and decision-making (Akinyele & Rayudu, 2016; Kumar, Mohanty, Palit, & Chaurey, 2009). This is because the historical RE data of a location is similar over the years, and different from the historical data of another location. While some components will be replaced during the 25-year project lifetime, the yearly energy yield is considered as the baseline energy generation level for any year during the system's useful operating years. Therefore, the energy production of each hybrid system components for in one-year horizon is discussed in the following section.

4.5.1 Solar PV

The capacity as well as number of solar panel selected in each sites depends on the amount of solar radiation received at each location and the site load profile. In order to achieve maximum power output from each module, the PV panel is expected to be inclined at optimal tilt angles and adjusted on seasonal basis as earlier computed for each sites in Table 4.7. The maximum PV output power, annual PV production (kWh) and percentage PV contribution in the optimal hybrid system at each sites is presented in Table 4.20.

At this juncture, it should be noted that out of all the high solar radiation potential sites, only Maiduguri has higher PV contribution (74.9%) in the energy mix, while the other site (Sokoto and Jos) gives priority to wind turbine contribution than PV, due to high wind speed potential of the sites. On the other hand, both Iseyin and Port Harcourt favors high PV contribution despite the medium-high solar radiation potential experience

at the site, but due to low wind speed experience in both sites since the developed energy management prioritize the use of RE sources over the diesel generator.

Table 4. 20: PV output power contribution at the selected site

Sites	Maximum power output (kW)	Total annual energy production (kWh)	Percentage contribution (%)
Iseyin	4.866	7,179	72.5
Sokoto	3.241	5,600	36.3
Maiduguri	4.941	8,840	74.9
Jos	3.400	5,672	34.3
Enugu	4.468	6,665	54.2
Port Harcourt	5.642	8,189	83.5

4.5.2 Wind turbine

The selection of types and sizes of wind turbine is based on the potential of a high wind speed regime in any particular site. Table 4.21 present the maximum power output, total annual wind energy production and percentage contribution of wind energy at each site. We observe a higher percentage contribution of wind turbine at both Jos and Sokoto site due to a high wind speed regime experienced in both sites.

Table 4. 21: Wind turbine contribution at the selected site

Sites	Maximum Power output (kW)	Total annual energy production (kWh)	Percentage contribution (%)
Iseyin	1.230	1,474	14.9
Sokoto	2.460	9,441	61.2
Maiduguri	1.230	2,603	22.1
Jos	2.460	10,572	63.9
Enugu	2.460	5,207	42.3
Port Harcourt	-	-	-

4.5.3 Diesel generator

Since the diesel generator consumed diesel fuel to produce power, therefore, the higher the diesel operating hours the more the fuel consumption leading to more pollutant emission into the surrounding environment causing global warming and can as well deteriorate the health of patient and medical personnel in the rural clinic. To avoid this, the generator operating hour needed to be kept to the minima. Table 4.22 presents the

maximum power output, total annual energy output, hours of operation and percentage contribution of diesel generator in the optimal hybrid system configuration in each site

Table 4. 22: Diesel generator contribution at the selected site

Sites	Maximum Power output (kW)	Total annual energy production (kWh)	Operating hours (hr/yr.)	Percentage contribution (%)
Iseyin	5.0	1,245	288	12.6
Sokoto	5.0	376	144	2.44
Maiduguri	5.0	353	113	2.99
Jos	5.0	297	119	1.79
Enugu	5.0	432	126	3.51
Port Harcourt	5.0	1,617	380	16.5

4.5.4 Battery energy storage capacity

Due to random behaviors of renewable energy resources at all the sites considered, battery capacity changes constantly in the hybrid system. At any time of the year, the battery capacity depends on its previous state of charge (SOC), available energy from the RE sources in the HRES, and the system loads. Global engineering standards (IEEE & IEC standards) have been carefully considered for the analysis presented in this thesis. IEEE 1561, 1562 and IEC/TS 62257 recommend that systems performance analysis should cover all the seasons in a calendar year (IEC, 2007; IEEE, 2007a, 2007b) . This is represented by the 8760-hr (one year) analysis, which is the standard for evaluating the outputs and performance of PV and wind generator. This is because of the intermittency or variability of renewable energy resources. The analysis should show how RE can provide reliable energy to the users over the year. The hourly battery SOC is an evidence-based analysis to show the variability of the renewable energy resources considered in this thesis, and of course, it covers a year. In Nigeria, there is high solar irradiation cycle during the dry season and low irradiation cycle during the rainy season, likewise the wind energy resources. Therefore, 8760-hr analysis is acceptable according to standards and best practices (Akinyele & Rayudu, 2016).

The charging process of the battery occurs whenever the energy output of PV modules and wind turbines is greater than the load demand, while the battery discharges whenever the energy available from the RE sources is insufficient to meet the clinic load demand. According to the developed energy management algorithm in HOMER (Figure 3.13), priority is given to RE sources to supply the load, this implied that under the normal operating condition the power output of solar PV (P_{pv}) and wind turbine (P_{wt}) will supply the load while excess energy will be used to charge the battery until maximum state of charge (SOC_{max}) is reached. However, in the event of insufficient energy from either the RE sources or the battery to supply the load, a conventional diesel generator will be operated automatically to supply the load and charge the battery. Figure 4.13 represents the hourly battery SOC over a period of one year in the selected locations.

We observed from Figure 4.13 that the battery SOC at both Sokoto and Jos sites is constantly at full capacity over the year except for few hours. This is due to the enormous potential of RE resources at both sites, resulting in the availability of RE sources to meet the clinic load demand at all time. Iseyin and Port Harcourt sites, on the other hand, experienced higher battery depletion compare to other sites especially during the Month of July, August and September (rainy season). This experience is due to low potential of RE sources in meeting the clinic load demand, thus resulting in depletion of the battery to its minimum state of charge (SOCmin) before the generator comes up to supply the load and charges the batteries. As earlier discussed, the number of hours of operation of a diesel generator at these sites is more than the other sites due to the above reason.

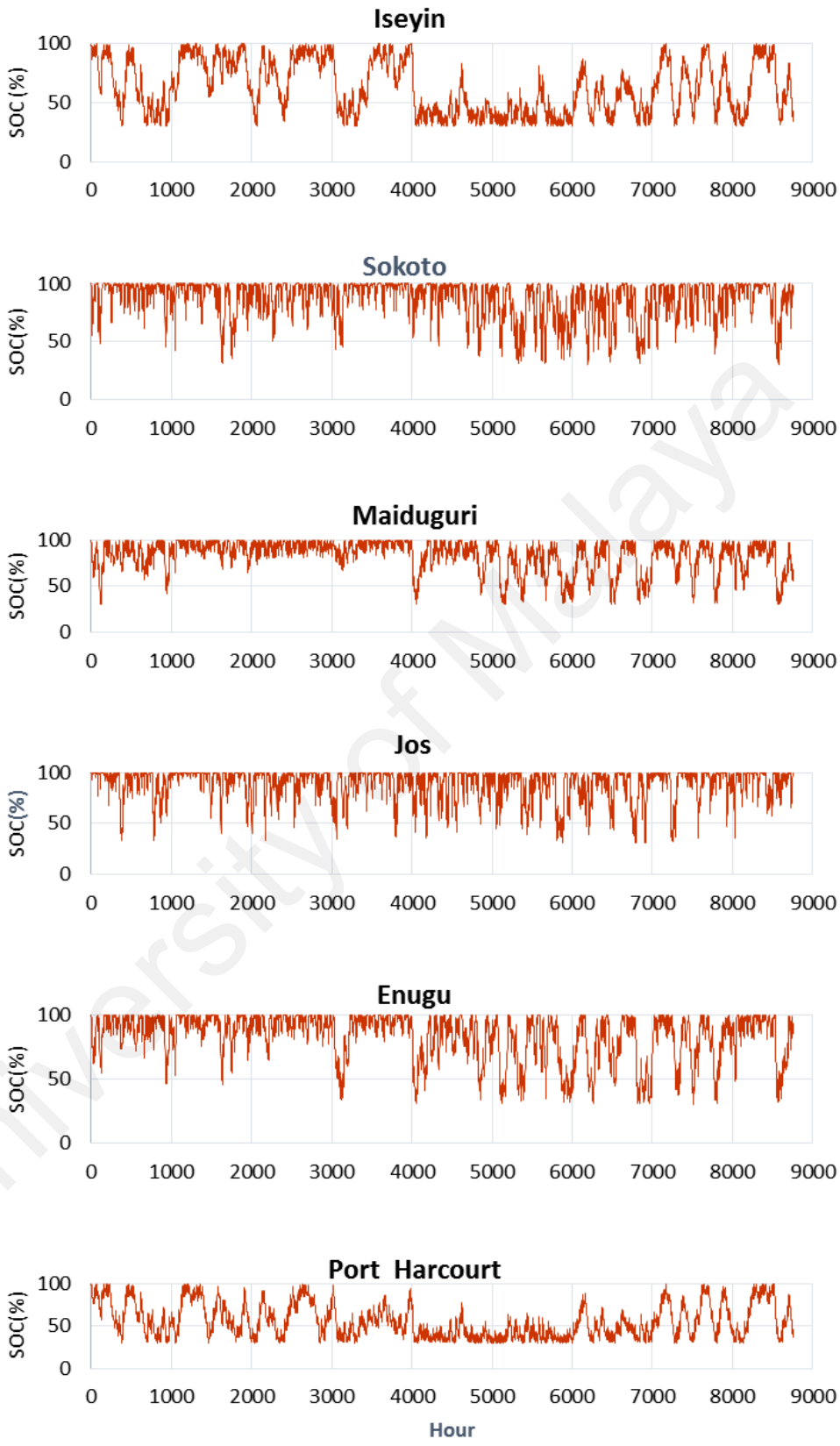

Figure 4. 13: Hourly battery SOC over a year at the selected sites

4.5.5 Combined energy production

Contribution of each energy source (wind turbine, solar panel and diesel generator) in meeting the load demand and the state of charge of batteries for the optimal hybrid system configuration case in Iseyin rural healthcare facility for two specific month of in a year ; January (dry season) and August (rainy season) is shown in Figures 4.14 and 4.15 respectively. These plots show the typical operation hour of the diesel generator in each of the specified months. A typical month of January in Nigeria is considered as dry season month due to clear sky conditions usually experienced during this month and more sunshine hours, leading to a good amount of solar radiation that encouraged PV power production. While August month in the entire region in Nigeria is considered as a rainy season month due to a large amount of rainfall during this period, hence cloudy sky leading low solar radiation potential that adversely affects PV power production.

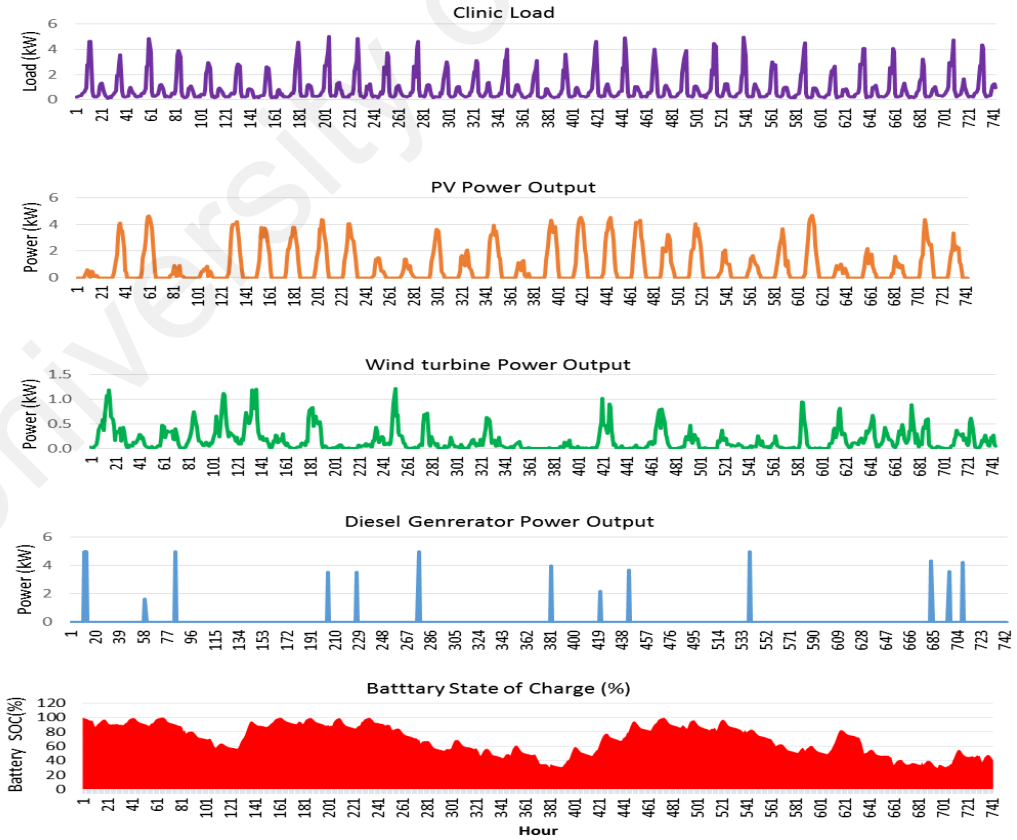

Figure 4. 14: Energy production of various energy sources and battery SOC of typical January month in Iseyin

As can be observed from Figure 4. 14, the battery state of charge remained full due to good amount of solar radiation incident on the PV panel during this month, leading to high power output from the PV panel to meet the load demand. Wind turbine also contributed in meeting the load demand as can been seen in the Figure. During this period, the number of hour of operation of diesel generator is limited due to sufficient amount of energy from RE sources to power the load and charges the battery.

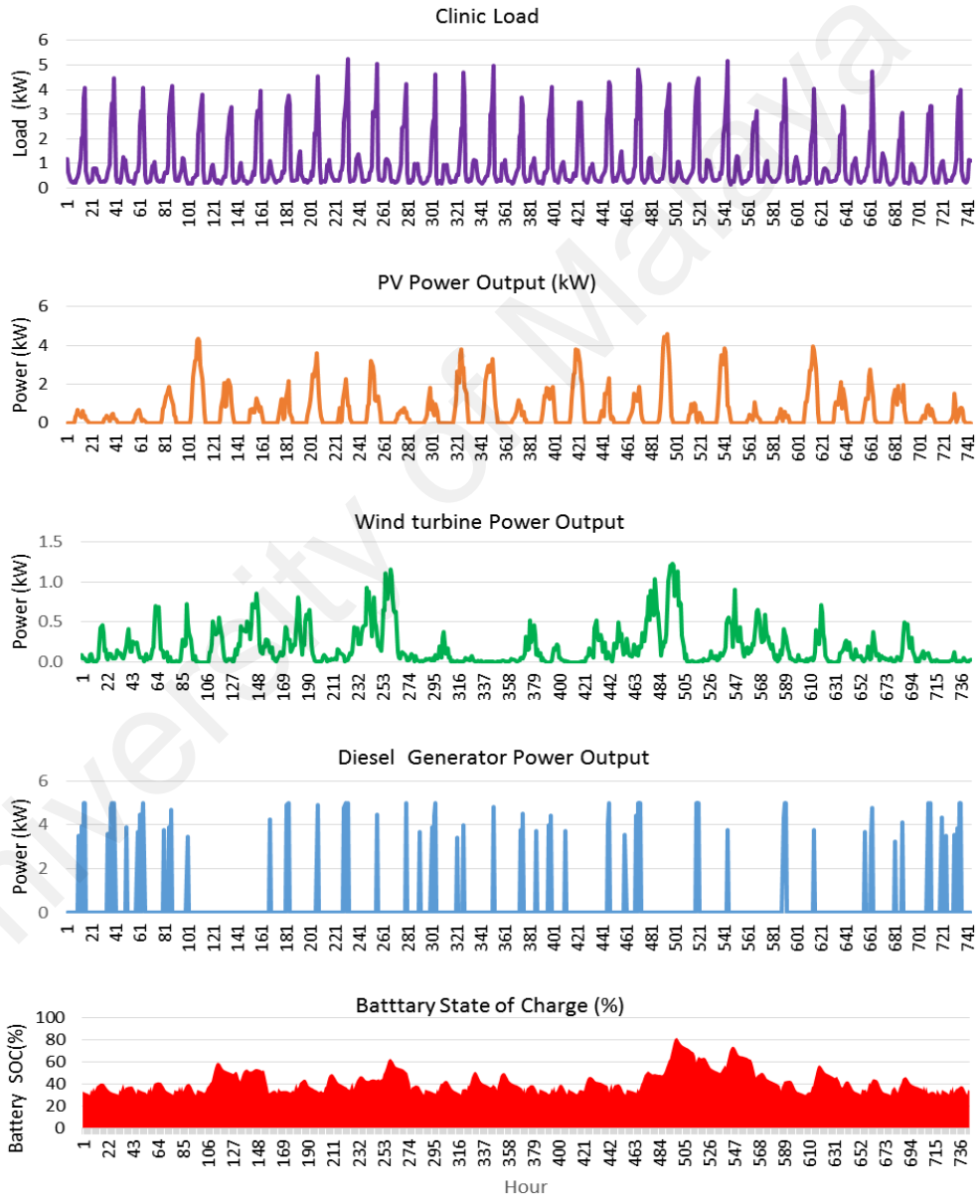

Figure 4. 15: Energy production of various energy sources and battery SOC of a typical August month in Iseyin

However, in the second scenario (August month), we observed constant depletion in battery storage capacity due to insufficient power production from both PV and wind energy sources as a result of changes in the weather condition. During this period, high number of start/stop of diesel generator operation is expected to meet the deficit of RE sources in meeting the clinic load demand as well as for charging the battery. It should, however, be noted that the battery capacity should not be depleted beyond the specified (30%) limit as already been designed with the energy management approach. This is done in order to avoid shorten the lifespan of the batteries.

4.6 Pollutant emission analysis

Figure 4.16 shows the annual carbon dioxide (CO_2) pollutant emission for the best optimal configurations in each of the selected sites, while Figure 4.17 shows the same analysis in comparison with diesel-only system configuration. The optimal hybrid renewable system configurations emitted 1,119.8, 374.4, 337.13, 298.66, 404.83 and 1,459.2 kg/year of CO_2 at Iseyin, Sokoto, Maiduguri, Jos, Enugu and Port-Harcourt respectively, while the diesel-only system emits 24,107kg/yr representing 86% to total CO_2 emission.

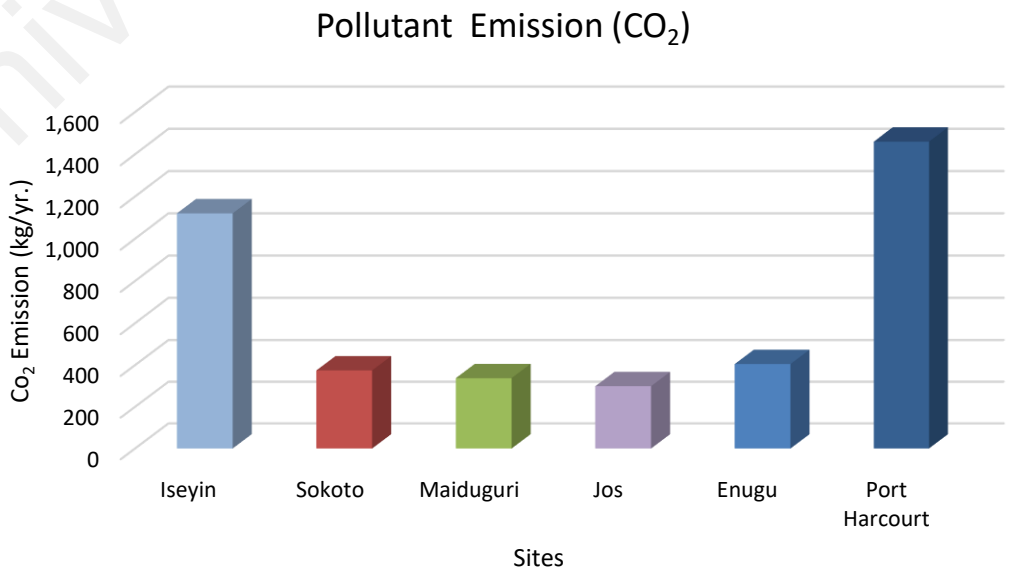

Figure 4.16: Comparison of CO_2 pollutant emission in the entire site

Since diesel generator consumed diesel fuel to produce power, thus the higher diesel operating hours experienced at both Port Harcourt and Iseyin site has led to high CO_2 emission as seen in Figure 4.16. On the other hand, the remaining sites experienced low emission due to high availability of renewable energy resources leading to utilization of hybrid PV/wind to power the rural health clinics majority of the time during the year rather than diesel generator system.

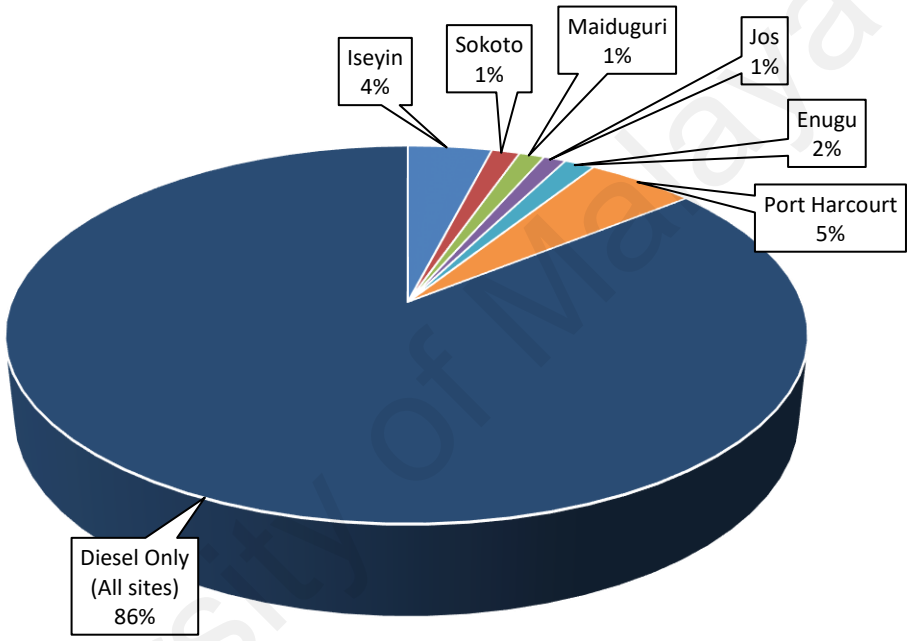

Table 4.17: Comparison of CO_2 emission in optimal system configuration and diesel-only system in the selected sites

As a result, a total of 95.4, 98.4, 98.6, 98.8, 98.3 and 93.9% of CO_2 emission would be curtailed if a hybrid renewable energy system configuration is adopted at Iseyin, Sokoto, Maiduguri, Jos, Enugu and Port-Harcourt respectively. Based on the observation from Fugure 4.16 and bearing in mind the effect of pollution into the environment, it can be concluded that the best suitable sites for HRES configuration comprising PV, wind, diesel and battery are Jos, Maiduguri, Sokoto and Enugu rural healthcare facilities. This is basically due to the highest percentage of CO_2 emission reduction in the locations as well as low NPC compared to other locations as earlier stated.

4.7 Sensitivity analysis

In this study, various uncertainty variables were explored to analyze the effect of the changes in uncertainty parameters on the optimal hybrid system configuration in the selected site. The sensitivity analysis in this thesis is carried out to study the effect of changes in the parameters of the hybrid system on the cost of energy (COE). To this aim, three important parameters in HRES are selected as sensitivity variable viz; global solar radiation on the horizontal surface, wind speed and diesel price. These parameters were varied by ± 20% to give room for wider analysis. The resulting sensitivity values were previously presented in Table 3.11, where 0% represent the present values of the parameter at the selected sites before variation.

The result of sensitivity analysis is presented in Figure 4.18. From this figure, we observed that COE is more sensitive to the variation in wind speed and solar radiation than diesel prices in the selected sites. That is, as the renewable energy resource's parameters (wind speed and solar radiation) increased from one site to another, the COE of the optimal system configuration decreases given more room to the adoption of RE sources in meeting the load demand. While in the case of diesel price, COE slightly increases with an increase in diesel price, therefore, the higher the cost of diesel fuel coupled with associated maintenance cost of diesel generator with make the configuration not feasible.

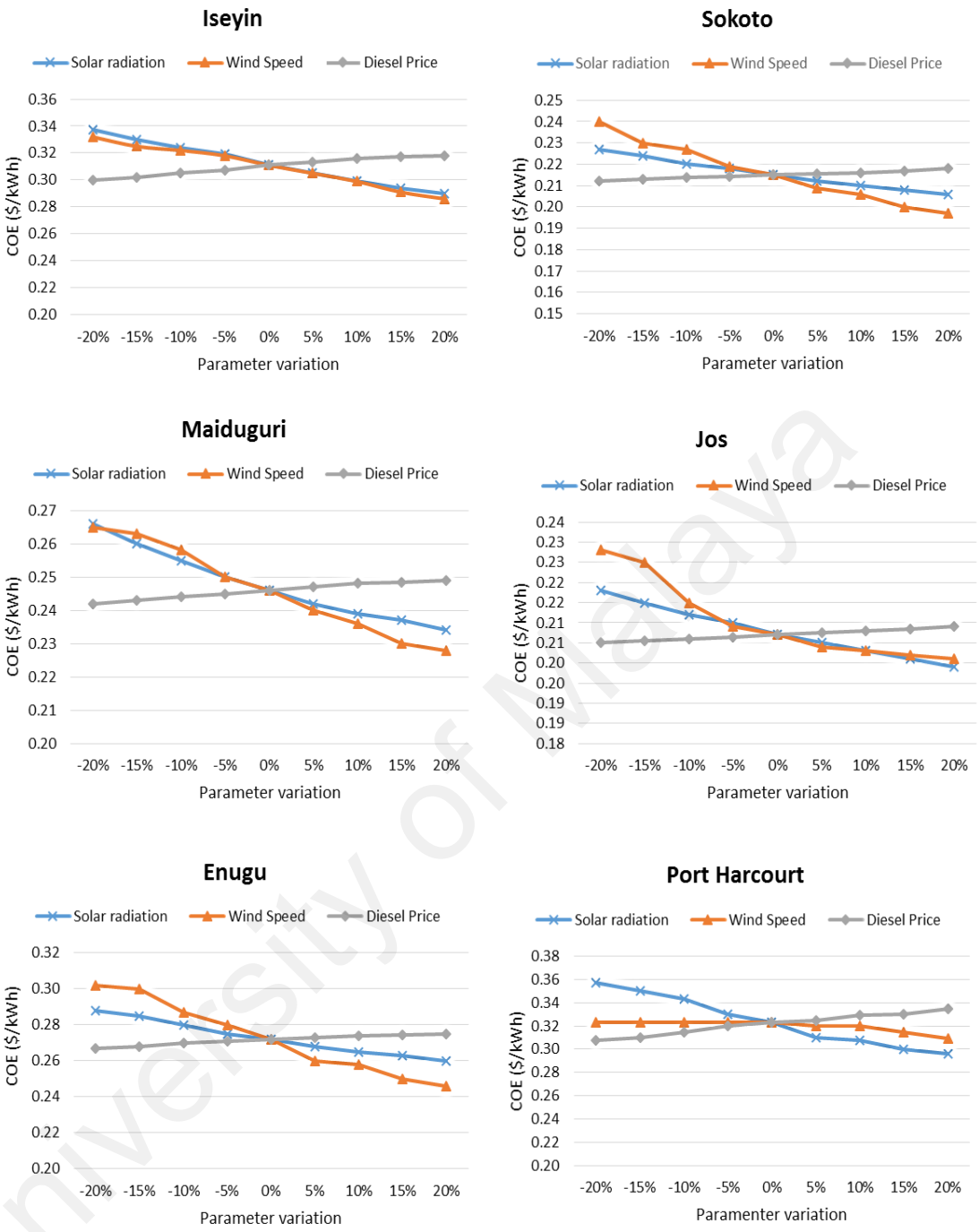

Figure 4. 18: Effect of parameter variation on cost of energy production

4.8 Chapter summary

In this chapter, the results of various sections of the study earlier highlighted in the previous chapters are presented and discussed. Foremost in this chapter is the results of solar radiation prediction with ANFIS. The performance analysis of the proposed ANFIS model in comparison with other models proved the proposed model as an efficient

technique for global solar radiation prediction with a greater degree of reliability for practical purposes. The results of renewable energy resources assessments in the selected sites indicate Sokoto and Jos as most suitable sites for wind energy application, while the values obtained for global, beam and diffuse radiation, as well as clearness index, showed that all the sites considered in this study enjoy considerable solar energy potential suitable for solar energy conversion applications.

In the PV modeling, the tabulation of numerical results shows the correlation of the PV module parameters with module characteristic curve as an indicator of PV model performance based on the developed PV model in MATLAB/Simulink. Furthermore, the performance of the selected wind turbines at various sites shows that, Jos and Sokoto to be good sites for wind turbine applications irrespective of the wind turbine model adopted, this is due to enormous potential of wind energy resources at these sites compared to other sites. Meanwhile, a 1kW wind turbine models (FDQ-3.0-1) is considered the best in terms of energy production and capacity factor in all the sites; this is due to relatively low cut-in wind speed and rated wind speed compared other models.

Finally, the results of optimal sizing of the hybrid renewable energy system configuration in each of the selected rural healthcare facilities, considered hybrid PV-diesel-battery system as the best system configuration for Port Harcourt sites. While PV-wind-diesel-battery is considered optimal for the rest locations (Iseyin, Sokoto, Maiduguri, Jos and Enugu). The optimal configuration obtained for Jos has the lowest NPC and COE of all the sites considered, followed by Sokoto site. The lowest NPC and COE obtained from these sites are due to high solar and wind resources availability in the sites as compared to other sites.

CHAPTER 5: CONCLUSIONS AND RECOMMENDATIONS

5.1 Conclusions

This thesis focused on the feasibility of off-grid hybrid renewable energy in delivering basic healthcare services in rural areas where there is no grid extension or unreliable power supply. Since it has been reported that many rural locations far away from the grid center have difficulties in accessing electricity, and this has resulted in inability of rural healthcare facilities located in such places to deliver its intended mandate. This has often led to many problems, including obstetric complications, which is one of the root causes of the high maternal mortality rates in the rural area. Lack of antenatal care, absences of skilled birth attendants and limited availability of emergency obstetrics procedures due to lack of electricity are reasons for this situation. Therefore, the provision of portable hybrid renewable power supply will enable certain medical equipment, critical lighting and mobile communication devices to be powered in an off-grid area for timely delivery and critical medical care for the rural dwellers.

To this aim, the potentials of wind and solar energy in six selected rural locations in Nigeria has been statistically analysis based on long-term hourly and daily available meteorological data. This is followed by optimal configurations assessment, sizing of system components as well as techno-economic assessment of employing hybrid renewable energy system in providing electricity access to the healthcare facilities located in these areas. To assess the techno-economic feasibility of employing hybrid renewable energy system comprising wind and solar, hybrid optimization software (HOMER) developed by US National Renewable Energy Lab. (NREL) has been used. This software has the capacity to simulate, optimize and conduct sensitivity analysis on different parameter of the system to select the optimal configuration that meet the clinic load demand and offer best performance with minimum life-cycle cost.

Therefore, the major finding in the study is summarized as follows:

- The monthly mean as well as the annual mean power density for Iseyin and Port-Harcourt fall into Class 1. In Enugu and Maiduguri, the wind power classification exists under Class 3. For Sokoto, the annual mean power density stand at 515.5 W/m^2, while the average annual power density in Jos exists as 741.2 W/m^2, making both sites to fall into Class 7 of the wind power classification. The classification places Sokoto and Jos in a high potential site for large-scale wind turbine applications and the rest of the selected locations as low wind potential sites.
- All the sites considered in this study enjoy a considerable solar energy potential suitable for solar energy conversion applications. However, better contribution of solar energy will be enhanced if the solar panel is inclined at optimal tilt. Since monthly tilt adjustment of solar panel may be impracticable owing to its financial implications, therefore the average seasonal (dry season) optimum tilt angle for Iseyin, Sokoto, Maiduguri, Jos, Enugu and Port-Harcourt are 29.6^o, 34.6^o, 34.4^o, 32.9^o, 28.0^o and 26.1^o respectively. While, 3.4^o, 4.9^o, 4.9^o, 4.1^o, 3.1^o and 2.5^o optimal tilts is applicable for Iseyin, Sokoto, Maiduguri, Jos, Enugu and Port-Harcourt respectively during the rainy season. Inclination of the solar panel in this positions has led to considerable solar energy gain.
- Put together, the complementary nature as well as the abundance of wind and solar resources in the considered locations makes it ideal to include renewable energy systems, such as solar PV and wind turbine in the design of standalone hybrid power supply system to improve rural healthcare delivery at the selected location. The reliability of hybrid systems is found to be enhanced when solar, wind and diesel production are used together; the size of battery storage is also reduced because there is less dependence on one method of energy production.

- Modelling and prediction of global solar radiation using soft computing methodology (ANFIS) has shown a good prediction performance compared to other models used in predicting solar radiation for the purpose of filling up any missing data in the dataset employed for solar energy resources assessments.
- The modelling of PV module performance and the determination of module parameters using an iterative algorithm developed in MATLAB has shown a good performance when compare with manufacturer datasheet. The obtained results has demonstrated good accuracy of the model under varying environmental condition. Wind turbine performance on the other hand, modelled based on wind turbine's power curves and equation has shown a good results for the selection of appropriate wind turbine in each sites.
- The PV/wind/diesel/battery hybrid system configuration is considered optimum for applications concerning rural healthcare facility at Iseyin, Sokoto, Maiduguri, Jos and Enugu, while hybrid systems involving PV/diesel/battery is considered ideal at Port-Harcourt site. Hence, the hybrid system configurations which meet the desired load largely depend on the renewable energy potential. For instance, the optimal configuration obtained for Jos has the lowest NPC and COE of all the sites considered, due to the high solar and wind resources availability compared to other locations; more than half of the total energy production of the optimal system configuration in this site, is found to be provided by the solar and wind generator. The wind system hybrid configuration is not considered best option for healthcare applications at Port Harcourt, owing to its relatively low wind speed. Nonetheless, the simulation results shows that it is still better than diesel-only configuration.
- The diesel-only system provides the highest COE, and emits 24,107kg of CO_2 per year in all the site considered. This pollutant emission is high and can have adverse

effect on the surrounding environment as well as the health of patients and staffs in the rural health facilities. Therefore, if a small/medium-size healthcare facility hybrid renewable energy system is properly managed, it can lead to yearly fuel savings of about 75–80% while delivering reliable power supply.

- The entire results indicated that not only did the considered hybrid system configurations perform better than diesel-alone configuration with respect to the NPC in all the six sites; it additionally showed good performance in fuel consumption and CO_2 reduction category.
- The inclusion of the wind and solar energy in the hybrid power system has greatly increased the reliability of the entire system due to the complimentary nature of wind and solar, while the use of diesel generator has reduce the battery energy storage requirements. This is demonstrated by the contribution of each energy sources, the battery state of charge and energy balance in the hybrid system at any point in time. The energy contribution from PV and wind turbine varies from one month to another during which the battery is set to supply the load in the event of incapability of the RE sources in meeting load demand, thereafter the diesel generator operates to supply the load and charges the battery in order to ensure it did not discharge beyond its minimum state of charge.
- The minimization of life-cycle cost in the optimal system configuration is not only achieved by considering optimal sizing of system components but also by employing appropriate energy management strategy to control the operation of the diesel generator and for effective charging/discharging of the battery storage system.
- The implementation of the proposed hybrid renewable energy model in the rural health clinics will among other lead to the following benefits; elongation of the operating hours in rural health clinic due to availability of general lighting;

attraction of more medical personnel (doctors and nurses), leading to availability of wider range of medical services, since experts tends to be attracted to rural areas having access to electricity; improved cold-chain vaccines, drugs, blood and other medical perishable preservation due to availability of electricity to power refrigerators; better emergency services and improved referral system via radio communication to the secondary healthcare centers.

5.2 Recommendations

In view of the above findings, the following are recommended;

- Owing to the capital intensive nature of the proposed hybrid renewable energy system, which usually pose as barrier to its implementation compare to conventional generators-alone system, the Nigeria government should intensify more effort to innovate financial solutions that can ease capital cost barriers which hindered the adoption of clean and efficient energy systems in rural healthcare facilities.
- Due to the highlighted benefits of reliable energy access to rural healthcare development, the energy commission in the country need to design new policies, standards and regulations to support procurement, installation, and sustainable operation of renewable energy technologies, as well as innovative financing structures to ease investments in the technology. The policy should also be channeled towards research and development (R&D) in other alternative energy sources and its effective utilization in healthcare applications.

5.3 Suggestions for future work

In this thesis, optimal configuration assessment and design of hybrid renewable energy system comprising PV, wind, diesel generator and battery energy storage for powering rural healthcare facilities located in six selected sites in Nigeria, which each site representing different climatic zone of the country have been proposed. Although various analysis have been carried out in this study to ensure the achievements of the set objectives; therefore, the following are suggested for further studies:

- Assessments of other alternative energy sources (such as small hydro, and biomass) in conjunction with wind and solar to form hybrid power supply system suitable for health facilities application in other resource-constrained areas need to be consider
- In order to enhance operational performance of the hybrid system configurations and improvement in energy management strategies, application of modern control techniques is required. This will allow better utilization of constituent energy sources in the hybrid system.
- Future studies can be conducted using the developed ANFIS model by considering several other combinations of meteorological and geographical data such as air pressure, humidity, cloud factor, latitude, longitude and altitude as inputs to the model. This will help to assess the possibility of achieving further accuracy of ANFIS model prediction.
- Development of a new optimization algorithm for sizing hybrid power scheme, especially dealing with operation and sizing of battery system.

REFERENCES

Abdalla, Y. A. (1994). New correlations of global solar radiation with meteorological parameters for Bahrain. *International Journal of Solar Energy, 16*(2), 111-120.

Adair-Rohani, H., Zukor, K., Bonjour, S., Wilburn, S., Kuesel, A. C., Hebert, R., & Fletcher, E. R. (2013). Limited electricity access in health facilities of sub-Saharan Africa: a systematic review of data on electricity access, sources, and reliability. *Global Health: Science and Practice, 1*(2), 249-261.

Adaramola, M. S. (2012). Estimating global solar radiation using common meteorological data in Akure, Nigeria. *Renewable Energy, 47*, 38-44.

Adaramola, M. S., Oyewola, O. M., Ohunakin, O. S., & Akinnawonu, O. O. (2014). Performance evaluation of wind turbines for energy generation in Niger Delta, Nigeria. *Sustainable Energy Technologies and Assessments, 6*, 75-85.

Adaramola, M. S., Paul, S. S., & Oyewola, O. M. (2014). Assessment of decentralized hybrid PV solar-diesel power system for applications in Northern part of Nigeria. *Energy for Sustainable Development, 19*, 72-82.

Ajayi, O., Ohijeagbon, O., Nwadialo, C., & Olasope, O. (2014). New model to estimate daily global solar radiation over Nigeria. *Sustainable Energy Technologies and Assessments, 5*(1), 28-36.

Akdağ, S. A., & Dinler, A. (2009). A new method to estimate Weibull parameters for wind energy applications. *Energy Conversion and Management, 50*(7), 1761-1766.

Akikur, R. K., Saidur, R., Ping, H. W., & Ullah, K. R. (2013). Comparative study of stand-alone and hybrid solar energy systems suitable for off-grid rural electrification: A review. *Renewable and Sustainable Energy Reviews, 27*(0), 738-752.

Akinyele, D., & Rayudu, R. (2016). Strategy for developing energy systems for remote communities: Insights to best practices and sustainability. *Sustainable Energy Technologies and Assessments, 16*, 106-127.

Al-Alawi, S., & Al-Hinai, H. (1998). An ANN-based approach for predicting global radiation in locations with no direct measurement instrumentation. *Renewable Energy, 14*(1), 199-204.

Allen, R. G., Pereira, L. S., Raes, D., & Smith, M. (1998). Crop evapotranspiration-Guidelines for computing crop water requirements-FAO Irrigation and drainage paper 56. *FAO, Rome, 300*, 6541.

Azoumah, Y., Yamegueu, D., Ginies, P., Coulibaly, Y., & Girard, P. (2011). Sustainable electricity generation for rural and peri-urban populations of sub-Saharan Africa: the "flexy-energy" concept. *Energy Policy, 39*(1), 131-141.

Bahramara, S., Moghaddam, M., & Haghifam, M. (2016). Optimal planning of hybrid renewable energy systems using HOMER: A review. *Renewable and Sustainable Energy Reviews, 62*, 609-620.

Bajpai, P., & Dash, V. (2012). Hybrid renewable energy systems for power generation in stand-alone applications: A review. *Renewable and Sustainable Energy Reviews, 16*(5), 2926-2939.

Bakirci, K. (2009). Correlations for estimation of daily global solar radiation with hours of bright sunshine in Turkey. *Energy, 34*(4), 485-501.

Behrang, M., Assareh, E., Ghanbarzadeh, A., & Noghrehabadi, A. (2010). The potential of different artificial neural network (ANN) techniques in daily global solar radiation modeling based on meteorological data. *Solar energy, 84*(8), 1468-1480.

Behrang, M., Assareh, E., Noghrehabadi, A., & Ghanbarzadeh, A. (2011). New sunshine-based models for predicting global solar radiation using PSO (particle swarm optimization) technique. *Energy, 36*(5), 3036-3049.

Benghanem, M. (2011). Optimization of tilt angle for solar panel: Case study for Madinah, Saudi Arabia. *Applied Energy, 88*(4), 1427-1433.

Benghanem, M., Mellit, A., & Alamri, S. (2009). ANN-based modelling and estimation of daily global solar radiation data: A case study. *Energy Conversion and Management, 50*(7), 1644-1655.

Besarati, S. M., Padilla, R. V., Goswami, D. Y., & Stefanakos, E. (2013). The potential of harnessing solar radiation in Iran: Generating solar maps and viability study of PV power plants. *Renewable Energy, 53*, 193-199.

Besharat, F., Dehghan, A. A., & Faghih, A. R. (2013). Empirical models for estimating global solar radiation: A review and case study. *Renewable and Sustainable Energy Reviews, 21*(1), 798-821.

Bilal, B. O., Sambou, V., Ndiaye, P., Kébé, C., & Ndongo, M. (2010). Optimal design of a hybrid solar–wind-battery system using the minimization of the annualized cost system and the minimization of the loss of power supply probability (LPSP). *Renewable Energy, 35*(10), 2388-2390.

Borowy, B. S., & Salameh, Z. M. (1996). Methodology for optimally sizing the combination of a battery bank and PV array in a wind/PV hybrid system. *IEEE Transactions on Energy Conversion, 11*(2), 367-375.

Bortolini, M., Gamberi, M., Graziani, A., Mora, C., & Regattieri, A. (2013). Multi-parameter analysis for the technical and economic assessment of photovoltaic systems in the main European Union countries. *Energy Conversion and Management, 74*, 117-128.

Burton, T., Jenkins, N., Sharpe, D., & Bossanyi, E. (2011). *Wind energy handbook*: John Wiley & Sons.

Caló, A., & Pongrácz, E. (2011). Assessing the potential for smart energy grids in the Northern Periphery: Oulu University, Master's Thesis, Part.

Celik, A. (2003). A simplified model for estimating the monthly performance of autonomous wind energy systems with battery storage. *Renewable Energy, 28*(4), 561-572.

Cha, H. J., & Enjeti, P. N. (2003). *A three-phase AC/AC high-frequency link matrix converter for VSCF applications.* Paper presented at the IEEE 34th Annual Power Electronics Specialist Conference, PESC'03. .

Chang, T. P. (2011). Estimation of wind energy potential using different probability density functions. *Applied Energy, 88*(5), 1848-1856.

Chauhan, A., & Saini, R. (2014). A review on integrated renewable energy system based power generation for stand-alone applications: configurations, storage options, sizing methodologies and control. *Renewable and Sustainable Energy Reviews, 38*, 99-120.

Chaurey, A., & Kandpal, T. C. (2010). Assessment and evaluation of PV based decentralized rural electrification: An overview. *Renewable and Sustainable Energy Reviews, 14*(8), 2266-2278.

Chedid, R., & Rahman, S. (1997). Unit sizing and control of hybrid wind-solar power systems. *IEEE Transactions on Energy Conversion, 12*(1), 79-85.

Chouder, A., Silvestre, S., Sadaoui, N., & Rahmani, L. (2012). Modeling and simulation of a grid connected PV system based on the evaluation of main PV module parameters. *Simulation Modelling Practice and Theory, 20*(1), 46-58.

Colson, C., Wang, C., Nehrir, M., Guda, S., & Li, J. (2007). *Stand-alone Hybrid Wind-Microturbine Distributed Generation System: A Case Study.* Paper presented at the 39th North American Power Symposium, NAPS'07. .

Connolly, D., Lund, H., Mathiesen, B. V., & Leahy, M. (2010). A review of computer tools for analysing the integration of renewable energy into various energy systems. *Applied Energy, 87*(4), 1059-1082.

Dadhania, A., Venkatesh, B., Nassif, A., & Sood, V. (2013). Modeling of doubly fed induction generators for distribution system power flow analysis. *International Journal of Electrical Power & Energy Systems, 53*, 576-583.

Dalton, G., Lockington, D., & Baldock, T. (2009). Feasibility analysis of renewable energy supply options for a grid-connected large hotel. *Renewable Energy, 34*(4), 955-964.

Daud, A.-K., & Ismail, M. S. (2012). Design of isolated hybrid systems minimizing costs and pollutant emissions. *Renewable Energy, 44*, 215-224.

De, A., & Musgrove, L. (1988). The optimization of hybrid energy conversion systems using the dynamic programming model—RAPSODY. *International journal of energy research, 12*(3), 447-457.

Diaf, S., Diaf, D., Belhamel, M., Haddadi, M., & Louche, A. (2007). A methodology for optimal sizing of autonomous hybrid PV/wind system. *Energy Policy, 35*(11), 5708-5718.

Dihrab, S. S., & Sopian, K. (2010). Electricity generation of hybrid PV/wind systems in Iraq. *Renewable Energy, 35*(6), 1303-1307.

Duffie, J. A., & Beckman, W. A. (2013). *Solar engineering of thermal processes*: John Wiley & Sons.

Dufo-López, R., & Bernal-Agustín, J. L. (2008). Multi-objective design of PV–wind–diesel–hydrogen–battery systems. *Renewable Energy, 33*(12), 2559-2572.

ECN. (1997). *Potentials for renewable energy application*. Lagos: Gilspar Co. Ltd.

ECN. (2006). *Renewable Energy Master Plan (REMP)*. Abuja: Federal Goverment of Nigeria.

ECN. (2013). Energy Commission of Nigeria. Retrieved 13 March, 2013, from http://www.energy.gov.ng/

El-Hefnawi, S. H. (1998). Photovoltaic diesel-generator hybrid power system sizing. *Renewable Energy, 13*(1), 33-40.

El Alimi, S., Maatallah, T., Dahmouni, A. W., & Nasrallah, S. B. (2012). Modeling and investigation of the wind resource in the gulf of Tunis, Tunisia. *Renewable and Sustainable Energy Reviews, 16*(8), 5466-5478.

El Ouderni, A. R., Maatallah, T., El Alimi, S., & Nassrallah, S. B. (2013). Experimental assessment of the solar energy potential in the gulf of Tunis, Tunisia. *Renewable and Sustainable Energy Reviews, 20*, 155-168.

El Shahat, A. (2010). Maximum power point genetic identification function for photovoltaic system. *International Journal of Research and Reviews in Applied Sciences, 3*(3), 264-273.

Elbaset, A. (2011). Design, Modeling and Control Strategy of PV/FC Hybrid Power System. *J. Electrical Systems, 7*(2), 270-286.

Elhadidy, M., & Shaahid, S. (1999). Optimal sizing of battery storage for hybrid (wind+ diesel) power systems. *Renewable Energy, 18*(1), 77-86.

Elliott, D., & Schwartz, M. (1993). Wind energy potential in the United States. *Pacific Northwest Laboratory PNL-SA-23109, Richland, WA*.

Entchev, E. (2004). Hybrid Fuel Cell/Microturbine Energy System Modelling and Simulation. *WSEAS Transactions on Systems, 3*(8), 2623-2627.

Erbs, D., Klein, S., & Duffie, J. (1982). Estimation of the diffuse radiation fraction for hourly, daily and monthly-average global radiation. *Solar energy, 28*(4), 293-302.

EWEA. (2011). *Wind in power–2010 European statistics*. Retrieved from http://www.ewea.org/.

Farret, F. A. (2006). *Integration of alternative sources of energy*: John Wiley & Sons.

Giannoulis, E. D., & Haralambopoulos, D. A. (2011). Distributed Generation in an isolated grid: Methodology of case study for Lesvos – Greece. *Applied Energy, 88*(7), 2530-2540.

Gökçek, M., Bayülken, A., & Bekdemir, Ş. (2007). Investigation of wind characteristics and wind energy potential in Kirklareli, Turkey. *Renewable Energy, 32*(10), 1739-1752.

Graham, V., & Hollands, K. (1990). A method to generate synthetic hourly solar radiation globally. *Solar energy, 44*(6), 333-341.

Gupta, S., Tiwari, H., Fozdar, M., & Chandna, V. (2012). *Development of a two diode model for photovoltaic modules suitable for use in simulation studies.* Paper presented at the Power and Energy Engineering Conference (APPEEC), 2012 Asia-Pacific.

Hansen, J. W. (1999). Stochastic daily solar irradiance for biological modeling applications. *Agricultural and forest meteorology, 94*(1), 53-63.

Hargreaves, G. H., & Samani, Z. A. (1982). Estimating potential evapotranspiration. *Journal of the Irrigation and Drainage Division, 108*(3), 225-230.

Hay, J. E., & Davies, J. A. (1980). *Calculation of the solar radiation incident on an inclined surface.* Paper presented at the Proc. of First Canadian Solar Radiation Data Workshop (Eds: JE Hay and TK Won), Ministry of Supply and Services Canada.

Hiendro, A., Kurnianto, R., Rajagukguk, M., & Simanjuntak, Y. M. (2013). Techno-economic analysis of photovoltaic/wind hybrid system for onshore/remote area in Indonesia. *Energy, 59*, 652-657.

Hossain, M. K., & Ali, M. H. (2016). Transient stability augmentation of PV/DFIG/SG-based hybrid power system by parallel-resonance bridge fault current limiter. *Electric Power Systems Research, 130*, 89-102.

Hottel, H., & Woertz, B. (1942). Performance of flat-plate solar-heat collectors. *Trans. ASME (Am. Soc. Mech. Eng.);(United States), 64*.

Hunt, L., Kuchar, L., & Swanton, C. (1998). Estimation of solar radiation for use in crop modelling. *Agricultural and forest meteorology, 91*(3), 293-300.

Ibrahim, A., Othman, M. Y., Ruslan, M. H., Mat, S., & Sopian, K. (2011). Recent advances in flat plate photovoltaic/thermal (PV/T) solar collectors. *Renewable and Sustainable Energy Reviews, 15*(1), 352-365.

IEA. (2008). World Energy Outlook. from http://www.worldenergyoutlook.org/

IEC. (2007). Recommendations for small renewable energy and hybrid systems for rural electrification, IEC Std. 62257 (pp. 1-27): IEC.

IEEE. (2007a). Guide for array and battery sizing in stand-alone photovoltaic (PV) systems, IEEE Std. 1562 (pp. 1-34): IEEE.

IEEE. (2007b). IEEE Guide for Optimizing the Performance and Life of Lead-Acid Batteries in Remote Hybrid Power Systems. IEEE Std. 1561 (pp. 1-35).

IFAD. (2012). Enabling poor rural people to overcome poverty in Nigeria, International Fund for Agricultural Development from http://www.ifad.org/operations/projects/regions/pa/factsheets/ng.pdf).

Ikeme, J., & Ebohon, O. J. (2005). Nigeria's electric power sector reform: what should form the key objectives? *Energy Policy, 33*(9), 1213-1221.

Iqbal, M. (2003). Modeling and control of a wind fuel cell hybrid energy system. *Renewable Energy, 28*(2), 223-237.

IRENA. (2012). International Off-Grid Renewable Energy Conference :Key findings and recommendations. from http://www.irena.org

Ishaque, K., Salam, Z., & Taheri, H. (2011). Simple, fast and accurate two-diode model for photovoltaic modules. *Solar Energy Materials and Solar Cells, 95*(2), 586-594.

Islam, M., Saidur, R., & Rahim, N. (2011). Assessment of wind energy potentiality at Kudat and Labuan, Malaysia using Weibull distribution function. *Energy, 36*(2), 985-992.

Ismail, M., Moghavvemi, M., & Mahlia, T. (2013). Techno-economic analysis of an optimized photovoltaic and diesel generator hybrid power system for remote houses in a tropical climate. *Energy Conversion and Management, 69*, 163-173.

Izgi, E., Öztopal, A., Yerli, B., Kaymak, M. K., & Şahin, A. D. (2012). Short–mid-term solar power prediction by using artificial neural networks. *Solar energy, 86*(2), 725-733.

Jang, J.-S. (1993). ANFIS: adaptive-network-based fuzzy inference system. *IEEE Transactions on Systems, Man and Cybernetics, 23*(3), 665-685.

Jiang, Y. (2009). Computation of monthly mean daily global solar radiation in China using artificial neural networks and comparison with other empirical models. *Energy, 34*(9), 1276-1283.

Kalantar, M., & Mousavi G, S. (2010). Dynamic behavior of a stand-alone hybrid power generation system of wind turbine, microturbine, solar array and battery storage. *Applied Energy, 87*(10), 3051-3064.

Kaldellis, J. (2004). Optimum technoeconomic energy autonomous photovoltaic solution for remote consumers throughout Greece. *Energy Conversion and Management, 45*(17), 2745-2760.

Kaldellis, J., Simotas, M., Zafirakis, D., & Kondili, E. (2009). Optimum autonomous photovoltaic solution for the Greek islands on the basisof energy pay-back analysis. *Journal of Cleaner Production, 17*(15), 1311-1323.

Kaldellis, J., Zafirakis, D., Kaldelli, E., & Kavadias, K. (2009). Cost benefit analysis of a photovoltaic-energy storage electrification solution for remote islands. *Renewable Energy, 34*(5), 1299-1311.

Karaki, S., Chedid, R., & Ramadan, R. (1999). Probabilistic performance assessment of wind energy conversion systems. *IEEE Transactions on Energy Conversion, 14*(2), 217-224.

Kellogg, W., Nehrir, M., Venkataramanan, G., & Gerez, V. (1996). Optimal unit sizing for a hybrid wind/photovoltaic generating system. *Electric Power Systems Research, 39*(1), 35-38.

Khatod, D. K., Pant, V., & Sharma, J. (2010). Analytical approach for well-being assessment of small autonomous power systems with solar and wind energy sources. *IEEE Transactions on Energy Conversion, 25*(2), 535-545.

Klucher, T. M. (1979). Evaluation of models to predict insolation on tilted surfaces. *Solar energy, 23*(2), 111-114.

Koza, J. R. (1992). *Genetic programming: on the programming of computers by means of natural selection* (Vol. 1): MIT press.

Kumar, A., Mohanty, P., Palit, D., & Chaurey, A. (2009). Approach for standardization of off-grid electrification projects. *Renewable and Sustainable Energy Reviews, 13*(8), 1946-1956.

Kusakana, K., & Vermaak, H. J. (2013). Hybrid renewable power systems for mobile telephony base stations in developing countries. *Renewable Energy, 51*, 419-425.

Lambert, T., Gilman, P., & Lilienthal, P. (2006). Micropower system modeling with HOMER. *Integration of alternative sources of energy, 1*(1), 379-385.

Li, J., Wei, W., & Xiang, J. (2012). A simple sizing algorithm for stand-alone PV/wind/battery hybrid microgrids. *Energies, 5*(12), 5307-5323.

Li, X., Song, Y.-J., & Han, S.-B. (2007). *Study on power quality control in multiple renewable energy hybrid microgrid system.* Paper presented at the IEEE Lausanne Power Tech Confernce, 2007.

Liu, B., & Jordan, R. (1961). Daily insolation on surfaces tilted towards equator. *ASHRAE J.;(United States), 10*.

Liu, X., Islam, S., Chowdhury, A., & Koval, D. (2008). *Reliability evaluation of a wind-diesel-battery hybrid power system.* Paper presented at the IEEE/IAS Industrial and Commercial Power Systems Technical Conference, ICPS 2008. .

Liu, X., Mei, X., Li, Y., Wang, Q., Jensen, J. R., Zhang, Y., & Porter, J. R. (2009). Evaluation of temperature-based global solar radiation models in China. *Agricultural and forest meteorology, 149*(9), 1433-1446.

Lu, B., & Shahidehpour, M. (2005). Short-term scheduling of battery in a grid-connected PV/battery system. *IEEE Transactions on Power Systems, 20*(2), 1053-1061.

Luque, A., & Hegedus, S. (2011). *Handbook of photovoltaic science and engineering*: Wiley. com.

Mahmoud, M. M., & Ibrik, I. H. (2006). Techno-economic feasibility of energy supply of remote villages in Palestine by PV-systems, diesel generators and electric grid. *Renewable and Sustainable Energy Reviews, 10*(2), 128-138.

Markvart, T., Fragaki, A., & Ross, J. (2006). PV system sizing using observed time series of solar radiation. *Solar energy, 80*(1), 46-50.

Massardo, A. F., McDonald, C. F., & Korakianitis, T. (2002). Microturbine/fuel-cell coupling for high-efficiency electrical-power generation. *Journal of engineering for gas turbines and power, 124*(1), 110-116.

Mathew, S. (2006). *Wind energy: fundamentals, resource analysis and economics* (Vol. 1): Springer.

Mellit, A., Benghanem, M., & Kalogirou, S. (2006). An adaptive wavelet-network model for forecasting daily total solar-radiation. *Applied Energy, 83*(7), 705-722.

Mellit, A., Menghanem, M., & Bendekhis, M. (2005). *Artificial neural network model for prediction solar radiation data: application for sizing stand-alone photovoltaic power system.* Paper presented at the Power Engineering Society General Meeting, 2005. IEEE.

Mohammadi, K., & Mostafaeipour, A. (2013). Using different methods for comprehensive study of wind turbine utilization in Zarrineh, Iran. *Energy Conversion and Management, 65*, 463-470.

Mohandes, M. A. (2012). Modeling global solar radiation using Particle Swarm Optimization (PSO). *Solar energy, 86*(11), 3137-3145.

Morgan, E. C., Lackner, M., Vogel, R. M., & Baise, L. G. (2011). Probability distributions for offshore wind speeds. *Energy Conversion and Management, 52*(1), 15-26.

Mulder, G., Six, D., Claessens, B., Broes, T., Omar, N., & Van Mierlo, J. (2013). The dimensioning of PV-battery systems depending on the incentive and selling price conditions. *Applied Energy, 111*, 1126-1135.

mygadgetsmall. Retrieved May 20, 2015, from http://www.mygadgetsmall.com/

Naikodi, A. (2011). *Solar-wind hybrid power for rural Indian cell sites.* Paper presented at the IEEE International Energy Conference and Exhibition (EnergyCon), Manama.

Nandi, S. K., & Ghosh, H. R. (2010a). Prospect of wind–PV-battery hybrid power system as an alternative to grid extension in Bangladesh. *Energy, 35*(7), 3040-3047.

Nandi, S. K., & Ghosh, H. R. (2010b). Techno-economical analysis of off-grid hybrid systems at Kutubdia Island, Bangladesh. *Energy Policy, 38*(2), 976-980.

NBS. (2013). *Annual Abstract of Statistics, National Bureau of Statistics. Federal Republic of Nigeria.*: Retrieved from www.nigerianstat.gov.ng.

Nehrir, M. H., Wang, C., Strunz, K., Aki, H., Ramakumar, R., Bing, J., . . . Salameh, Z. (2011). A review of hybrid renewable/alternative energy systems for electric power generation: configurations, control, and applications. *IEEE Transactions on Sustainable Energy, 2*(4), 392-403.

Ngpricehunter. Retrieved May 12, 2015, from http://www.ngpricehunter.com/

NIMET. (2014). Nigerian Meteorological Agency from htttp://www.nimet.gov.ng

Nnaji, C., Uzoma, C., & Chukwu, J. (2010). The role of renewable energy resources in poverty alleviation and sustainable development in Nigeria. *Continental Journal of Social Sciences, 3*, 31-37.

NREL. (2009). HOMER. from http://www.homerenergy.com

NREL. (2015). HOMER PRO Index. Retrieved from http://www.homerenergy.com/HOMER_pro.html

Ohunakin, O., Adaramola, M., & Oyewola, O. (2011). Wind energy evaluation for electricity generation using WECS in seven selected locations in Nigeria. *Applied Energy, 88*(9), 3197-3206.

Ohunakin, O. S. (2010). Energy utilization and renewable energy sources in Nigeria. *Journal of Engineering and Applied Sciences, 5*(2), 171-177.

Ohunakin, O. S. (2011a). Assessment of wind energy resources for electricity generation using WECS in North-Central region, Nigeria. *Renewable and Sustainable Energy Reviews, 15*(4), 1968-1976.

Ohunakin, O. S. (2011b). Wind resource evaluation in six selected high altitude locations in Nigeria. *Renewable Energy, 36*(12), 3273-3281.

Ohunakin, O. S., Adaramola, M. S., Oyewola, O. M., & Fagbenle, R. O. (2014). Solar energy applications and development in Nigeria: drivers and barriers. *Renewable and Sustainable Energy Reviews, 32*, 294-301.

Ohunakin, O. S., Ojolo, S. J., & Ajayi, O. O. (2011). Small hydropower (SHP) development in Nigeria: an assessment. *Renewable and Sustainable Energy Reviews, 15*(4), 2006-2013.

Okundamiya, M., & Nzeako, A. (2011). Empirical model for estimating global solar radiation on horizontal surfaces for selected cities in the six geopolitical zones in Nigeria. *Journal of Control Science and Engineering, 2011*, 9.

Olatomiwa, L., Mekhilef, S., Shamshirband, S., Mohammadi, K., Petković, D., & Sudheer, C. (2015). A support vector machine–firefly algorithm-based model for global solar radiation prediction. *Solar energy, 115*, 632-644.

Olatomiwa, L., Mekhilef, S., Shamshirband, S., & Petkovic, D. (2015). Potential of support vector regression for solar radiation prediction in Nigeria. *Natural Hazards, 77*(2), 1055-1068.

Onar, O., Uzunoglu, M., & Alam, M. (2006). Dynamic modeling, design and simulation of a wind/fuel cell/ultra-capacitor-based hybrid power generation system. *Journal of Power Sources, 161*(1), 707-722.

Pan, W., Gao, W., & Muljadi, E. (2009). *The dynamic performance and effect of hybrid renewable power system with diesel/wind/PV/battery.* Paper presented at the International Conference on Sustainable Power Generation and Supply, SUPERGEN'09. .

Payman, A., Pierfederici, S., & Meibody-Tabar, F. (2009). Energy management in a fuel cell/supercapacitor multisource/multiload electrical hybrid system. *IEEE Transactions on Power Electronics, 24*(12), 2681-2691.

Petković, D., Ćojbašić, Ž., & Lukić, S. (2013). Adaptive neuro fuzzy selection of heart rate variability parameters affected by autonomic nervous system. *Expert Systems with Applications, 40*(11), 4490-4495.

Petković, D., Issa, M., Pavlović, N. D., Pavlović, N. T., & Zentner, L. (2012). Adaptive neuro-fuzzy estimation of conductive silicone rubber mechanical properties. *Expert Systems with Applications, 39*(10), 9477-9482.

Pinker, R., Frouin, R., & Li, Z. (1995). A review of satellite methods to derive surface shortwave irradiance. *Remote Sensing of Environment, 51*(1), 108-124.

Practical Action (2013). [Poor people's energy outlook].

Rajashekara, K. (2005). Hybrid fuel-cell strategies for clean power generation. *IEEE Transactions on Industry Applications, 41*(3), 682-689.

Ramedani, Z., Omid, M., & Keyhani, A. (2013). Modeling solar energy potential in a Tehran Province using artificial neural networks. *International Journal of Green Energy, 10*(4), 427-441.

Ramedani, Z., Omid, M., Keyhani, A., Shamshirband, S., & Khoshnevisan, B. (2014a). Potential of radial basis function based support vector regression for global solar radiation prediction. *Renewable and Sustainable Energy Reviews, 39*(1), 1005-1011.

Ramedani, Z., Omid, M., Keyhani, A., Shamshirband, S., & Khoshnevisan, B. (2014b). Potential of radial basis function based support vector regression for global solar radiation prediction. *Renewable and Sustainable Energy Reviews, 39*, 1005-1011.

Rehman, S., & Al-Hadhrami, L. M. (2010). Study of a solar PV–diesel–battery hybrid power system for a remotely located population near Rafha, Saudi Arabia. *Energy, 35*(12), 4986-4995.

Rehman, S., Mahbub Alam, M., Meyer, J. P., & Al-Hadhrami, L. M. (2012). Feasibility study of a wind–pv–diesel hybrid power system for a village. *Renewable Energy, 38*(1), 258-268.

Reindl, D., Beckman, W., & Duffie, J. (1990). Evaluation of hourly tilted surface radiation models. *Solar energy, 45*(1), 9-17.

Rinne, H. (2010). *The Weibull distribution: a handbook*: CRC Press.

Roy, A., Kedare, S. B., & Bandyopadhyay, S. (2010). Optimum sizing of wind-battery systems incorporating resource uncertainty. *Applied Energy, 87*(8), 2712-2727.

Saha, A., Chowdhury, S., Chowdhury, S., & Gaunt, C. (2009). *Integration of wind turbine, SOFC and microturbine in distributed generation.* Paper presented at the IEEE Power & Energy Society General Meeting, PES'09. .

Sambo, A. (1986). Empirical models for the correlation of global solar radiation with meteorological data for northern Nigeria. *Solar & wind technology, 3*(2), 89-93.

Sambo, A. S. (2009). Strategic Developments in Renewable Energy in Nigeria. . *International Association for Energy Economics*, 15 – 19.

Sandrolini, L., Artioli, M., & Reggiani, U. (2010). Numerical method for the extraction of photovoltaic module double-diode model parameters through cluster analysis. *Applied Energy, 87*(2), 442-451.

Sathyajith, M. (2006). *Wind energy: fundamentals, resource analysis and economics*: Springer.

Schalkoff, R. J. (1997). *Artificial neural networks*: McGraw-Hill Higher Education.

Sen, R., & Bhattacharyya, S. C. (2014). Off-grid electricity generation with renewable energy technologies in India: an application of HOMER. *Renewable Energy, 62*, 388-398.

Sera, D., Teodorescu, R., & Rodriguez, P. (2007). *PV panel model based on datasheet values.* Paper presented at the 2007 IEEE international symposium on industrial electronics.

Shaahid, S., & El-Amin, I. (2009). Techno-economic evaluation of off-grid hybrid photovoltaic–diesel–battery power systems for rural electrification in Saudi Arabia—A way forward for sustainable development. *Renewable and Sustainable Energy Reviews, 13*(3), 625-633.

Shaahid, S., El-Amin, I., Rehman, S., Al-Shehri, A., Ahmad, F., Bakashwain, J., & Al-Hadhrami, L. M. (2010). Techno-economic potential of retrofitting diesel power systems with hybrid wind-photovoltaic-diesel systems for off-grid electrification

of remote villages of Saudi Arabia. *International Journal of Green Energy, 7*(6), 632-646.

Shamshirband, S., Petković, D., Hashim, R., & Motamedi, S. (2014). Adaptive neuro-fuzzy methodology for noise assessment of wind turbine. *PloS one, 9*(7), 1-11.

Singh, M., & Chandra, A. (2009). *Control of PMSG based variable speed wind-battery hybrid system in an isolated network.* Paper presented at the IEEE Power & Energy Society General Meeting, 2009. PES'09.

Sinha, S., & Chandel, S. (2014). Review of software tools for hybrid renewable energy systems. *Renewable and Sustainable Energy Reviews, 32*, 192-205.

Sinha, S., & Chandel, S. (2015). Review of recent trends in optimization techniques for solar photovoltaic–wind based hybrid energy systems. *Renewable and Sustainable Energy Reviews, 50*, 755-769.

Solex. (2014). from http://solex.in/

Sugeno, M., & Kang, G. (1988). Structure identification of fuzzy model. *Fuzzy sets and systems, 28*(1), 15-33.

Talei, A., Chua, L. H. C., & Quek, C. (2010). A novel application of a neuro-fuzzy computational technique in event-based rainfall–runoff modeling. *Expert Systems with Applications, 37*(12), 7456-7468.

Tchinda, R., Kendjio, J., Kaptouom, E., & Njomo, D. (2000). Estimation of mean wind energy available in far north Cameroon. *Energy Conversion and Management, 41*(17), 1917-1929.

Thapar, V., Agnihotri, G., & Sethi, V. K. (2011). Critical analysis of methods for mathematical modelling of wind turbines. *Renewable Energy, 36*(11), 3166-3177.

Tina, G., Gagliano, S., & Raiti, S. (2006). Hybrid solar/wind power system probabilistic modelling for long-term performance assessment. *Solar energy, 80*(5), 578-588.

Torres, M., & Lopes, L. A. (2013). Inverter-based diesel generator emulator for the study of frequency variations in a laboratory-scale autonomous power system. *Energy and Power Engineering, 5*(03), 274.

Ucar, A., & Balo, F. (2009). Evaluation of wind energy potential and electricity generation at six locations in Turkey. *Applied Energy, 86*(10), 1864-1872.

UN. (2014). *World Urbanization Prospects: The 2014 Revision, Highlights*. Retrieved from http://esa.un.org/unpd/wup/Highlights/WUP2014-Highlights.pdf.

USAID. (2014). Powering Health. *Electrification Option for Developing Country Health Facilities.* from http://www.poweringhealth.org/index.php

Uzoma, C. C., Nnaji, C. E., Ibeto, C. N., Okpara, C. G., Nwoke, O. O., Obi, I. O., . . . Oparaku, O. U. (2011). Renewable Energy Penetration in Nigeria: A Study of The South-East Zone. *Continental Journal of Environmental Sciences, 5*(1), 1-5.

Villalva, M. G., & Gazoli, J. R. (2009). Comprehensive approach to modeling and simulation of photovoltaic arrays. *IEEE Transactions on Power Electronics, 24*(5), 1198-1208.

Vincent-Akpu, I. (2012). *Renewable energy potentials in Nigeria*. Paper presented at the Energy Future The Role of Impact Assessment, 32nd Annual Meeting of the International Association for Impact Assessment, Centro de Congresso da Alfândega, Porto-Portugal

Vosen, S., & Keller, J. (1999). Hybrid energy storage systems for stand-alone electric power systems: optimization of system performance and cost through control strategies. *international journal of hydrogen energy*, *24*(12), 1139-1156.

Wang, C. (2006). *Modeling and control of hybrid wind/photovoltaic/fuel cell distributed generation systems.* Montana State University, Bozeman.

Wang, C., & Nehrir, M. H. (2008). Power management of a stand-alone wind/photovoltaic/fuel cell energy system. *IEEE Transactions on Energy Conversion, 23*(3), 957-967.

Wang, W., Mao, C., Lu, J., & Wang, D. (2013). An Energy Storage System Sizing Method for Wind Power Integration. *Energies, 6*(7), 3392-3404.

Willmott, C. J., & Matsuura, K. (2005). Advantages of the mean absolute error (MAE) over the root mean square error (RMSE) in assessing average model performance. *Climate Research, 30*(1), 79.

Wood, D. (2010). Small wind turbines for remote power and distributed generation. *Wind engineering, 34*(3), 241-254.

WorldBank. (2013). *Initiating the World Bank's peri-urban Rural and Renewable Energy activities in Nigeria.* Paper presented at the workshop organized under the auspices of the World Bank's Energy Sector Management Assistance Program. ESMAP Abuja, Nigeria.

Worldbank. (2015). *World Development Indicators*. Retrieved from http://databank.worldbank.org/data/.

Wu, C., Chau, K., & Fan, C. (2010). Prediction of rainfall time series using modular artificial neural networks coupled with data-preprocessing techniques. *Journal of hydrology, 389*(1), 146-167.

Yacef, R., Benghanem, M., & Mellit, A. (2012). Prediction of daily global solar irradiation data using Bayesian neural network: a comparative study. *Renewable Energy, 48*, 146-154.

Yohanna, J. K., Itodo, I. N., & Umogbai, V. I. (2011). A model for determining the global solar radiation for Makurdi, Nigeria. *Renewable Energy*, *36*(7), 1989-1992.

Zagrouba, M., Sellami, A., Bouaïcha, M., & Ksouri, M. (2010). Identification of PV solar cells and modules parameters using the genetic algorithms: application to maximum power extraction. *Solar energy, 84*(5), 860-866.

Zhou, W., Lou, C., Li, Z., Lu, L., & Yang, H. (2010). Current status of research on optimum sizing of stand-alone hybrid solar–wind power generation systems. *Applied Energy, 87*(2), 380-389.

LIST OF PUBLICATIONS AND PAPERS PRESENTED

Journals

1. **Lanre Olatomiwa**, Saad Mekhilef, Shahaboddin Shamshirb (**2015**). *Adaptive neuro-fuzzy approach for solar radiation prediction in Nigeria.* ***Published in "Renewable & Sustainable Energy Reviews"*** (Elsevier). ISSN: 1364-0321. Vol. 51. pp: 1784-1791 (*ISI-cited publication, I.F: 6.798,* ***Q1***).
2. **Lanre Olatomiwa**, Saad Mekhilef, M.S. Ismail , M. Moghavvemi **(2016)**. *Energy management strategies in hybrid renewable energy systems: A review.* ***Published in "Renewable & Sustainable Energy Reviews"*** (Elsevier). ISSN: 1364-0321. Vol. 62. pp: 821-835 (*ISI-cited publication, I.F: 6.798,* ***Q1***).
3. **Lanre Olatomiwa**, Saad Mekhilef, A.S.N. Huda, Olayinka S.Ohunakin **(2015).** *Economic evaluation of hybrid energy systems for rural electrification in six geo-political zones of Nigeria.* ***Published in "Renewable Energy"*** (Elsevier). ISSN: 0960-1481. Vol. 83. pp: 435-446. (*ISI-cited publication, I.F: 3.476,* ***Q1***).
4. **Lanre Olatomiwa**, Saad Mekhilef, Olayinka S.Ohunakin **(2015)**. *Hybrid renewable power supply for rural health clinics (RHC) in six geo-political zone of Nigeria.* ***Published in*** "***Sustainable Energy Technologies and Assessments.*** (Elsevier). ISSN: 2213-1388. Vol. 13. 1-12: . (*ISI-cited publication, I.F: 0.842*)
5. **Lanre Olatomiwa**, Saad Mekhilef, Shahaboddin Shamshirband (**2015**). *A support vector machine-firefly algorithm-based model for global solar radiation prediction.* ***Published in "Solar Energy"*** (Elsevier). ISSN: 0038-092X. Vol. 115. pp: 632–644. (*ISI-cited publication, I.F: 3.469.* ***Q1***)
6. **Lanre Olatomiwa**, Saad Mekhilef, Shahaboddin Shamshirb, Dalibor Petkovic (**2015**) *Potential of support vector regression for solar radiation prediction in Nigeria.* ***Published in "Natural Hazards Journal"*** (Springer) Netherlands. Vol. 75, Issue 2, pp. 1055-1068. ISSN: 0921-030X (Print), 1573-0840 (Online). (*ISI-cited publication, I.F:1.718,* ***Q2***)
7. **Lanre Olatomiwa,** Saad Mekhilef (**2016**). Optimal configuration assessments of hybrid renewable power supply for rural healthcare facilities. ***Published in Energy Reports*** (Elsevier). ISSN: 2352-4847. Vol. 2, pp: 141–146 (Scopus-cited publication).
8. **Lanre Olatomiwa**, Saad Mekhilef, A.S.N. Huda (**2015**). *Techno-economic analysis of hybrid PV-diesel-battery and PV-wind-diesel-battery power systems:*

The way forward for rural development. ***Published in "Energy Science & Engineering Journal"*** (Wiley & Sons). ISSN: 2050-0505, Vol. 4, Issue 4, pp. 271-285. *(Scopus-cited publication).*

9. **Lanre Olatomiwa**, Saad Mekhilef, Shahaboddin Shamshirband. *Global Solar Radiation Forecasting Based on SVM-Wavelet Transform Algorithm.* ***Published in "International Journal of Intelligent Systems and Applications (IJISA)"***. ISSN: 2074-904X (Print), ISSN: 2074-9058 (Online).Vol 8, Issue 5 pp. 19-26. *(Scopus-cited publication).*

Conferences

1. **Lanre Olatomiwa**, Saad Mekhilef, A.S.N **(2014)**. *Optimal Sizing of Hybrid Energy System: A Case Study in Nigeria.* ***Presented*** *at 2014* IEEE conference on Energy Conversion (CENCON 2014) held at KSL Resort, Johor Bahru, Malaysia (13-14 October 2014).
2. **Lanre Olatomiwa**, Saad Mekhilef. **(2015)**. *Techno-economic feasibility of hybrid renewable energy system for rural health centre (RHC): The wayward for quality health delivery.* ***Presented*** at 2015 IEEE conference on Energy Conversion held at Berjaya Waterfront Hotel, Johor Bahru, Malaysia (19-20 October 2015).
3. **Lanre Olatomiwa**, Saad Mekhilef. *Assessments of Hybrid Renewable Energy System Optimal Configuration for Rural Healthcare Facilities.****Presented*** at 4th European Conference on Renewable Energy System (ECRES 2016) held in Istanbul, Turkey (28-31, August, 2016).

APPENDIX A

MATLAB code for determination of Optimal tilt angle

```
%%%%%%%%%%%%%%%%%%%%%%%%%%%%%%%%%%%%%%%%%%%%%%%%%%%%%%%%%%%%%%%%%%%%%%%%%%%%
 This Program determine optimal tilt angle and optimal solar radiation
on tilted surface
%%%%%%%%%%%%%%%%%%%%%%%%%%%%%%%%%%%%%%%%%%%%%%%%%%%%%%%%%%%%%%%%%%%%%%%%%%%%
d= [17 47 75 105 135 162 198 228 258 288 318 344]; Average day of each
month of calendar year.
%H=[4.76    5.14    4.74    4.76    4.54    4.13    3.35    3.53    3.70
4.24    4.55    4.82];  Average radiation on horizontal surface
%%%%%%%%%%%%%%%%%%%%%%%%%%%%%%%%%%%%%%%%%%%%%%%%%%%%%%%%%%%%%%%%%%%%%%%%%%%%
  clc
  d= 17; % Insert a typical average day of each month
  H=4.76; % Average global solar radiation on horizontal surface
  Pg=0.2;                              % Ground reflectivity
  phi=25.3*pi/180;                     % Convert from degree to Rad
  I_sc=1.367;                          % Solar constant
  s=0.409*sin(2*pi/365*(284+d));       % Solar declination angle
  w= acos(-tan(s)*tan(phi));           % Sunrise hour angle
  Ho=(24*I_sc/pi)*(1+0.033*cos(2*pi*d/365)).*(w*sin(s)*sin(phi)+cos(s)
*cos(phi)*sin(w));                     % extraterrestrial radiation
  Kt=H/Ho;                             % Clearness index
  if w<=81.4*pi/180
      Hd= H*(1.391-3.560*Kt+4.189*Kt^2 -2.137*Kt^3);
  else
      Hd= H*(1.311-3.022*Kt+3.427*Kt^2 -1.821*Kt^3);
  end
  Hb=H-Hd;
  H_tilt_vary_B=[];                    %Tilt angle
  Ht_max=0;
  B_max=0;
  for B=0:pi/1800:pi/2
      w1=min(w,acos(-tan(s)*tan(phi-B)));

      Rb=(cos(phiB)*cos(s)*sin(w1)+w1*sin(phiB)*sin(s))/(cos(phi)*cos(
      s)*sin(w)+w*sin(phi)*sin(s));
       Rd = Hb*Rb/Ho+(1-Hb/Ho)*((1+cos(B))/2);
       Ht= Hb*Rb+Hd*Rd+ H*Pg*(1-cos(B))/2;
       H_tilt_vary_B=[H_tilt_vary_B;Ht];
  if Ht>Ht_max
       Ht_max =Ht;
       B_max=B;                        % Optimal tilt angle
  end
  end
  Ht_max                        % Optimal radiation on tilted surface

  B_max_Degree=B_max*180/pi   %Optimal tilt angle (in degree)
```

APPENDIX B

Table B1 : Indicative power requirements of electrical devices for health services

	Health services	Electrical devices	Indicative power rating[W]	AC power supply	DC power supply
Infrastructure	Basic amenities	Lightings :			
		✓ Incandescent Bulb	10.8W/m2	110/220V	-
		✓ Halogen Bulb	1.8W/m2	110/220V	12V
		✓ CFL Bulb	2.16W/m2	110/220V	-
		✓ LED Bulb	1.8-2.14W/m2	110/220V	10-30V
		Security lighting/outdoors	40-160W CFL/LED	110/220V	10-30V
			200-600W incandescent	110/220V	10-30V
		Mobile phone battery (charging)	5-20W	110/220V	5-16.5V
		Desktop Computer	15-200W	110/220V	8-20V
		Laptop Desktop	20-60W	110/220V	12-20V
		Printer(ink jet)	65-100W	110/220V	12-20V
		VHF radio receiver: Stand-by	2W	110/220V	12V
		Transmitting	30W	110/220V	12V
		Ceiling fan	50-100W	110/220V	-
		Refrigerator (for food& water)	150-200W	110/220V	-
		Portable Air-conditioner (AC)	1000-1500W	110/220V	48V
Specific services	General outpatient services	Nebulizer	80-90W	110/220V	-
		Oxygen concentrator	270-310W	110/220V	-
		Pulse oximeter	50W	110/220V	-
	Antenatal child & adolescent health	Vaccine refrigerator	60-115W	110/220V	N/A
	Obstetric & new born	LED lighting (phototherapy)	440W	110/220V	-
		Suction apparatus	90-200W	110/220V	-
		Vacuum aspirator	36-96W	110/220V	3-6V
		Neo-natal incubator	800-1035W	110/220V	-
		Ultrasound	800-1000W	110/220V	-
	General diagnostics, blood analysis & laboratory equipment	Laboratory refrigerator	60-160W	110/220V	-
		Centrifuge	250-400W	110/220V	-
		Haematology analyser	230-400W	110/220V	-
		Blood chemistry analyser	45-88W	110/220V	-
		CD4 counter	200W	110/220V	12V
		Microscope (with LED light)	20-30W	110/220V	3-6V
		x-ray machine (portable)	3-4kW	110/220V	-
		Laboratory incubator	200W	110/220V	12V
	Basic surgical services	Suction apparatus	90-200W	110/220V	-
		Anaesthesia machine	1440W	110/220V	

APPENDIX C

Table C1: Annual mean energy density of Sokoto site

Wind speed Range (m/s)	Mid-range V(i) (m/s)	Duration (hr)	Prob. of Occurrence f(vi)	Power (W/m2)	Power density_data (W/m2)	Weibull PDF fw(vi)	Power density_Weibull (W/m^2)	Energy density_Weibull (kWh/m^2)	Energy density_data (kWh/m^2)
0-1	0.5	104	0.012	0.08	0.00	0.00	0.00	0.00	0.01
1-2	1.5	318	0.036	2.04	0.07	0.00	0.00	0.00	0.65
2-3	2.5	540	0.062	9.45	0.58	0.00	0.01	0.05	5.10
3-4	3.5	709	0.081	25.94	2.10	0.00	0.08	0.72	18.39
4-5	4.5	823	0.094	55.13	5.18	0.01	0.62	5.44	45.37
5-6	5.5	900	0.103	100.66	10.34	0.03	3.08	27.01	90.59
6-7	6.5	874	0.100	166.15	16.58	0.07	11.32	99.15	145.21
7-8	7.5	846	0.097	255.23	24.65	0.13	32.27	282.68	215.93
8-9	8.5	759	0.087	371.55	32.19	0.19	71.62	627.36	282.00
9-10	9.5	651	0.074	518.71	38.55	0.23	119.20	1044.23	337.68
10-11	10.5	556	0.063	700.36	44.45	0.20	137.74	1206.60	389.40
11-12	11.5	435	0.050	920.13	45.69	0.11	97.84	857.11	400.26
12-13	12.5	347	0.040	1181.64	46.81	0.03	35.95	314.96	410.03
13-14	13.5	264	0.030	1488.53	44.86	0.00	5.42	47.47	392.97
14-15	14.5	196	0.022	1844.42	41.27	0.00	0.25	2.17	361.51
15-16	15.5	142	0.016	2252.94	36.52	0.00	0.00	0.02	319.92
16-17	16.5	101	0.012	2717.74	31.33	0.00	0.00	0.00	274.49
17-18	17.5	70	0.008	3242.42	25.91	0.00	0.00	0.00	226.97
18-19	18.5	46	0.005	3830.63	20.12	0.00	0.00	0.00	176.21
19-20	19.5	31	0.004	4486.00	15.88	0.00	0.00	0.00	139.07
20-21	20.5	20	0.002	5212.15	11.90	0.00	0.00	0.00	104.24
21-22	21.5	11	0.001	6012.72	7.55	0.00	0.00	0.00	66.14
22-23	22.5	12	0.001	6891.33	9.44	0.00	0.00	0.00	82.70
23-24	23.5	4	0.000	7851.61	3.59	0.00	0.00	0.00	31.41
23-25	24.5	1	0.000	8897.21	1.02	0.00	0.00	0.00	8.90
Sum		8760	1.000		516.57		515.41	4514.97	4525.14

Table C2: Annual mean energy density of Maiduguri site

Wind speed Range (m/s)	Mid-range V(i) (m/s)	Duration (hr)	Prob. of Occurrence f(vi)	Power (W/m2)	Power density_data (W/m2)	Weibull PDF fw(vi)	Power density_ Weibull (W/m^2)	Energy density_ Weibull (kWh/m^2)	Energy density_ data (kWh/m^2)
0-1	0.5	214	0.02	0.08	0.00	0.00	0.00	0.00	0.02
1-2	1.5	648	0.07	2.04	0.15	0.01	0.02	0.16	1.32
2-3	2.5	1023	0.12	9.45	1.10	0.04	0.34	3.01	9.67
3-4	3.5	1228	0.14	25.94	3.64	0.09	2.22	19.44	31.85
4-5	4.5	1291	0.15	55.13	8.12	0.15	8.18	71.63	71.17
5-6	5.5	1175	0.13	100.66	13.50	0.20	20.13	176.31	118.27
6-7	6.5	997	0.11	166.15	18.91	0.21	34.82	305.03	165.65
7-8	7.5	750	0.09	255.23	21.85	0.17	42.43	371.68	191.43
8-9	8.5	548	0.06	371.55	23.24	0.10	35.50	310.99	203.61
9-10	9.5	363	0.04	518.71	21.49	0.04	19.54	171.16	188.29
10-11	10.5	223	0.03	700.36	17.83	0.01	6.69	58.60	156.18
11-12	11.5	142	0.02	920.13	14.92	0.00	1.33	11.68	130.66
12-13	12.5	74	0.01	1181.64	9.98	0.00	0.14	1.26	87.44
13-14	13.5	45	0.01	1488.53	7.65	0.00	0.01	0.07	66.98
14-15	14.5	20	0.00	1844.42	4.21	0.00	0.00	0.00	36.89
15-16	15.5	12	0.00	2252.94	3.09	0.00	0.00	0.00	27.04
16-17	16.5	3	0.00	2717.74	0.93	0.00	0.00	0.00	8.15
17-18	17.5	1	0.00	3242.42	0.37	0.00	0.00	0.00	3.24
18-19	18.5	1	0.00	3830.63	0.44	0.00	0.00	0.00	3.83
19-20	19.5	2	0.00	4486.00	1.02	0.00	0.00	0.00	8.97
20-21	20.5	0	0.00	5212.15	0.00	0.00	0.00	0.00	0.00
Sum		8760	1.00		172.45		171.35	1501.03	1510.67

Table C3: Annual mean energy density of Jos site

Wind speed Range (m/s)	Mid-range V(i) (m/s)	Duration (hr)	Prob. of Occurrence f(vi)	Power (W/m2)	Power density_data (W/m2)	Weibull PDF fw(vi)	Power density_Weibull (W/m^2)	Energy density_Weibull (kWh/m^2)	Energy density_data (kWh/m^2)
0-1	0.5	96	0.01	0.08	0.00	0.00	0.00	0.00	0.01
1-2	1.5	269	0.03	2.04	0.06	0.00	0.00	0.00	0.55
2-3	2.5	441	0.05	9.45	0.48	0.00	0.01	0.07	4.17
3-4	3.5	581	0.07	25.94	1.72	0.00	0.09	0.80	15.07
4-5	4.5	676	0.08	55.13	4.25	0.01	0.56	4.88	37.27
5-6	5.5	737	0.08	100.66	8.47	0.02	2.34	20.52	74.18
6-7	6.5	768	0.09	166.15	14.57	0.05	7.58	66.37	127.60
7-8	7.5	773	0.09	255.23	22.52	0.08	19.96	174.81	197.30
8-9	8.5	724	0.08	371.55	30.71	0.12	43.88	384.38	269.00
9-10	9.5	664	0.08	518.71	39.32	0.16	80.86	708.32	344.42
10-11	10.5	591	0.07	700.36	47.25	0.18	123.33	1080.37	413.91
11-12	11.5	519	0.06	920.13	54.51	0.16	151.61	1328.09	477.55
12-13	12.5	446	0.05	1181.64	60.16	0.12	144.30	1264.11	527.01
13-14	13.5	352	0.04	1488.53	59.81	0.07	100.80	883.04	523.96
14-15	14.5	295	0.03	1844.42	62.11	0.03	48.30	423.15	544.10
15-16	15.5	222	0.03	2252.94	57.10	0.01	14.63	128.12	500.15
16-17	16.5	172	0.02	2717.74	53.36	0.00	2.54	22.23	467.45
17-18	17.5	134	0.02	3242.42	49.60	0.00	0.22	1.97	434.48
18-19	18.5	94	0.01	3830.63	41.10	0.00	0.01	0.08	360.08
19-20	19.5	67	0.01	4486.00	34.31	0.00	0.00	0.00	300.56
20-21	20.5	51	0.01	5212.15	30.34	0.00	0.00	0.00	265.82
21-22	21.5	41	0.00	6012.72	28.14	0.00	0.00	0.00	246.52
22-23	22.5	23	0.00	6891.33	18.09	0.00	0.00	0.00	158.50
23-24	23.5	13	0.00	7851.61	11.65	0.00	0.00	0.00	102.07
23-25	24.5	9	0.00	8897.21	9.14	0.00	0.00	0.00	80.07
23-26	25.5	1	0.00	10031.73	1.15	0.00	0.00	0.00	10.03
23-27	26.5	1	0.00	11258.82	1.29	0.00	0.00	0.00	11.26
Sum		8760	1.00		741.22		741.02	6491.32	6493.12

Table C4: Annual mean energy density of Enugu site

Wind speed Range (m/s)	Mid-range V(i) (m/s)	Duration (hr)	Prob. of Occurrence f(vi)	Power (W/m^2)	Power density _data (W/m^2)	Weibull PDF fw(vi)	Power density_ Weibull (W/m^2)	Energy density_ Weibull (kWh/m^2)	Energy density_ data (kWh/m^2)
0-1	0.5	213	0.02	0.08	0.00	0.00	0.00	0.00	0.02
1-2	1.5	645	0.07	2.04	0.15	0.00	0.01	0.05	1.32
2-3	2.5	1017	0.12	9.45	1.10	0.02	0.17	1.51	9.61
3-4	3.5	1249	0.14	25.94	3.70	0.06	1.53	13.36	32.40
4-5	4.5	1277	0.15	55.13	8.04	0.13	7.21	63.12	70.40
5-6	5.5	1177	0.13	100.66	13.52	0.21	21.57	188.93	118.47
6-7	6.5	986	0.11	166.15	18.70	0.25	42.15	369.19	163.82
7-8	7.5	758	0.09	255.23	22.09	0.20	51.35	449.80	193.47
8-9	8.5	550	0.06	371.55	23.33	0.09	35.28	309.08	204.35
9-10	9.5	367	0.04	518.71	21.73	0.02	11.81	103.47	190.37
10-11	10.5	224	0.03	700.36	17.91	0.00	1.59	13.96	156.88
11-12	11.5	139	0.02	920.13	14.60	0.00	0.07	0.60	127.90
12-13	12.5	78	0.01	1181.64	10.52	0.00	0.00	0.01	92.17
13-14	13.5	41	0.00	1488.53	6.97	0.00	0.00	0.00	61.03
14-15	14.5	21	0.00	1844.42	4.42	0.00	0.00	0.00	38.73
15-16	15.5	8	0.00	2252.94	2.06	0.00	0.00	0.00	18.02
16-17	16.5	6	0.00	2717.74	1.86	0.00	0.00	0.00	16.31
17-18	17.5	1	0.00	3242.42	0.37	0.00	0.00	0.00	3.24
18-19	18.5	3	0.00	3830.63	1.31	0.00	0.00	0.00	11.49
Sum		8760	1.00		172.37		172.73	1513.10	1510.00

Table C5: Annual mean energy density of Port Harcourt site

Wind speed Range (m/s)	Mid-range V(i) (m/s)	Duration (hr)	Prob. of Occurrence f(vi)	Power (W/m^2)	Power Density_ data (W/m^2)	Weibull PDF fw(vi)	Power density_ Weibull (W/m^2)	Energy density_ Weibull (kWh/m^2)	Energy density_ data (kWh/m^2)
0-1	0.5	544	0.06	0.08	0.00	0.00	0.00	0.00	0.04
1-2	1.5	1417	0.16	2.04	0.33	0.03	0.05	0.45	2.89
2-3	2.5	1827	0.21	9.45	1.97	0.12	1.13	9.93	17.27
3-4	3.5	1731	0.20	25.94	5.13	0.28	7.14	62.54	44.90
4-5	4.5	1360	0.16	55.13	8.56	0.34	18.74	164.14	74.98
5-6	5.5	893	0.10	100.66	10.26	0.20	19.76	173.09	89.89
6-7	6.5	528	0.06	166.15	10.01	0.04	6.72	58.85	87.73
7-8	7.5	263	0.03	255.23	7.66	0.00	0.52	4.58	67.13
8-9	8.5	118	0.01	371.55	5.00	0.00	0.01	0.05	43.84
9-10	9.5	50	0.01	518.71	2.96	0.00	0.00	0.00	25.94
10-11	10.5	19	0.00	700.36	1.52	0.00	0.00	0.00	13.31
11-12	11.5	6	0.00	920.13	0.63	0.00	0.00	0.00	5.52
12-13	12.5	4	0.00	1181.64	0.54	0.00	0.00	0.00	4.73
13-14	13.5	0	0.00	1488.53	0.00	0.00	0.00	0.00	0.00
14-15	14.5	0	0.00	1844.42	0.00	0.00	0.00	0.00	0.00
Sum		8760	1.00		54.58		54.07	473.63	478.16